UNIVERSITÀ DEL PIEMONTE ORIENTALE

"A. AVOGADRO"

Department of Translational Medicine

PhD PROGRAM IN BIOTECHNOLOGIES FOR HUMAN HEALTH

XXVII cycle
Academic years 2011-2014

PhD THESIS

ROLE OF GHRELIN PEPTIDES IN SKELETAL MUSCLE: IMPLICATIONS FOR MUSCLE WASTING AND CANCER CACHEXIA

Tutor:

Prof. Andrea Graziani

Co-tutor:

Prof. Nicoletta Filigheddu

PhD Coordinator:

Prof. Claudio Santoro

PhD Student:

Michele Ferrara

TABLE OF CONTENTS

SUMMARY

I spent my PhD fellowship in Prof. Graziani's Lab, at the Department of Translational Medicine in Novara with the supervision of Prof. Filigheddu.

During the three years of my PhD program I contributed to the discovery that ghrelin peptides activate anti-atrophic signaling by acting directly in the skeletal muscle, thus protecting from muscle wasting both *in vitro* and *in vivo*. In addition, we showed that such anti-atrophic activity is mediated by the binding to a novel yet unidentified receptor, herein referred as "GhrlR2", providing the first genetic evidence for a novel ghrelin receptor. These findings have been published in the *Journal of Clinical Investigation* in 2013 (Porporato, 2013). We also showed that the mechanisms underlying ghrelin anti-atrophic activity do not overlap with the IGF-1 pathway, the best characterized anabolic factor in skeletal muscle. Differently from IGF-1, AG and UnAG inhibit only protein degradation, without stimulating protein synthesis and hypertrophy. Although the identity of the novel receptor is still missing, the data presented here demonstrate that the GhrlR2 is *bona fide* a $G\alpha_s$-coupled receptor. Finally, we investigated the role of UnAG in counteracting cancer cachexia. The finding that ghrelin protects cancer-associated muscle wasting far more weakly than denervation- and fasting-induced atrophy, suggesting that cachectic muscle may acquire a condition of ghrelin resistance. Indeed, we showed that pro-cachectic cytokines, TNFα and IFNγ, induce ghrelin resistance in muscle cell *in vitro*, by inducing p101 regulatory subunit of PI3Kγ, an enzyme known to promote $G\alpha_s$-coupled receptors downregulation. Overall, these findings may have important translational implications in pathologies involving inflammation-associated muscle wasting such as cachexia, muscle dystrophies, and aging-associated sarcopenia.

INTRODUCTION

Regulation of skeletal muscle mass

Cell size is the result of a balance between protein breakdown and protein synthesis. In the skeletal muscle, when the first exceeds the protein synthesis, there is the onset of atrophy, whereas in the opposite condition skeletal muscle grows or becomes hypertrophic [1]. Recent findings have highlighted multiple levels of connections between catabolic pathways, mainly the ubiquitin-proteasome system and the autophagy-lysosome pathway, and biosynthetic pathways.

Skeletal muscle grows in the postnatal period, and increases its mass becoming hypertrophic in adults, for example in response to mechanical overload, through two main signaling pathways triggered by: the positive regulator insulin-like growth factor (IGF-1), and the negative regulator myostatin [2].

- IGF-1 is the best characterized hypertrophic factor in skeletal muscle (Fig. 1, from [3]). It binds to IGF1R inducing phosphorylation of insulin receptors substrate 1 (IRS1), that is a highly regulated component for the majority of IGF-1 activities [4]. Indeed, several E3 ubiquitin ligases control IRS1 under different conditions [4]: for example, SOCS1 and SOCS3 elicit insulin resistance induced by inflammation through ubiquitination of IRS1 and IRS2 [5], and Fbox40-SCF complex degrades IRS1 soon after IGF-1 stimulation, limiting the activation of the downstream pathway [6]. IGF-1 activates both mitogen-activated protein kinase/extracellular signal-regulated kinase (MAPK/ERK) and the phosphoinositide 3-kinase (PI3K)/Akt pathways. It has been demonstrated that the major hypertrophic signal comes from PI3K/Akt pathway, and that, conversely, ERK pathway is negligible [7]. The IGF-1-triggered Akt inhibits GSK3β and activates mTOR signaling to induce protein synthesis [8-10]. The serine/threonine kinase mTOR is regulated by multiple factors, including amino acids, AMPK, phosphatidic acid, and Akt, and forms two multiprotein complex, mTORC1 and mTORC2, characterized by the two key components raptor and rictor, respectively [11]. Protein synthesis is mainly attributable to mTORC1 activation, while mTORC2 blunts

protein degradation [11, 12]. Indeed, genetic studies revealed that mice without raptor in the skeletal muscle show a reduced postnatal growth, but mice lacking rictor had not abnormalities [13]. Consistently, treatment with rapamycin, that inhibits mTORC1 and, in chronic treatment, impairs also mTORC2 activity, blunts skeletal muscle growth, regeneration, and compensatory hypertrophy [14-16].

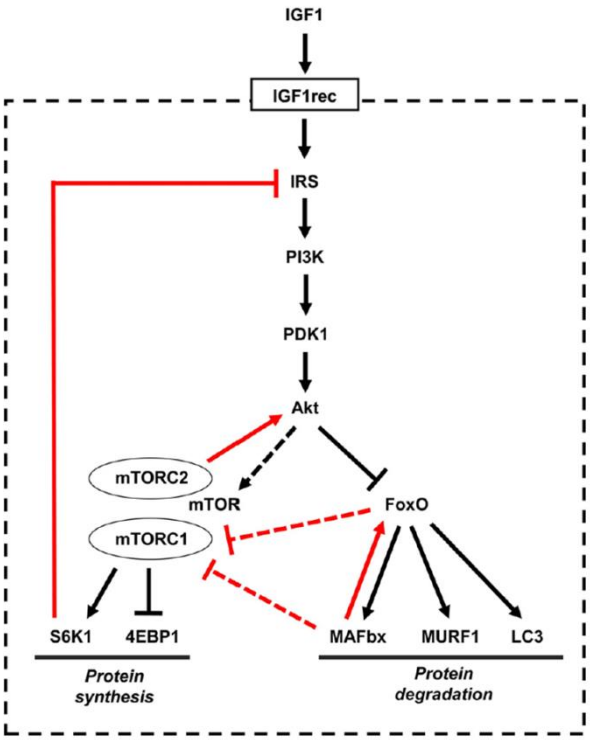

Figure 1: The IGF-1 pathway regulating skeletal muscle mass [3]

- Conversely to IGF-1, myostatin reduces skeletal muscle mass. Myostatin is a member of TGFβ family, and induces atrophy both *in vitro* and *in vivo* [17, 18], by activating Smad2 and Smad3 transcription factors [19]. It is likely that myostatin, similar to Activin A, another member of TGFβ family, deregulates Akt/mTOR pathway [19-21], enforcing its ability to induce muscle wasting.

Among the other factors involved in skeletal muscle growth and hypertrophy, such as serum response factor (SRF), androgens, PGC-1α4, and nNOS [2], β-adrenergic receptors (β-ARs) (Navegantes, 2002; Lynch, 2008) [22, 23], in particular β_2-AR agonists, and Wnt7a/Fzd7 play a

crucial role in the regulation of skeletal muscle mass [22-27]. Both β2-ARs and Wnt7a/Fzd7 trigger, besides Akt pathway, cAMP signaling, pointing out the crucial role of this second messenger in the regulation of skeletal muscle mass [28]. Indeed, at least four receptors coupled to $G\alpha_s$ induce skeletal muscle hypertrophy: Fzd7, β2-AR, CRFR2, and LPAR (Fig. 2, from [28]). It has been also demonstrated that cAMP affects not only differentiated myofibers, but also finely regulates myogenesis [28]. Surprisingly, it has been recently reported that the expression of $G\alpha_{i2}$ is sufficient to induce muscle hypertrophy and regeneration [29], however, it seems that the modulation of cAMP production in skeletal muscle is not the primary role of $G\alpha_{i2}$, which mainly acts through phospholipase C and protein kinase C [28].

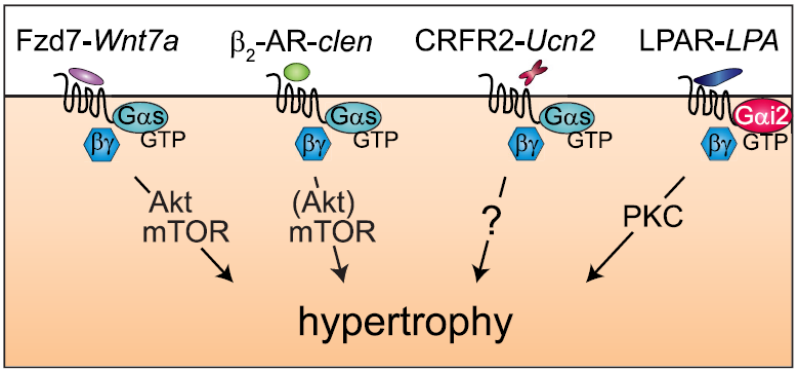

Figure 2: G protein-coupled receptors (GPCRs) inducing skeletal muscle hypertrophy [28]

Conversely, when protein degradation exceeds protein synthesis skeletal muscle loses its mass becoming atrophic. Skeletal muscle wasting is induced by several stimuli: loss of muscle mass may occurs locally, in response to denervation or inactivity, but also as a systemic response during fasting or different diseases, such as cardiac and renal failure, excessive glucocorticoids, AIDS, sepsis, trauma, and cachexia [30]. It is worth noting that the modulation of skeletal muscle mass not always follow the simple rule in which hypertrophy occurs when protein synthesis increases and protein degradation decreases, and conversely for muscle atrophy [2]. Indeed, it has been reported, among others, that muscle denervation is characterized by an increase in both protein synthesis and degradation [2]. However, it is undoubted that skeletal muscle atrophy shows an accelerated proteolysis of both myofibrillar and soluble proteins, leading to the loss of muscle

mass, leading to reduced body weight, fatigue, weakness and increased disability [30]. Specifically, the accelerated proteolysis derives from two highly conserved pathways: the ubiquitin-proteasome system (UPS) and autophagy [30, 31]. Both these pathways in skeletal muscle are constitutively active in physiological condition, but in pathological states there is an increase of their activity [32-39].

Skeletal muscle atrophy is an active process that is managed by a definite transcriptional program. Through microarray analysis it has been discovered a pool of genes regulated in different atrophic conditions, called atrogenes [33-36]. Globally, it has been identified 120 atrophy-related genes, including those related to UPS and autophagy, and, among these, Atrogin-1/MAFbX and MuRF1, two muscle specific E3-ubiquitin ligases, are the most induced genes in several atrophic states [33-35, 40], and are the principal proteins involved in the UPS. Atrogin-1 and MuRF1 are both dispensable for skeletal muscle growth, but their ablation reduces denervation-, starvation-, and glucocorticoid-induced atrophy [40, 41]. The PI3K/Akt/mTOR pathway discussed above, although in dividing cells regulates proliferation, in non-dividing cells, such as muscle cells, is the major regulator of skeletal muscle mass not only stimulating protein synthesis, but also inhibiting protein degradation [3]. Indeed, mTOR inhibits both UPS and autophagy [42-44], and Akt phosphorylates the transcription factors belong the family of forkhaed box protein O (FoxO), impairing their ability to translocate into the nucleus and induce atrogenes program [30]. Among these, FoxO1 and FoxO3 are likely activated in all types of skeletal muscle wasting [30], and FoxO3 alone is sufficient to induce skeletal muscle atrophy upregulating UPS and autophagy [38, 39, 45]. Beyond FoxO transcription factors, other crucial regulators of atrogenes expression are NF-kB, activated by cytokines, SMAD2 and SMAD3, triggered by myostatin, and glucocorticoid receptors [30]. Interestingly, although Atrogin-1 and MuRF1 are the best characterized E3 ubiquitin ligases, it has been demonstrated that also others ubiquitin ligases are involved in skeletal muscle, such as E3alpha-II, activated upon tumor necrosis factor a (TNFα) and interleukin-6 (IL-6) treatment [46], Mul1, inducing mitophagy during muscle wasting [47], and Musa1, inhibited by bone morphogenetic protein to induce muscle hypertrophy [48].

In conclusion, skeletal muscle mass is finely regulated by several different pathways, that own multiple cross-talks and feedback regulations, and the upregulation of a particular signaling leads to a net increase or decrease in muscle mass (Fig. 3, from [30]).

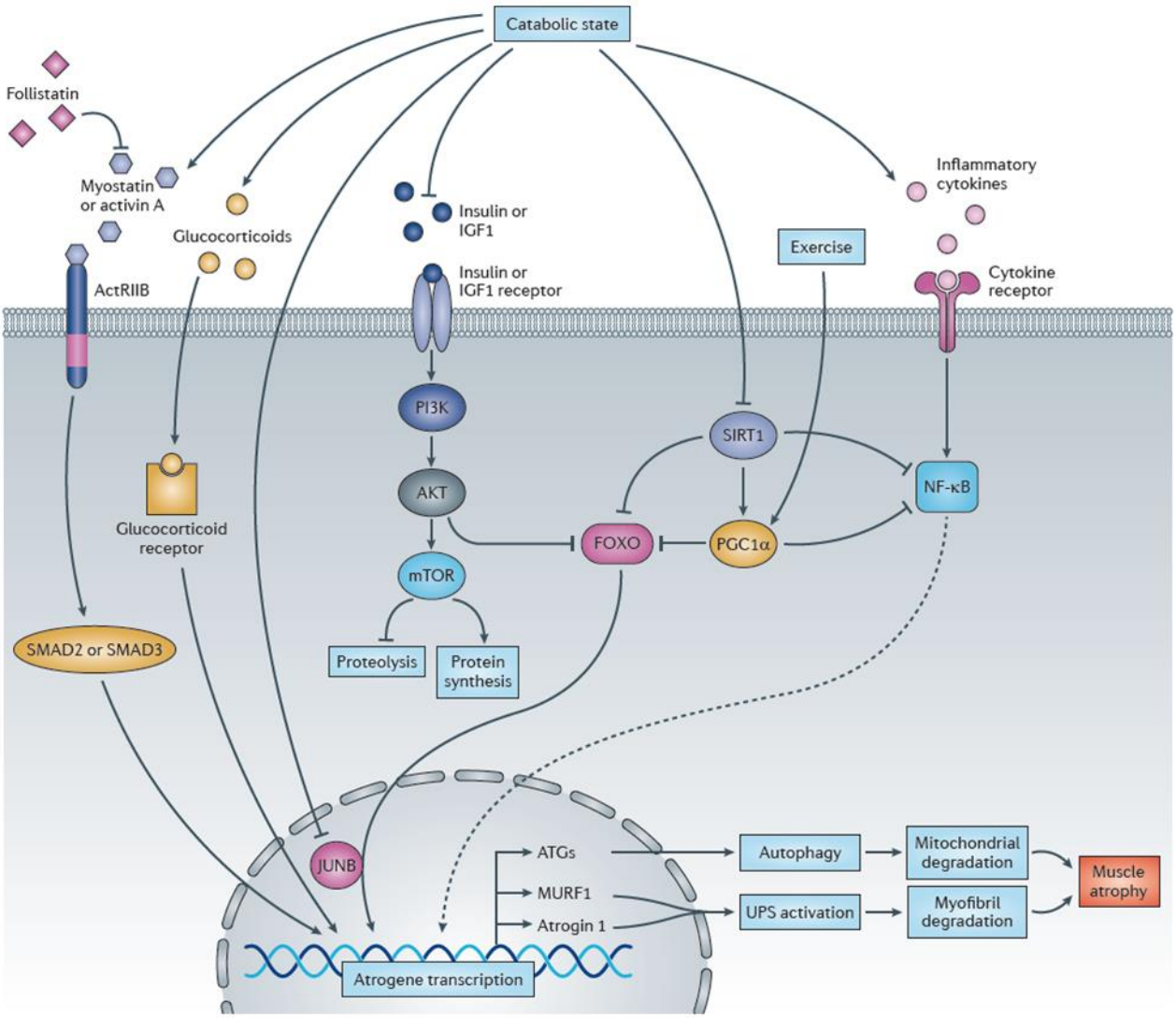

Figure 3: Signaling pathways leading to skeletal muscle atrophy [30]

Cancer cachexia

The term "cachexia" derives etymologically from the Greek *kakos* and *hexis*, meaning "bad condition". It is a multifactorial syndrome associated with several diseases, such as cancer, heart and renal failure, AIDS, and rheumatoid arthritis [49]. Development of cachexia reflects poor prognosis, and, despite the heterogeneity of the pathological causes of cachexia, there are two

major common factors: weight loss and inflammation [50]. Consistently, the only drugs currently utilized to counteract cachexia are glucocorticoids, to inhibit inflammation, and megestrol acetate, to stimulate appetite, although both become ineffective in the long term [50].

It has been reported that 30-80% of cancer patients develop cachexia, depending on tumor type, and in the 15% of cases the body weight loss is extremely severe, exceeding the 10% of initial body weight [51]. Cancer cachexia is characterized by a strong reduction of quality of life, related mainly to symptoms such as fatigue, weakness, asthenia, anaemia, anorexia, and psychosocial distress [50, 51], and leads to more than 20% of all cancer deaths via respiratory failure, cardiac failure, and metabolic derangement [49]. Despite several definitions of cancer cachexia, it has been recently achieved a consensus [52]: *"Cancer cachexia is defined as a multifactorial syndrome characterized by an ongoing loss of skeletal muscle mass (with or without loss of fat mass) that cannot be fully reversed by conventional nutritional support and leads to progressive functional impairment. The pathophysiology is characterized by a negative protein and energy balance driven by a variable combination of reduced food intake and abnormal metabolism"*. Clinically, progression of cachexia may be classified into three different stages, although not all cancer patients follow the entire process: precachexia, cachexia, and refractory cachexia [52]. Patients in the last stage, associated with very advanced or rapidly progressive cancer, show low performance status and a life expectancy of less than 3 months, without any possibility to manage weight loss [52].

It has been proposed that cancer cachexia may be considered as a state of "autocannibalism", in which tumor orchestrates a host response to obtain fuel for its growth, such as glucose, amino acids, and free fatty acids (Fig. 4, from [50]), or a generic host response to stress and injury leading to a "double-edged sword" [53]. Interestingly, tumors with the same origins and similar growth patterns may present or not cachexia [53], suggesting that little differences in genetic background strongly influence cachexia development. For example, cachexia prevalence in pancreatic and gastric cancer has been associated with single-nucleotide polymorphisms in the genes encoding IL-6, IL-1 and IL-10 [53]. Finally, also treatments such as surgery, chemotherapy, and radiotherapy contribute to cachexia, making cancer cachexia an extremely complex syndrome to understand and to counteract.

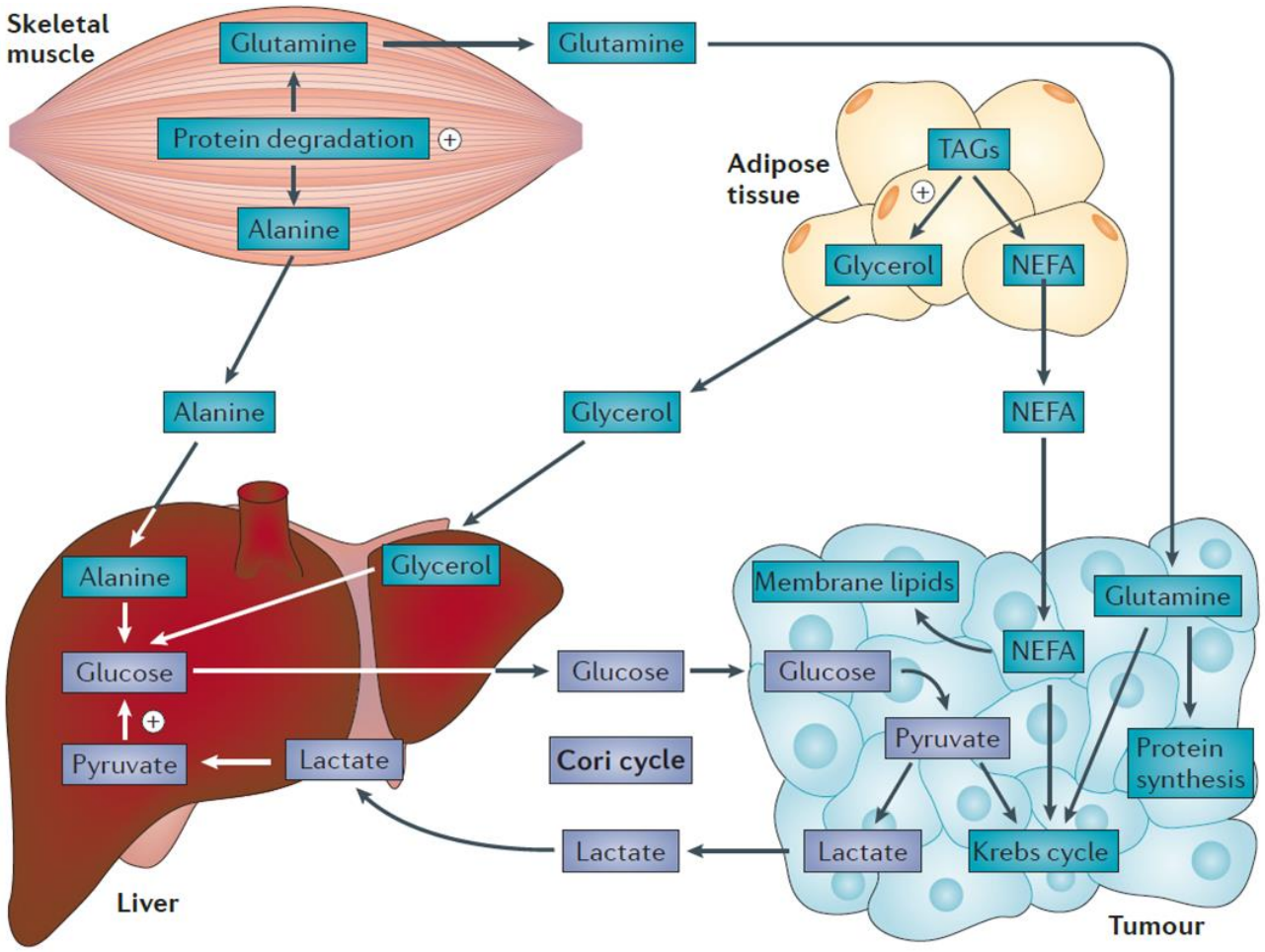

Figure 4: Metabolic response to tumor in cancer cachexia [50]

Tumor affects the functions of skeletal muscle, brain, liver, heart, gut, and adipose tissue, leading to the definition of cancer cachexia as a multi-organ syndrome (Fig. 5, from [50]). However, the critical issue is the loss of skeletal muscle mass, which contributes to more than 40% of body weight [50]. Hence, the main goal of current investigations are to counteract skeletal muscle wasting during cachexia.

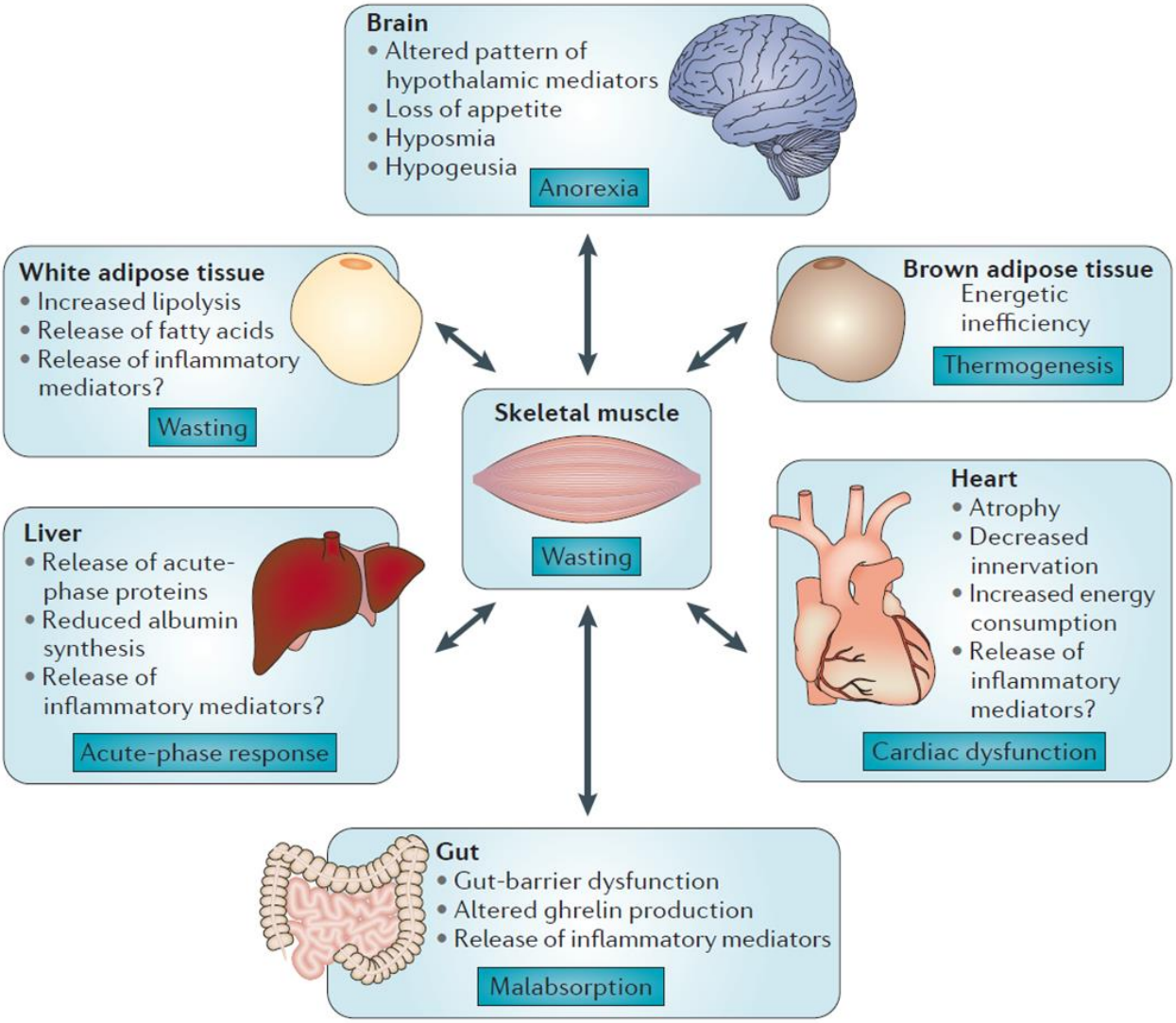

Figure 5: Multi-organ affection in cancer cachexia [50]

In cancer cachexia skeletal muscle is affected by multiple mechanisms. Indeed, the severe wasting is the result of an unbalance between anabolic and catabolic signaling, mainly due by a reduction a IGF-1/Akt signaling and by an up-regulation of UPS, although also autophagy plays a crucial role [54]. Moreover, in cancer cachexia there is a loss of dystrophin and nNOS, a dystrophin-associated complex member, destroying the membrane integrity, and thus inducing atrogenes activity [55, 56]. Interestingly, it has been reported that cancer cachexia is associated also with an impairment skeletal muscle regeneration [57-61]. In particular, cachectic serum induces a NF-kB-mediated

overexpression of myogenic Pax7 transcription factor [61], leading to a block of the differentiation process, as previously reported [62].

Skeletal muscle is affected by the tumor both directly, releasing pro-inflammatory cytokines and cachectic factors, and indirectly, inducing chronic inflammation and multi-organ response that leads to anorexia, hormonal deregulation, acute phase response, autonomic nervous system deregulation, and insulin resistance [51, 53]. Among the cachectic factors released by tumor, zinc-α2-glycoprotein (ZAG) and proteolysis-inducing factor (PIF) are the best characterized [51]:

- ZAG, or lipid mobilizing factor (LMF), induces lipolysis both directly, through cAMP-mediated activation of hormone-sensitive lipase (HSL), and indirectly, increasing the white adipose tissue (WAT) response to catecholamine [51, 63]. Moreover, LMF enhances lipid oxidation, likely through β3-AR-mediated increase in the expression of uncoupling protein 1 (UCP1) [51]. The UCPs dissipate mitochondrial proton gradient, thus decreasing ATP synthesis, and, among the three isoforms, UCP1 is expressed only in the brown adipose tissue (BAT), UCP2 is present in several tissues, and UCP3 is produced in BAT, heart, and skeletal muscle [64]. Besides UCP1, LMF/ZAG increases the expression of both UCP2, in skeletal muscle and tumor cells, and UCP3, in skeletal muscle [51]. Notably, it has been reported that LMF is detectable in serum cancer patients proportionally to weight loss extent [65]. Interestingly, LFM/ZAG, acting through β-ARs, stimulates protein synthesis and inhibits protein degradation in murine myotubes [66], that could account for the initial loss of fat, instead of skeletal muscle mass, in some cancer patients [63].

- PIF is a sulfated glycoprotein, that has been found excreted in urine proportionally to the extent of weight loss in cancer patients [51]. The intravenously injection of PIF in mice induces a severe and rapid loss of lean body mass, affecting neither food nor water intake [67, 68]. Consistently, PIF decreases protein synthesis and triggers protein degradation, increasing the expression of components of UPS, through NF-kB activation. The receptor activated by PIF has been found in skeletal muscle and in liver, but not in adipose tissue [69]. Importantly, PIF induces NF-kB- and STAT3-mediated expression of cytokines acting directly in the liver [70, 71], contributing to elevation of pro-inflammatory cytokines in cancer cachexia.

Besides ZAG and PIF, it has been recently demonstrated that tumor release parathyroid-hormone-related protein (PTHrP), which induces adipose tissue browning enhancing thermogenesis and energy dissipation [72]. The block of PTHrP with specific antibodies impairs adipose tissue browning and, importantly, skeletal muscle wasting [72]. However, authors claimed that PTHrP does not act alone in the induction of skeletal muscle wasting, suggesting the involvement of others tumor factors [72]. Indeed, besides PIF, tumor produces pro-inflammatory cytokines, such as TNFα, IL-6, IL-1β, and interferon gamma (IFNγ), that, together with cytokines released by the host, play a crucial role in the development of cachexia, although the dissection of the activities of each cytokine may be extremely difficult, due to the high redundancy between their activities.

- TNFα, or cachectin, inhibits differentiation of both adipocytes and skeletal myoblasts, and induces cachexia in mice [73-76]. In C2C12 myotubes, TNFα affects both canonical and alternative NF-kB pathways, chemokines network, Notch1 signaling, and proteasome pathway [77]. Specifically, TNFα triggers skeletal muscle atrophy, enhancing protein degradation [78-81], through ROS production and NF-kB-mediated increase of UPS components [82, 83]. Moreover, TNFα-activated NF-kB leads to MyoD downregulation, inhibiting myogenesis [74]. Moreover, TNFα induces insulin resistance in skeletal muscle through p38 activation [84]. In adipocytes, TNFα stimulates lipolysis likely through the MAPK- and NF-kB-mediated downregulation of PLIN, which is a barrier to lipolysis [85, 86]. However, in cancer patients the correlation between circulating TNFα levels and weight loss is questionable. Indeed, many studies failed to observe skeletal muscle wasting induced by TNFα, due to its several systemic effects, such as shock, anemia, and release of other pro-inflammatory cytokines [30]. It is possible that serum TNFα correlates better with the disease stage, reflecting tumor size, than with weight loss [51]. However, the relevance of TNFα in cancer patients is currently under investigation. Indeed, the inhibition of TNFα showed no benefit in patients [30]. It is possible that TNFα acts as a facilitator but it needs to synergize with other cachectic factors to induce atrophy, or that TNFα accounts only a subset of tumor types [53]. Indeed, TNFα activity on muscle cells *in vitro* depends on concentration and treatment duration [87-89].

- IL-6 levels, in contrast, correlates with weight loss and reduced survival of cancer patients [90-93]. Interestingly, TNFα promotes IL-6 secretion, and both synergize in several

activities [51]. IL-6 induces skeletal muscle wasting in several murine models of cancer cachexia, through induction of UPS and autophagy, and inhibition of mTORC1 pathway [95]. Moreover, IL-6 stimulates acute phase response (APR) [92, 95], and browning of WAT by increase UCP1 expression [96], while its role in lipid mobilization from adipose tissue is still debated [53]. Recently, based on encouraging results on animal models [97, 98], clinical trials revealed that the blockade of IL-6 pathway in cancer patients ameliorates some cachectic symptoms [95]. However, also IL-6 exerts different and contrasting roles, at least in skeletal muscle. Indeed, although IL-6 triggers severe muscle wasting in certain conditions, it is involved in myogenesis and skeletal muscle hypertrophy, and has beneficial effects on energy metabolism [99]. It is possible that detrimental effects of IL-6 rely on a persistent and systemic stimulation with this cytokine, and/or on a synergy of IL-6 with other factors [99].

Furthermore, other key mediators of skeletal muscle wasting in cancer cachexia are myostatin and activin A, both activating the activin receptor type II B (ActRIIB) [53]. Indeed, it has been demonstrated that the activity of this receptor increases in different tumors [100-103]. Myostatin induces skeletal muscle wasting and inhibits the expression of genes associated with muscle differentiation, such as MyoD and myogenin [19, 21]. Interestingly, the blockade of ActRIIB is one of the most promising therapeutic strategies for cancer cachexia. Indeed, ActRIIB antagonism effectively counteracts cancer cachexia and, importantly, improves survival [104]. In cancer cachexia also angiotensin II (ANGII) may contribute to skeletal muscle wasting. Indeed, it has been reported that infusion of ANGII results in a severe lean body mass depletion, together with an anorexigenic response [105]. ANGII both upregulates UPS activity and impairs muscle regeneration [106].

Furthermore, additional mechanisms, affected by inflammation and other factors, are involved in cancer cachexia, including anorexia, abnormal metabolism and energy expenditure, and elevated glucocorticoids [50, 51, 53].

- Anorexia is often associated with cancer cachexia, although it seems that there is no a cause-effect relationship between them [51]. Cancer cachexia and starvation differ for several aspects: for example non-muscle protein compartment is less affected during

cancer cachexia compared to starvation, and, importantly, wasting observed in cachexia cannot be reversed by nutritional supplementation [51]. Anorexia in cancer is likely a result of an unbalance between orexigenic and anorexigenic signals, accounted by different neuropeptides, in response to inflammatory cytokines, leptin and other mediators [107]. Hence, although non always present, anorexia is an important component of cancer cachexia, but it barely contributes directly to skeletal muscle wasting [51].

- Energy expenditure and hypermetabolism, associated with the presence of systemic inflammation and elevated adrenergic state [108, 109], significantly contribute to cancer cachexia [50, 53]. Indeed, patients on total parenteral nutrition still suffer of weight loss and other symptoms [110]. In cancer cachexia energy is dissipated by futile cycles, such as Cori cycle, and by thermogenesis due to upregulation of UCP proteins [50]. Moreover, skeletal muscle mitochondria are deregulated in cancer cachexia [111], in part due to the activation of PGC1α by TNFα-induced p38 activity. Indeed, it has been demonstrated that PGC1α increases expression of genes related to mitochondrial uncoupling, and thus energy expenditure [112]. Furthermore, PGC1α activates mitofusin 2 (MFN2) expression, that leads to Ca^{2+} deregulation, inducing muscle wasting. The energy expenditure in skeletal muscle may be associated also with metabolites generated by gut microbiota [113]. Finally, the synthesis of positive APR proteins by liver is not compensated by the downregulation of negative APR proteins, and this, during low food intake, leads to muscle mobilization and wasting [50]. Hence, the prolonged APR contributes significantly to the accelerated skeletal muscle mass loss [53].

- Similarly, a physiologic response to stress is the induction of glucocorticoids, but elevated or prolonged doses of glucocorticoids induce skeletal muscle wasting, upregulating Atrogin-1 and MuRF1 [114]. In this contest, it may be harmful the treatment of cachexia symptoms with glucocorticoids, to reduce inflammation and increase appetite [50, 51].

Furthermore, in cancer cachexia autonomic nervous system is deregulated, in particular the sympathetic branch, [115, 116], and gonadal function is impaired, leading to decrease in testosterone levels, negatively affecting skeletal muscle mass [107, 117]. A crucial role in cancer cachexia play also insulin-resistance, likely contributing to muscle wasting for the reduced anabolic

stimuli in response to meal [118, 119]. Finally, the two mainly affected tissues in cancer cachexia, skeletal muscle and adipose tissue, have a fine cross-talk mediated by myokines, adipokines, and free fatty acids [120]. Interestingly, it has been recently demonstrated that the genetic ablation of adipose triglyceride lipase impairs not only adipose tissue wasting, but also skeletal muscle degradation [121], and similar results were obtained with hormone-sensitive lipase null mice, although at lesser extent [121]. Although the factors mediating skeletal muscle and adipose tissue cross-talk have not been elucidated yet, several mechanisms have been proposed (Fig. 6, from [122]).

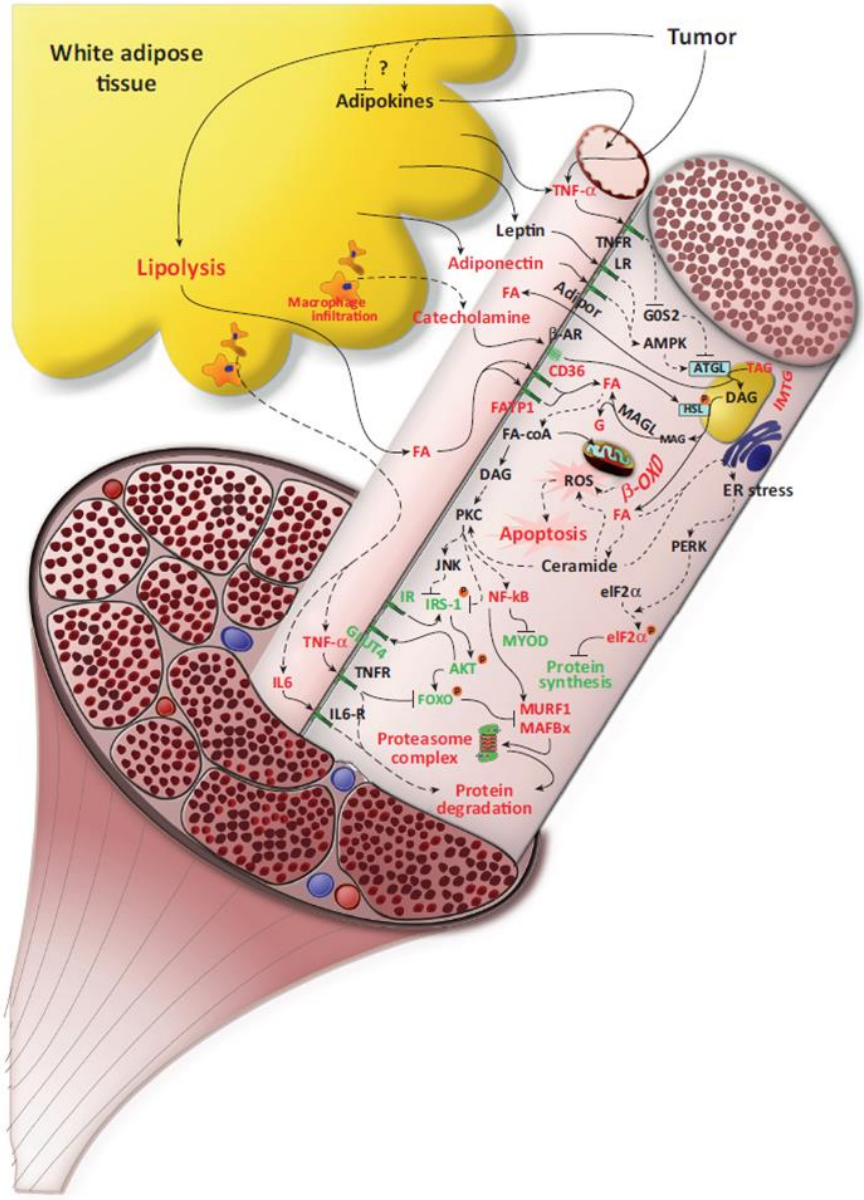

Figure 6: Cross-talk between WAT and skeletal muscle during cancer cachexia [122]

In conclusion, cancer cachexia is a highly complex and multifactorial syndrome, that needs to further investigations to better understand the molecular mechanisms underlying its pathogenesis. However, as discussed above, *"common themes emerge in terms of cytokine/neuroendocrine-driven changes in food intake, energy expenditure, adipocyte lipolysis, and altered hepatic and skeletal muscle protein synthesis/degradation"* [53]. It is likely that targeting one factor could be not efficacious in counteracting cancer cachexia, and a multi-target approach may be the correct path. Consistently, one promising approach appears to take advantage from the multiple functions of ghrelin hormone. Indeed, it has just concluded a Phase III clinical trial with anamorelin, a ghrelin analog, that revealed benefits in cachectic conditions of non-small-cell lung cancer (NSCLC) patients (ESMO 27/09/2014 Press Release: Anamorelin Shown to Improve Appetite and Body Mass in Patients with Cancer Anorexia-Cachexia).

Ghrelin

Acylated ghrelin (AG) is a circulating peptide hormone, released mainly from X/A-like stomach cells, discovered as the endogenous ligand of GHSR-1a, a G protein-coupled receptor known for its ability to induce growth hormone (GH)-release upon stimulation with synthetic compounds, named GH-secretagogues [123, 124]. As illustrated in Fig. 7 (from [125]), human ghrelin gene, *GHRL*, has two distinct transcriptional initiation sites, leading to transcript A and transcript B [126]. In humans, transcript A is the main form and encodes for the 117-aminoacid long preproghrelin [127]. Preproghrelin is cleaved into proghrelin (1-94) and 23-aminoacid long signal peptide by signal peptidase [128]. Proghrelin is further processed into mature ghrelin (1-28) by prohormone convertase 1/3 (PC1/3) [129]. The acylation with octanoic acid or, rarely, with decanoic or decenoic acids [128], seems to occur in the endoplasmic reticulum on the Ser3 of proghrelin peptide [130], and is mediated by the ghrelin *O*-acyl transferase (GOAT, a member of membrane-bound *O*-acyl transferases, MBOAT) [131, 132]. Interestingly, AG is the only known acylated peptide hormone [128]. Besides AG, also the unacylated form of ghrelin (UnAG) is released in circulation, and represents 90% of plasma ghrelin. Other peptides derives from ghrelin gene, by alternative splicing, although their function is largely unknown [133]. Notably, the C-terminal portion released from proghrelin cleavage is further processed into obestatin, a biological active

peptide originated by ghrelin gene. Obestatin was originally discovered as an antagonist of AG in the regulation of food intake through the activation of GPR39 orphan receptor [134], however the functions and receptor of obestatin are still controversial [135-138].

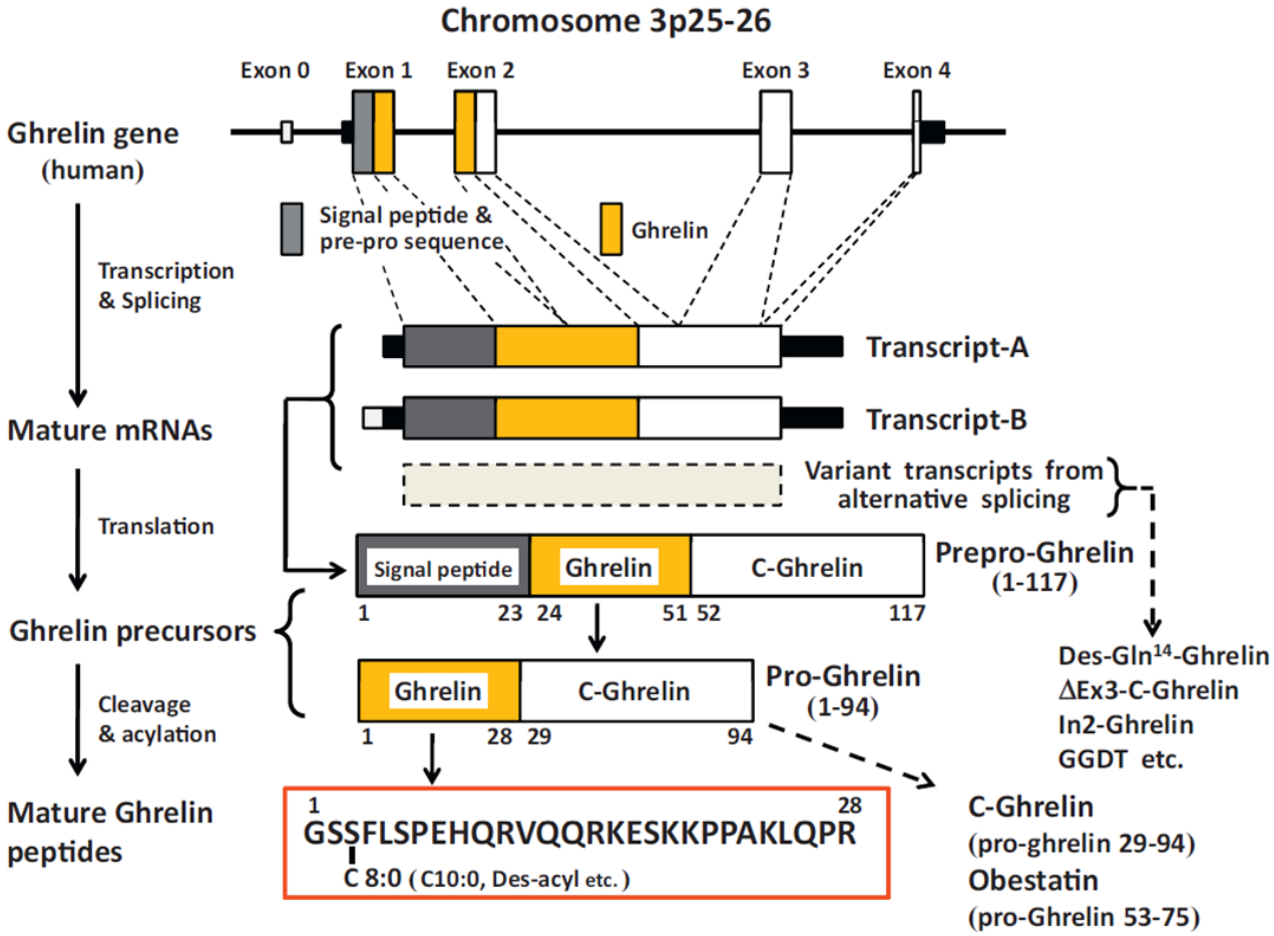

Figure 7: Structure of human *GHRL* gene and processing steps to mature ghrelin peptides [125]

The acylation of ghrelin is crucial for the binding to GHSR-1a [123], therefore GOAT is a crucial enzyme for AG activities. It has been reported that GOAT likely utilizes the most available fatty acid substrate for ghrelin acylation [138], and that the ingestion of medium-chain fatty acids or triglycerides enhances ghrelin acylation [139, 140]. Interestingly, GOAT mRNA is positively regulated by leptin administration, and the increase of GOAT expression in chronic restricted-nutritional conditions may account partially for the elevation of circulating AG [141, 142]. GOAT

knockout mice show different responses depending on the type of diet [128]. Hence, the regulation of ghrelin acylation by feeding behavior appears to be consistent to the stimulating activity of AG of food intake, adiposity and positive energy balance [143, 144]. Indeed, AG is the so called "hunger hormone", raising during fasting, and frequently deregulated in pathologies affecting body mass and/or body energy metabolism [145, 146]. However, the circulating peak of AG before meal may be an anticipation of eating, rather than a stimulation of feeding [147]. Indeed, it has been proposed that GOAT-ghrelin system is not only a feeding stimulus reflecting an empty stomach, but is a sensor that signals to the brain that nutrients are available [148]. Consistently, among other functions, AG induces GH-release and adiposity [123, 124, 143, 149], that are activities not suitable in fasting conditions [148]. Fasting affects differentially circulating AG and UnAG levels: although AG levels do not change, gastric GOAT decreases significantly, and UnAG circulating levels are strongly up-regulated [148]. Indeed, it has been reported that long-term fasting inhibits acylation, whereas it does not affect total secretion [150]. In contrast, feeding decreases secretion of both AG and UnAG [150]. These results suggest that secretion may be independent from acylation, which results from esterases activity, cleaving the acyl group, or by availability of nutrient [150]. Interestingly, it has been recently demonstrated that the GOAT and ghrelin gene are regulated by different transcriptional factors, enforcing the idea of a uncoupling between ghrelin expression and acylation [151].

AG is the only known peripheral peptide that acts centrally in the hypothalamus regulating food intake [128]. Notably, both *Ghsr* and *Ghrl* knockout mice show feeding behavior similar to WT mice [152, 153]. Besides the GH-releasing activity of AG, acting directly in the pituitary and hypothalamus [123, 124, 149], AG-GHSR-1a axis affects a plethora of other tissues and systems: stimulates prolactin (PRL) and proopiomelanocortin (POMC) secretion, affects gastric acid secretion and gastric emptying, exerts neuro- and cardio-protective actions, induces bone formation, controls female and male reproductive physiology, inhibits inflammation, and decreases insulin sensitivity [128, 133]. In the context of cancer cachexia, beside the activities on food intake, GH release, and energy balance, it is extremely relevant the strong anti-inflammatory properties exerted by in several conditions [154]. In particular, it has been shown that AG, through GHSR-1a, inhibits pro-inflammatory cytokines expression in T lymphocytes and monocytes, counteracting leptin actions [155, 156]. Moreover, AG is crucial in the maintenance of thymus functionality during aging [157], enforcing the concept that AG exerts key actions in immune system. Although the main source of ghrelin is the stomach, the ε-islets in the pancreas produce

and release ghrelin [158], In addition, also the α- and β-islets synthetize ghrelin [159-161], suggesting a key role of ghrelin in the regulation of endocrine pancreas. Indeed, AG inhibits insulin release in mice, rats and humans [133], and affects also glucagon synthesis and release [162]. Moreover, AG induces peripheral insulin resistance [163, 164], and insulin negatively affects ghrelin levels [165-168], although it has been published contrasting results [169-171]. Finally, AG stimulates glycogenolysis and gluconeogenesis, preventing the inhibitory effects of insulin on glucose production [172-174]. Notably, the ablation of either Ghrl, or Ghsr, or GOAT genes affects only marginally mice phenotype under standard diet, but induces important differences in regulation of body weight, adiposity and glucose levels during high-fat diet or calorie restriction [175, 176], suggesting that the major physiological role of ghrelin system may be the control of glucose and weight.

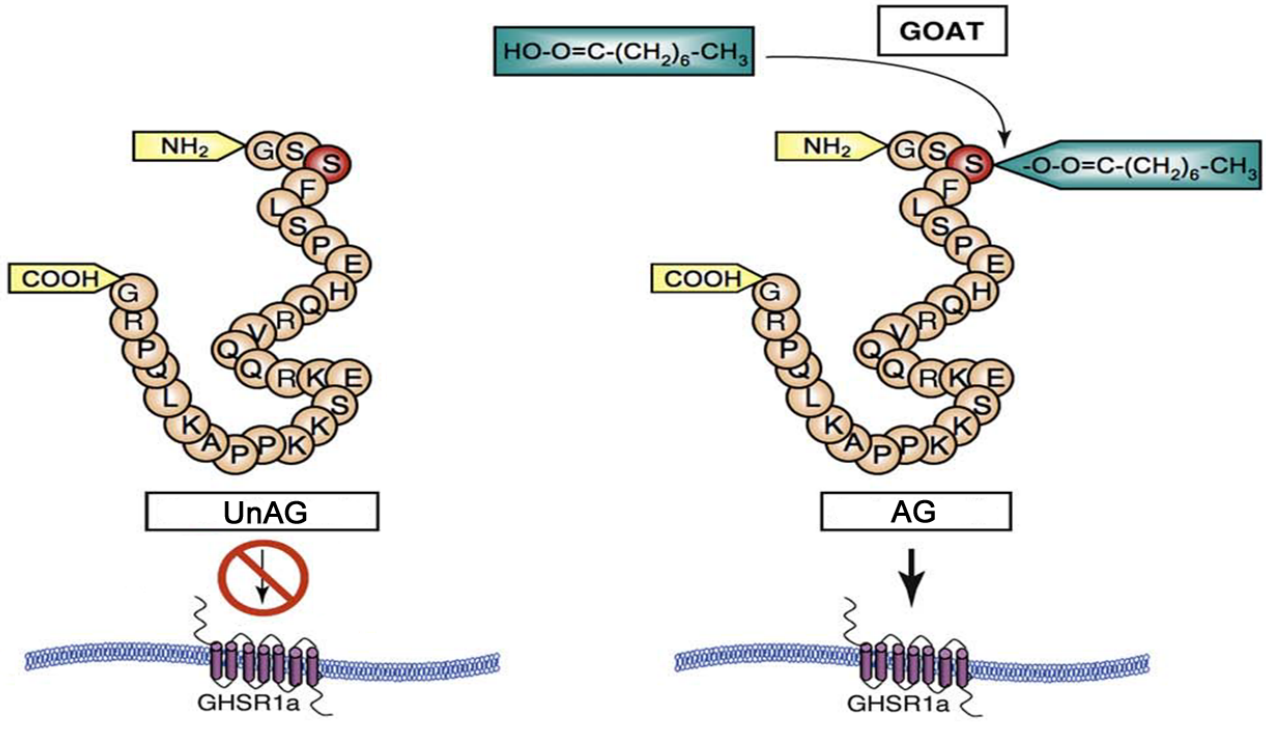

Figure 8: The acylation of ghrelin is necessary for the binding to GHSR1a (adapted from [179])

The unacylated form of ghrelin arises from the same AG precursor, but it lacks the fatty acid modification, making UnAG unable to activate GHSR-1a [123]. UnAG is far more abundant in plasma than AG, and, since it does not bind to GHSR-1a, and thus is devoid of any GH-releasing activity [177, 178], has been considered for many years the inactive product of ghrelin catabolism (Fig. 8, adapted from [179]). AG and UnAG relative levels are finely regulated by multiple mechanisms, such as GOAT activity and AG deacylation mediated by acyl-protein thioesterase 1/lysophospholipase I enzyme [180]. Moreover, it has been reported that in stomach mucosa the staining of AG and UnAG co-localizes in close-type round cells, whereas only UnAG is present in the open-type cells [181], suggesting that in the stomach different cell types are specialized in the production and release of AG and/or UnAG, pointing out a different biological significance of the two peptides. Indeed, several reports demonstrated that UnAG owns several biological activities, mediated by still unknown receptor(s). Besides the ability of UnAG to activate GHSR-1a in supra-physiological concentrations [177, 182, 183], UnAG shares with AG several activities also in cells lacking GHSR-1a [184-192], suggesting the existence of a common receptor, still unknown. Moreover, it has been demonstrated that UnAG negatively affects some AG actions both *in vitro* and *in vivo* [172, 193, 194], , or exerts own activities [195]. It has been reported that UnAG affects also food intake, in a mechanism likely independent from GHSR-1a [196-198]. UnAG shares with AG common binding sites on several cell types, regulating differentiation [189, 199-202], proliferation [186, 189, 190, 203-205], and anti-apoptotic/protective pathways [184, 190, 204, 206-209]. In contrast to AG, UnAG improves insulin sensitivity and inhibits the liver production of glucose [172, 210]. Interestingly, it has been observed in healthy human subjects that the injection of AG directly in skeletal muscle ameliorates insulin sensitivity, increasing glucose uptake [211]. Besides the interesting authors speculation about a second messenger affecting AG activity on glucose when it is injected systemically, their results suggest that the direct action of AG on skeletal muscle might be mediated by a still unidentified receptor. Indeed, it has been reported that skeletal muscle does not express GHSR-1a [212], which mediates the diabetogenic effects of systemically AG.

Since AG and UnAG activate the anti-atrophic PI3K/Akt pathway in several cell types [184, 186, 190, 204, 206], and it has been demonstrated that both peptides promote myoblast differentiation [189], in our laboratory raised the hypothesis that AG and UnAG could protect skeletal muscle from atrophy. Interestingly, in both human patients and experimental models, AG improves cachexia induced by several pathological conditions [213-220]. However, it reasonable

assume that anti-cachectic activity is mainly dependent on its GHSR-1a-mediated orexigenic, GH-secretagogue, and anti-inflammatory activities. However, we found that:

- in C2C12 myotubes, AG and UnAG inhibit dexamethasone-induced skeletal muscle atrophy through activation of a novel common receptor (herein referred as "GhrlR2"), triggering PI3Kβ/mTORC2 and p38 pathways, without stimulating mTORC1-mediated stimulation of S6K, protein synthesis, and hypertrophy, nor regulating myostatin expression;
- upregulation of circulating UnAG, obtained both in transgenic mice and by pharmacological treatment, impairs skeletal muscle atrophy induced by either fasting or denervation, without stimulating muscle hypertrophy, GHSR1-mediated activation of the GH/IGF-1 axis, and food intake;
- UnAG administration rapidly activates anti-atrophic signaling pathways in skeletal muscle;
- in GHSR1$^{-/-}$ mice, both AG and UnAG induce phosphorylation of Akt, FoxO3A and p38 in the skeletal muscle, and impair fasting-induced atrophy.

Hence, the anti-cachectic activities of AG may be attributable also to the direct protection of skeletal muscle in a GHSR-1a-independent manner, through a pathway not overlapping with IGF-1 (Fig. 9, from [221]). These data have been published in 2013 in the *Journal of Clinical Investigation* (Porporato, 2013), and are presented in the first part of the results of this thesis. For further details, refer to the paper in attachment.

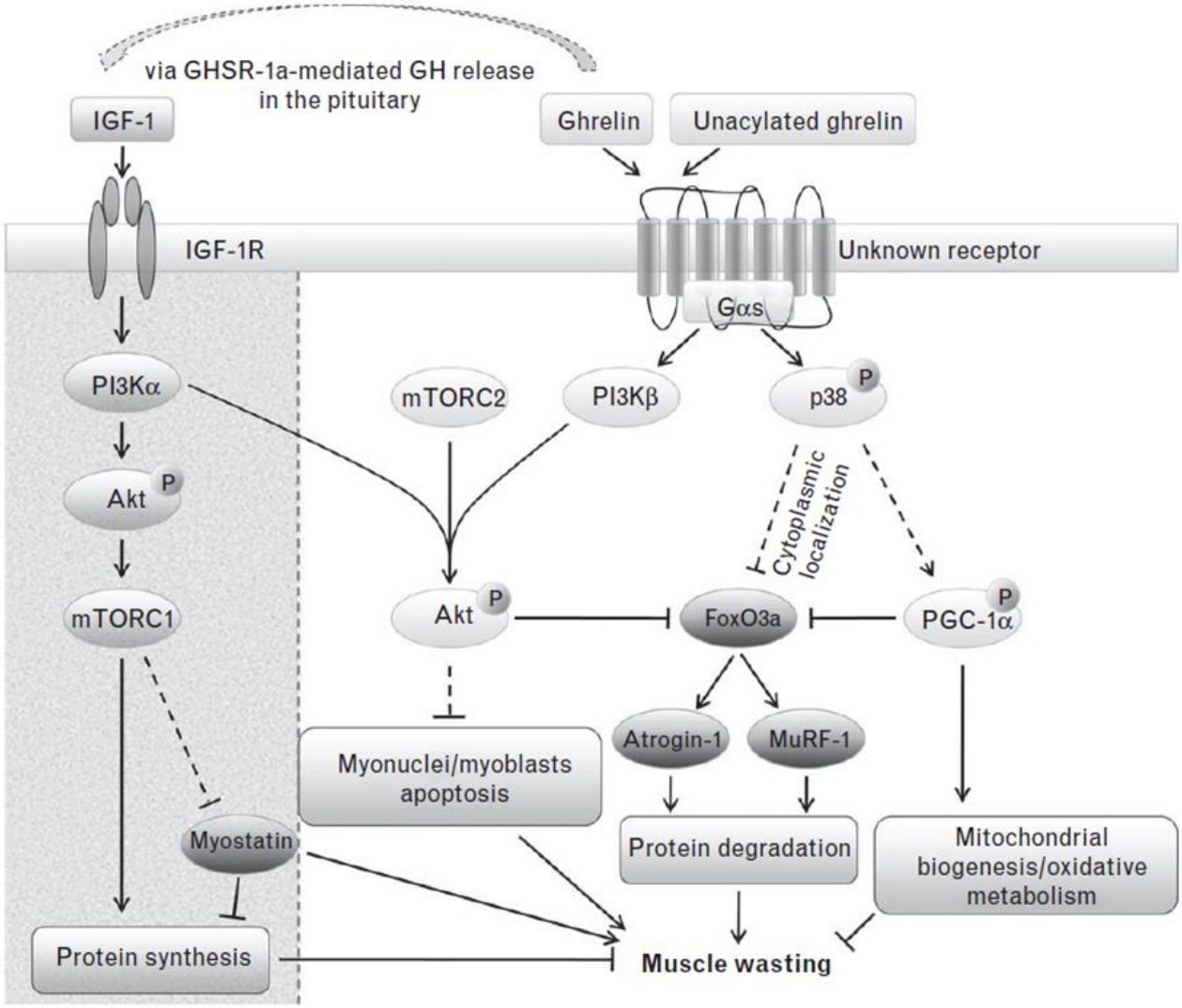

Figure 9: Anti-atrophic activities triggered by AG and UnAG in skeletal muscle, through GhrlR2 [221]

Furthermore, UnAG reduces burn-induced skeletal muscle proteolysis and local TNFα upregulation, and diminishes TNFα/IFNγ-induced cachexia in C2C12 myotubes [222]. Moreover, it has been reported that UnAG counteracts pro-inflammatory cytokines expression induced by insoluble fibrillary β-amyloid protein deposition in mice microglia [223], and that both AG and UnAG show anti-hyperalgesic and anti-inflammatory activities in rats [224]. Hence, although the role of UnAG on inflammation is not well investigated, these results suggest an inhibitory action of UnAG on inflammatory response. Thus, considering all these data, also UnAG may be take into account for cancer cachexia treatment [221]. Although UnAG lacks of orexigenic and GH-releasing

activity of AG, the clinical use of UnAG appears advantageous compared to AG, allowing directly skeletal muscle protection, without the diabetogenic side effects of AG and the potential cancer risk associated with IGF-1 treatment [210, 225].

In the second part of this thesis, we provide evidences of a ghrelin resistance thorugh the GhrlR2 in cancer cachexia. Indeed, although AG treatment counteracts cachexia both in humans and animals [213-220], its circulating concentration is upregulated in cachectic patients, independently from the underlying phatology [226-232], suggesting a compensative mechanism to a reduced AG response. Consistently, in cancer cachexia appetite does note correlate with AG levels [233], and only high dose of AG affects food intake in eicosanoid-related cachexia [234]. Moreover, heart failure-associated cachexia display ghrelin resistance, which is reverted upon heart transplantation in a small group of patients [235]. These findings, along with our demonstration that both AG and UnAG prevent protein degradation through GhrlR2, suggest that the establishment of a resistance to AG/UnAG activities may contribute to the development of cancer-induced muscle wasting.

Since our data support that GhrlR2 is a G protein-coupled receptor (GPCR) activating adenylate cyclase, we hypothesize that AG and UnAG signaling in the skeletal muscle might be desensitized through a mechanism dependent on the phosphoinositide 3-kinase gamma (PI3Kγ), as reported for β-adrenergic receptors [236].

Phosphoinositide 3-kinase gamma (PI3Kγ)

Phosphoinositide 3-kinases (PI3Ks) are enzymes that catalyze the conversion of PtdIns(4,5)P2 to PtdIns(3,4,5)P3 in response to several stimuli. Based on biochemical and structure characteristics, PI3Ks are subdivided into three classes: PI3Ks regulated by receptors belong into class I, PI3K-C2 kinases into class II, and the PtdIns-specific enzyme Vps34 into class III [237]. Class I members are characterized by the association of a catalytic subunit (p110α, p110β, p110γ, p110δ) with a regulatory subunit (5 distinct p85 isoforms, p101, and p84/87). All the p85 isoforms have a Src-homology 2 (SH2) domain, binding to phosphotyrosines, and associate with p110α, p110β and p110δ. In contrast, p110γ associates with either p101 or p84/87 regulatory subunits, both lacking SH2 domain. For these reasons, class I is further divided into class IA (PI3Kα, PI3Kβ, PI3Kδ), downstream Tyr-kinase receptors (RTKs), and class IB (PI3Kγ), downstream GPCRs [238, 239].

However, it has been demonstrated that PI3Kβ is mainly activated upon GPCR-stimulation [240], and it is redundant with PI3Kγ that, in turn, can be signal downstream also RTKs [241]. Currently, PI3Kα and PI3Kδ are considered the main isoforms activated by RTKs, while PI3Kβ and PI3Kγ by GPCRs, despite a certain grade of promiscuity [237, 238, 241], as illustrated in Fig. 9, from [238]).

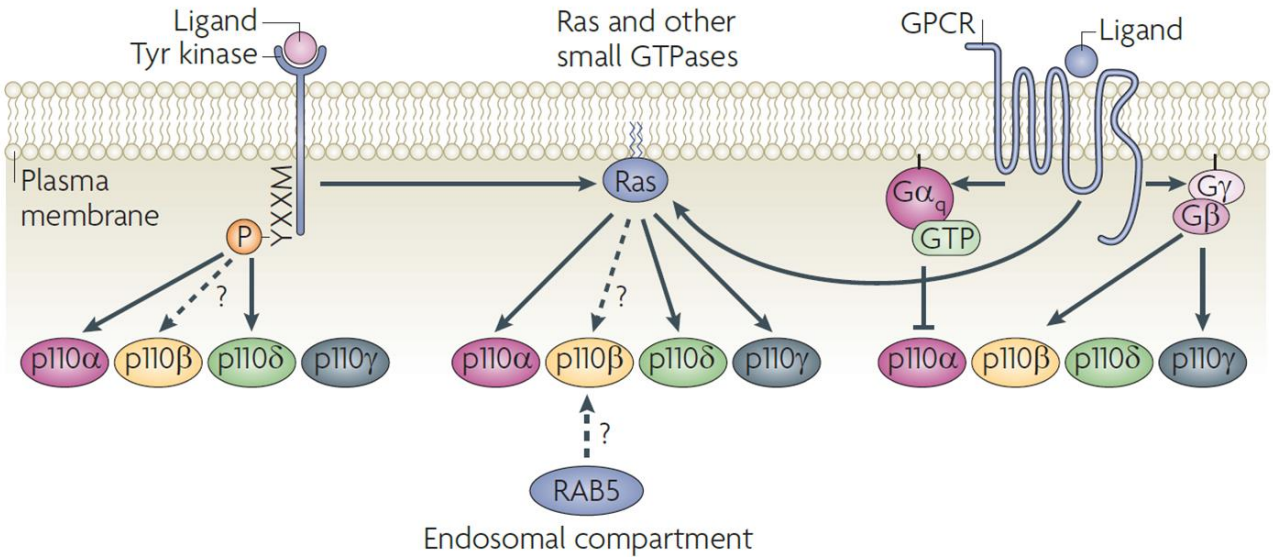

Figure 10: Upstream signals regulating Class I PI3Ks [238]

PI3Kβ and PI3Kγ isoforms are heterodimers with distinct regulatory subunits, p85 and p101/p87, respectively, and both are activated by GPCRs. However, their role in GPCR signaling appears to be distinct, at least when PI3Kγ is not greatly expressed, regulating reciprocally the downstream signaling upon ligand stimulation. Although PI3Kβ is ubiquitously expressed, PI3Kγ is the main isoform in white blood cells [239]. Consistently, PI3Kγ null mice show clear defects when immune system is stressed [242-244]. PI3Kγ regulates several pathways, such as Akt, JNK, Ras, and MAPK [245-247], and controls β-AR resensitization and internalization after stimulation [248-251]. Interestingly, PI3Kγ kinase-dependent and -independent actions are involved in the pathologic response to heart failure [252]. In the healthy heart, the role of PI3Kγ remains negligible given its low expression level and its rapid inhibition after receptor stimulation. Conversely, PI3Kβ is the major PI3K accountable for PIP3-mediated Akt activation in response to β-AR stimulation. However, in stress conditions, such as hypertension and pressure overload, PI3Kγ exerts a

detrimental response to cardiac stress [253]. Indeed, it has been shown that the PI3Kγ regulatory subunit p84/87 physiologically acts as a scaffolding protein by supporting a macromolecular complex that includes p110γ, protein kinase A (PKA) and cAMP-phosphodiesterases (PDEs). PI3Kγ is necessary to coordinate PDE activity by allowing to the active PKA to phosphorylate PDE3B. Moreover, p110γ is inhibited by PKA-induced phosphorylation, leading to a negative feedback after β-AR stimulation, to restore receptor density at the plasma membrane [236]. However, p110γ can escape from PKA-mediated inhibition through the association with p101, the second regulatory subunit of PI3Kγ, which is unable to associate with PKA [236]. These mechanisms have been clearly shown in the myocardial response to heart failure [236]. During heart failure, an upregulation of p101 expression instead of p84/87 leads to an increased PI3Kγ activity, resulting in a strong desensitization and downregulation of β-ARs at the plasma membrane [236]. In this context, pharmacological inhibition of PI3Kγ kinase activity restores β-AR density in heart failure, improving compromised cardiac contractility [236].

In conclusion, the mutual role of PI3Kβ and PI3Kγ in β-AR signaling may be a model for other receptors similar to β-AR, likely other $G\alpha_s$-coupled receptors, in several tissue distinct to immune compartment, where PI3Kγ is not the main isoform accountable for Akt activation. Consistently, since PI3Kγ is upregulated by stress and inflammatory cytokines, such as IL-6, TNFα, IFNγ, and IL-1 [239], we hypothesized that a sustained increase of PI3Kγ activity in cachectic muscles leads to a downregulation of GhrlR2, impairing ghrelin responiveness, as demonstated for β-AR in heart failure (Fig. 11, adapted from [236]).

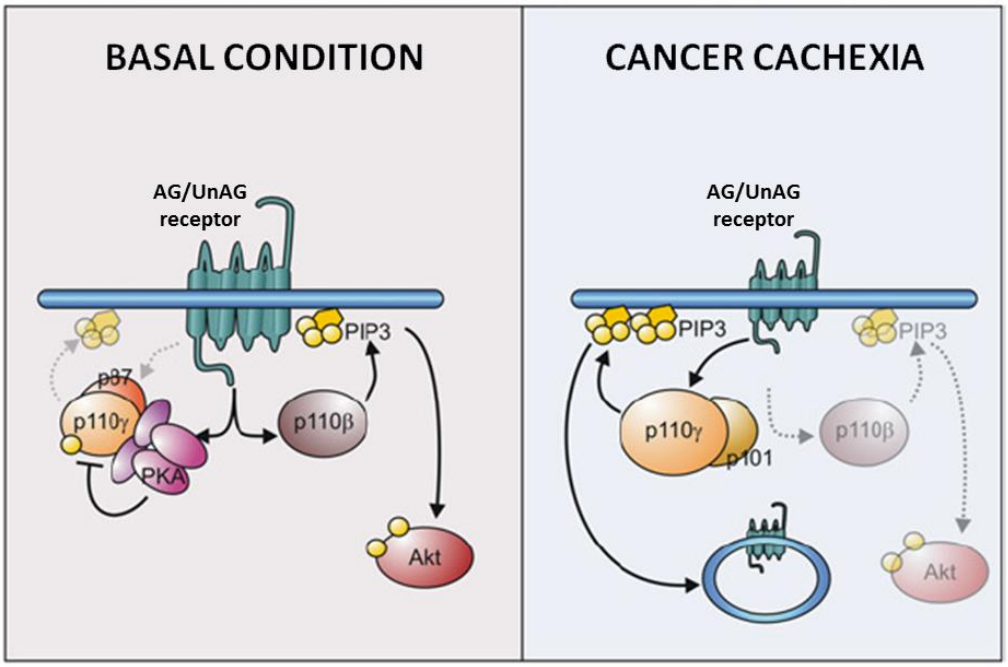

Figure 11: Model of p110γ/p101-mediated ghrelin resistance (adapted from [236])

MATERIALS AND METHODS

Reagents

AG-(1-28) and UnAG-(1-28) were purchased from PolyPeptide Laboratories. PIK-75 hydrochloride, inhibitor of PI3Kα, was purchased from Axon Medchem; TGX-221, PI3Kβ inhibitor was a kind gift from Dr. Ubaldina Galli (Synthetic Medicinal Chemistry group, Università del Piemonte Orientale, Novara, Italy); AS605240 and H89, PI3Kγ and PKA inhibitor, respectively, were a kind gift from Prof. Emilio Hirsch (Università di Torino, Italy). Water-soluble dexamethasone, as well as other reagents, was from Sigma-Aldrich, unless otherwise stated. Anti-phospho-Akt^{S473}, anti-phospho-S6K^{T389}, anti-phospho-S6$^{S235/236}$ were from Cell Signaling Technology; anti-actin and anti-GAPDH antibodies were from Santa Cruz Biotechnology.

Mice

All experiments were conducted on young adult (8-10 weeks) male C57BL/6J WT, PI3Kγ$^{KD/KD}$, *Myh6/Ghrl*, Ghsr$^{-/-}$, and Ghrl$^{-/-}$ mice, matched for age and weight. Mice were handled following the OACU-ARAC guidelines (NIH, Office of Animal Care and Use). All animal manipulations were done under anesthesia with sevoflurane (Baxter).

Cachexia was induced by subcutaneous injection of 5*10^6 LLC cells suspended in PBS [72, 254]. Mice and food intake were daily monitored, and the animals were euthanatized after 23-24 days from tumor cells injection [72]. The denervation-induced muscle atrophy was obtained by resection of the sciatic nerve of one hindlimb (Porporato, 2013), and evaluated 7 days later. Fasting-induced atrophy was achieved by 48-hour of food removal [255].

Skeletal muscle force was assessed using the BS-GRIP Grip Meter (2Biological Instruments). Each animal was tested 5 times, and the average value of the maximum weight that the animal managed to hold was recorded and normalized to the mouse's weight.

Blood was collected from retro-orbital sinus/plexus, in presence of EDTA (1 mM final concentration) and p-hydroxymercuribenzoic acid (1 mM final concentration) to prevent ghrelin degradation by proteases, and centrifuged at 3,500 rpm for 10 min at 4°C. Supernatant was split for UnAG and AG quantification. HCl was added to AG samples (0.1 N final concentration), that were then centrifuged at 3,500 rpm for 5 min at 4°C. Supernatant was then transferred in a new tube. Plasma sample was stored at -80°C prior to be assayed.

Cell cultures and myotubes analysis

C2C12 myotubes are a widely used model to study skeletal muscle wasting *in vitro* [40, 42, 45, 222, 256-258]. C2C12 myoblasts were maintained in Growth Medium (GM, DMEM 20% FBS) and differentiated in myotubes as previously described [189]. C2C12 myoblasts were transfected with Lipofectamine2000 (Life Technologies), according to the manufacturer's protocol. To induce muscle wasting, C2C12 myotubes were treated for 24h in differentiation medium (DM, DMEM 2% horse serum), in the presence or absence of 10 nM AG or UnAG [189], or 10 ng/ml IGF-1, with: 1 μM dexamethasone [40, 42, 45, 256]; 5 or 10 ng/ml each TNFα and IFNγ combination [222, 257]; 20 or 100 ng/ml IL-6 [95, 98, 259]. For myotubes diameter measurement, myotubes were fixed with acetone:methanol (1:1) and diameters were quantified by measuring a total of about 80 diameters from seven random fields in 3 replicates at 20X magnification using Image-Pro Plus software (MediaCybernetics).

C26 adenocarcinoma cells were grown in DMEM 5% FBS, and Lewis lung carcinoma (LLC) cells were maintained in DMEM 10% FBS [72, 258].

Muscle sampling and staining for fiber size assessment

Collected muscles were frozen in liquid nitrogen-cooled isopentane. Serial transverse cryosections (7 μm thick) of the midbelly region of muscles were cut at –20°C and mounted on glass slides (Super Frost ultra plus, Bio-optica). The sections were fixed for 10 min in 4% paraformaldehyde at 4°C, permeabilized with PBS 0.1% BSA-0.2% Triton X-100 for 15 min, and incubated with anti-laminin polyclonal antibody (Dako) for 90 min at room temperature. Therefore, sections were incubated for 1 h with anti-rabbit secondary antibody (Alexa Fluor 488 anti-rabbit IgG) at room

temperature. Images of whole muscles were acquired with Pannoramic Digital Slide Scanners (3DHISTECH), and fibers minimal Feret's diameter [260] were measured automatically with ImageProPlus (Media Cybernetics). Data are expressed as frequency distribution of myofibers diameter.

Conditioned medium (CM) preparation

For CCM and LCM collection, from C26 and LLC cells supernatant, respectively, cells were seeded at a density of $5*10^5$ cells/cm^2 and, after overnight attachment, were washed three times with PBS, followed by two washes with serum-free DMEM, and grown in serum-free DMEM for 24h. The resulting CCM/LCM was centrifuged at 500 g for 10 min, followed by an additional centrifugation at 5,000 g for 10 min. The CCM/LCM was filtered using a 0.2 µm syringe filter and either stored at -80°C or used immediately [258].

RNA extraction and analysis

Total RNA from cultured myotubes or frozen muscles was extracted with TRIreagent (Life Technologies). RNA was retro-transcribed with High Capacity cDNA Reverse Transcription Kit (Life Technologies) and real-time PCR was performed with the ABI7200 Sequence Detection System (Life Technologies) using the following assays: Mm00499518_m1 (*Fbxo32*, Atrogin-1/MAFbx), Mm01185221_m1 (*Trim63*, MuRF1), Mm004450358_m1 (*Pik3cg*, p110γ catalytic subunit), Mm00805205_m1 (*Pik3r5*, p101 regulatory subunit), Mm01335671_m1 (*Pik3r6*, p84/87 regulatory subunit), Mm00446953_m1 (*Gusb*), Mm00506384_m1 (Ppif), Mm01205647_g1 (*Actb*, β-actin).

Western Blot

C2C12 myotubes were serum-deprived overnight and then treated as indicated. Cells were washed with PBS 1X containing 1 mM Na_3VO_4, and then homogenized in RIPA buffer (1% Triton X-100, 1% sodium-deoxycholate, 0.1% SDS, 1 mM EDTA, 1 mM EGTA, 59 mM NaF, 160 mM NaCl and 20 mM Tris-HCl pH 7.4) containing 1 mM DTT, Protease Inhibitors Cocktail, and 1 mM Na_3VO_4. The homogenates were centrifuged at 14,000 g for 15 min to remove the debris and nuclei. The

supernatant were mixed with SDS loading buffer 3X (187.5 mM Tris-HCl pH 6.8, 6% w/v SDS, 30% glycerol and 0.03% w/v bromophenol blue) and boiled at 95°C for 5 min. The electrophoresis was performed with 8-10% polyacrylamide gel (Sigma Aldrich), and then the proteins were transferred on PVDF membranes (Hybond-P, GE Healthcare). After 1-hour of saturation in 3% BSA at room temperature, the membranes were incubated with primary antibody overnight at 4°C, and then with secondary antibody for 1h at room temperature. Finally, the membranes were visualized with Western Lightning Chemiluminescence Reagent Plus (PerkinElmer Life Sciences) and analyzed with Quantity One software (Bio-Rad).

Intracellular cAMP measurement

C2C12 myotubes were serum-deprived for 18h, and then treated for 5 min with 1 μM AG and UnAG in the presence of 100 μM IBMX (3-Isobutyl-1-methylxanthine, phosphodiesterase inhibitor). 1 μM CGS, agonist of adenosine receptor A2A, was used as positive control. Assay was performed following the producer's protocol (Cayman Chemical).

Ghrelin ELISA

Plasma AG and UnAG levels was measured by EIA kits (SPIbio Bertin Pharma), according to the manufacturer's instructions.

Statistical analysis

Data are presented as the mean ± SEM, or box and whiskers plots showing median (black line) and Min and Max (whiskers). The variation among groups was evaluated using Wilcoxon and Mann-Whitney U tests. Statistical significance was assumed for $P < 0.05$.

For further details about results published in Porporato, 2013, refer to the attached paper.

RESULTS

AG and UnAG counteract skeletal muscle atrophy *in vitro* in a PI3Kβ/mTORC2-, p38-, and cAMP/PKA-dependent manner

In our lab it has been demonstrated that AG and UnAG inhibit apoptotis in cardiomyocytes and promote myoblasts differentiation, by activating a novel receptor distinct from GHSR-1a [184, 189]. Moreover, in several cell types AG and UnAG trigger PI3K/Akt pathway [184, 190, 204, 206], that is the major hypertrophic and anti/atrophic signaling in skeletal muscle. Hence, we decided to test the hypothesis that both peptides may counteract skeletal muscle atrophy. After 24-hour treatment of C2C12 myotubes with the synthetic glucocorticoid dexamethasone, a widely adopted model to assay atrophy *in vitro*, we measured myotubes diameter, and Atrogin-1 and MuRF1 expression [40, 42, 45, 256]. We demonstrated that AG and UnAG counteract dexamethasone-induced atrophy, without inducing hypertrophy, in contrast to IGF-1 (Fig. 12, A-C). Moreover, both wortmannin (W) and rapamycin (R) blunt AG and UnAG activities, suggesting the involvement of the PI3K/mTOR pathway (Fig. 12D). Rapamycin is an inhibitor of mTOR complex 1 (mTORC1), which leads to protein synthesis stimulation, but upon long treatment also of mTOR complex 2 (mTORC2), which inhibits protein degradation [261-263]. Indeed, we showed that both peptides increase Akt^{S473} and $FoxO3a^{T32}$ phosphorylation, markers of mTORC2 activity, while do not induce, in contrast to IGF-1, mTORC1-associated $S6K^{T389}$ and $S6^{S235/236}$ phosphorylation, and leucine incorporation (Fig. 12, E-I). Accordingly, the knockdown of raptor and rictor, the specific components of mTORC1 and mTORC2, respectively, differently affects AG/UnAG and IGF-1 anti-atrophic activity: the silencing of raptor impairs IGF-1 action, while does not affect that of AG and UnAG; conversely, the knockdown of rictor blunts AG and UnAG activity, affecting to a lesser extent that of IGF-1 (Fig. 1, J and K). These data demonstrate that AG and UnAG activate selectively mTORC2 pathway, leading to inhibition of protein degradation, without stimulation of mTORC1 and protein synthesis.

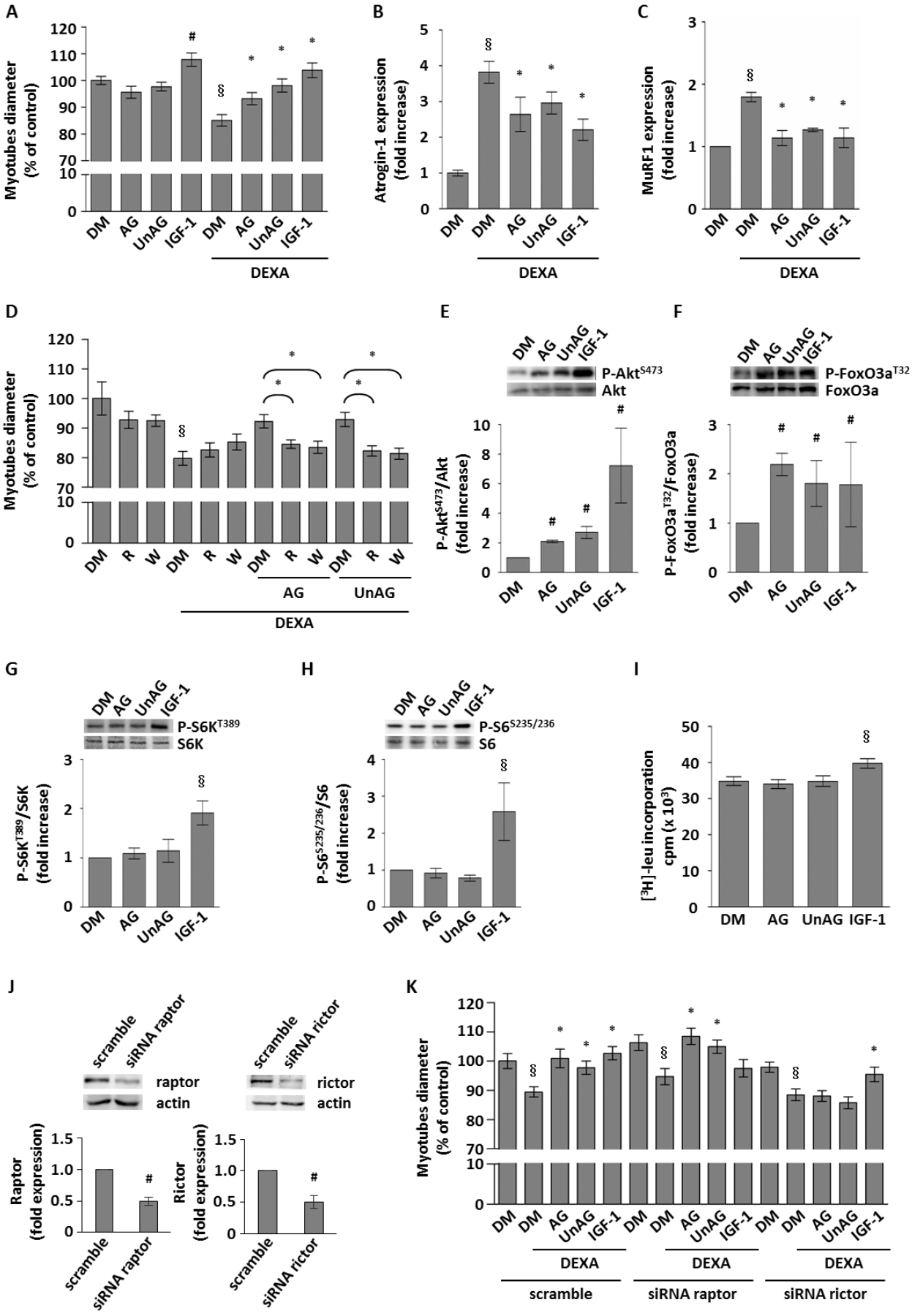
A
Myotubes diameter (% of control)
DM AG UnAG IGF-1 DM AG UnAG IGF-1
DEXA
B
Atrogin-1 expression (fold increase)
DM DM AG UnAG IGF-1
DEXA
C
MuRF1 expression (fold increase)
DM DM AG UnAG IGF-1
DEXA
D
Myotubes diameter (% of control)
DM R W DM R W DM R W DM R W
AG UnAG
DEXA
E
DM AG UnAG IGF-1
P-Akt S473
Akt
P-Akt S473/Akt (fold increase)
DM AG UnAG IGF-1
F
DM AG UnAG IGF-1
P-FoxO3a T32
FoxO3a
P-FoxO3a T32/FoxO3a (fold increase)
DM AG UnAG IGF-1
G
DM AG UnAG IGF-1
P-S6K T389
S6K
P-S6K T389/S6K (fold increase)
DM AG UnAG IGF-1
H
DM AG UnAG IGF-1
P-S6 S235/236
S6
P-S6 S235/236/S6 (fold increase)
DM AG UnAG IGF-1
I
[3H]-leu incorporation cpm (x 10³)
DM AG UnAG IGF-1
J
scramble siRNA raptor
raptor
actin
scramble siRNA rictor
rictor
actin
Raptor (fold expression)
scramble siRNA raptor
Rictor (fold expression)
scramble siRNA rictor
K
Myotubes diameter (% of control)
DM DM AG UnAG IGF-1 DM DM AG UnAG IGF-1 DM DM AG UnAG IGF-1
DEXA DEXA DEXA
scramble siRNA raptor siRNA rictor

Figure 12 (from Porporato, 2013): AG and UnAG protect C2C12 myotubes from dexamethasone-induced atrophy without induction of protein synthesis or hypertrophy. (**A**) Myotubes diameter was measured after 24-hour treatment in differentiation medium (DM) with 10 nM AG, 10 nM UnAG, and/or 1 μM dexamethasone (DEXA). In every experiments, 10 ng/ml IGF-1 was used as positive control for anti-atrophic/hypertrophic activity. (**B** and **C**) Atrogin-1 and MuRF1 expression analysis upon 24-hour treatment of 1 μM dexamethasone with or without 10 nM AG or 10 nM UnAG, determined by real-time RT-PCR. (**D**) Treatment with 100 nM wortmannin (W) or 20 ng/ml rapamycin (R) reverts the anti-atrophic activity of AG and UnAG on myotubes diameter. Control myotubes in differentiation medium were treated with DMSO, a vehicle for both wortmannin and rapamycin. (**E** and **F**) Phosphorylation of Akt^{S473} and $FoxO3a^{T32}$, detected by Western blotting, upon treatment for 20 min with 1 μM AG or UnAG. Shown are representative blots and quantification of 3 independent experiments. (**G**-**I**) IGF-1, but not AG and UnAG, induces protein synthesis, as determined by phosphorylation of $S6K^{T389}$ (**G**) or $S6^{S235/236}$ (**H**), and by incorporation of [^{3}H]-leucine (**I**). (**J**) Effect of raptor and rictor silencing on protein levels, detected by Western blotting. (**K**) Silencing of rictor, but not of raptor, reverts the anti-atrophic activity of AG and UnAG on the diameter of myotubes treated as in A. #$P < 0.05$, §$P < 0.01$ vs. DM control; *$P < 0.01$ vs. DEXA treatment.

Furthermore, it has been demonstrated that AG and UnAG activate p38 in C2C12 myoblasts [189], and that p38 can variably modulate Atrogin-1 expression in different conditions [78, 264-266]. We observed that AG and UnAG induce $p38^{T180/Y182}$ phosphorylation in C2C12 myotubes, and that p38 inhibition with SB203580 blunts the anti-atrophic effects of both peptides (Fig. 13, A-D).

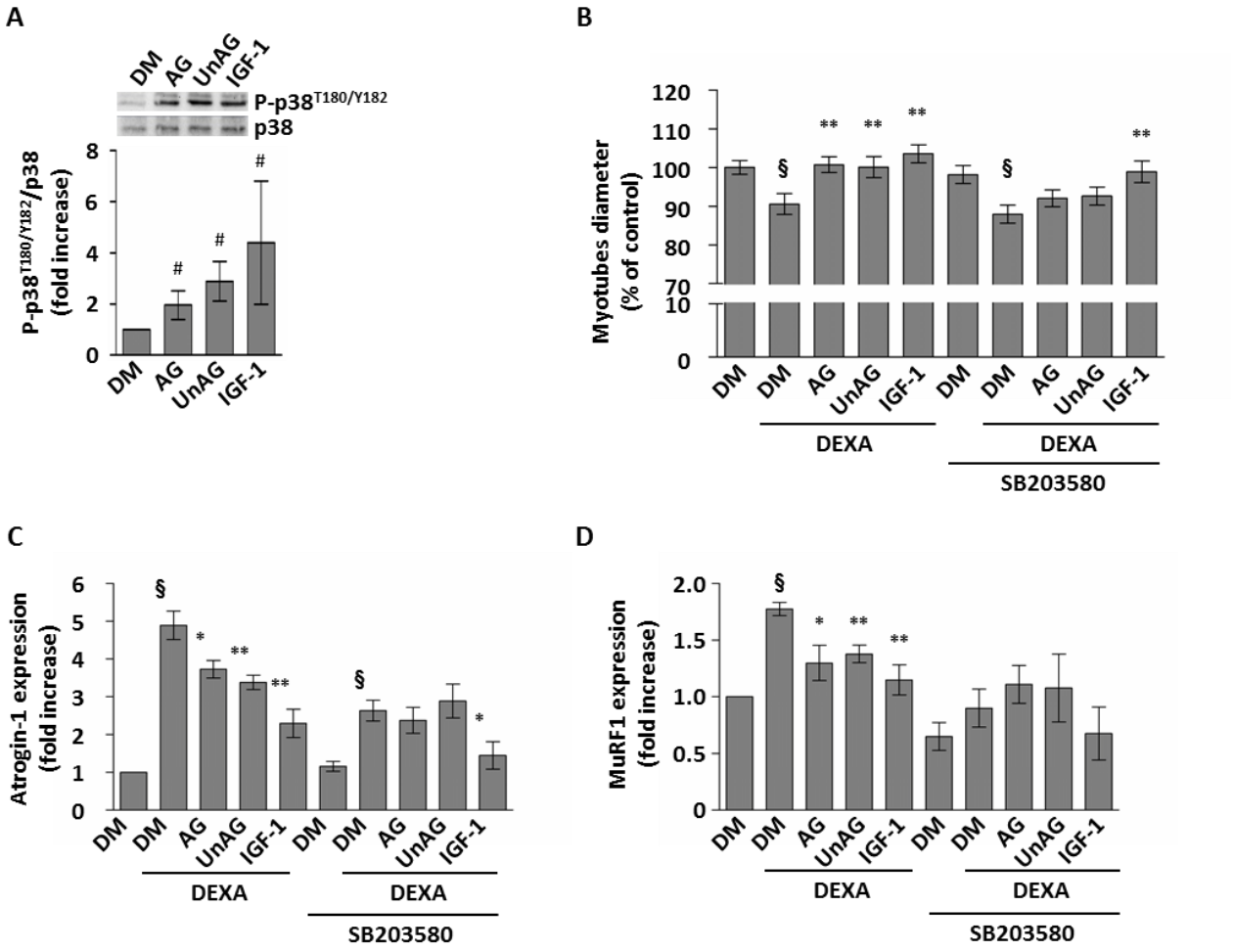

Figure 13 (from Porporato, 2013): AG and UnAG anti-atrophic signaling is mediated by p38. (**A**) Phosphorylation of $p38^{T180/Y182}$, detected by Western blotting, after 20-min treatment with 1 μM AG or UnAG. Shown are representative blots and quantification of 3 independent experiments. (**B**) Treatment with the p38 inhibitor SB203580 (5 μM) reverts the anti-atrophic activity of AG and UnAG on myotube diameter upon treatment with dexamethasone, without affecting IGF-1 activity. (**C** and **D**) Atrogin-1 and MuRF1 expression analysis upon dexamethasone treatment with or without AG and UnAG, in the presence or absence of 5 μM SB203580. #$P < 0.05$, §$P < 0.01$ vs. DM control; *$P < 0.05$, **$P < 0.01$ vs. DEXA treatment.

Since C2C12 myotubes do not express GHSR-1a receptor [189], these results suggest that AG and UnAG activate a novel common receptor, as already reported [184, 186, 189, 190, 206]. The receptor mediating AG and UnAG activities in β-cells is unaffected by pertussis toxin (PTX), an inhibitor of $G\alpha_i$, and, in contrast, is sensitive to NF449, a $G\alpha_s$-uncoupling drug, suggesting that the novel receptor is *bona fide* a $G\alpha_s$-coupled receptor [190]. Moreover, both AG and UnAG induce cAMP synthesis in β-cells [190]. Consistently, in C2C12 myotubes we demonstrated that NF449 inhibits AG/UnAG-induced Akt^{S473} phosphorylation and anti-atrophic activity, without affecting IGF-1 signaling (Fig. 14, A and B). In addition, both AG and UnAG rapidly increase intracellular concentration of cAMP (Fig. 14C), that, in turn, activates PKA, which is necessary for AG/UnAG anti-atrophic activities, as revealed by the loss of efficacy of both peptides in the presence of PKA-specific inhibitor H89 (Fig. 14D). In contrast, PTX do not affect AG and UnAG response (Fig. 14E). Interestingly, we demonstrated that the specific isoform of PI3K necessary to AG/UnAG anti-atrophic activity is PI3Kβ (Fig. 14, F and G), which mediates Akt activation mainly upon GPCRs activation [238]. In contrast, PI3Kα, associated with RTKs [238], is crucial for IGF-1 response but does not affect that of AG and UnAG (Fig. 14F).

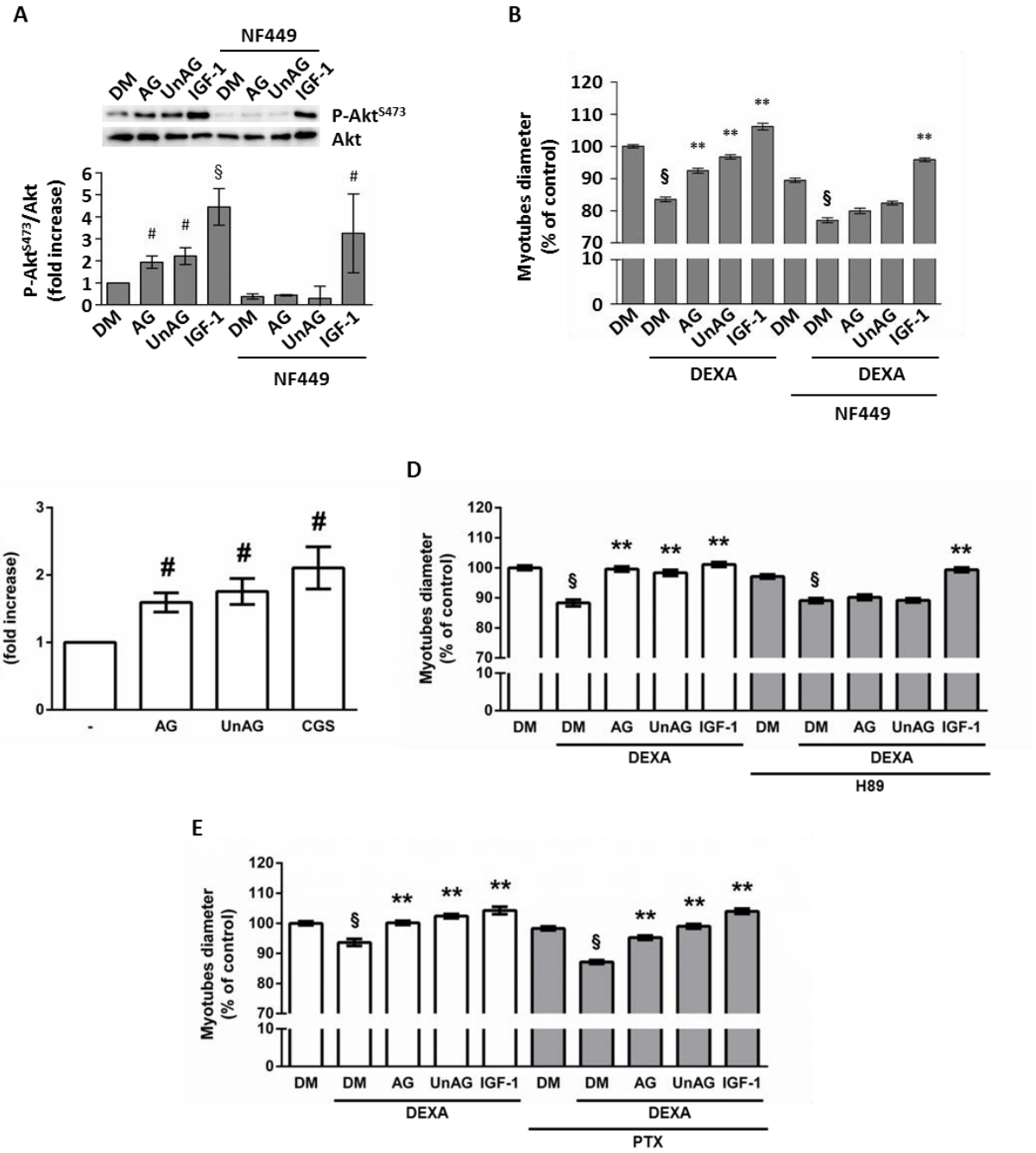
A
NF449
DM AG UnAG IGF-1 DM AG UnAG IGF-1
P-Akt^{S473}
Akt
P-Akt^{S473}/Akt (fold increase)
NF449
B
Myotubes diameter (% of control)
DEXA
DEXA
NF449
C
Intracellular cAMP (fold increase)
-
AG
UnAG
CGS
D
Myotubes diameter (% of control)
DEXA
DEXA
H89
E
Myotubes diameter (% of control)
DEXA
DEXA
PTX
F
Myotubes diameter (% of control)
DEXA
DEXA
DEXA
PIK-75
TGX-221
G
Atrogin-1 expression (fold increase)
DEXA
DEXA
TGX-221

Figure 14 (from Porporato, 2013 and unpublished): AG and UnAG activate a Gα$_s$-coupled receptor. (**A**) AG and UnAG phosphorylation of Akt^{S473} is abolished upon treatment with 10 μM NF449, a Gα$_s$ subunit–selective G protein antagonist. Shown are representative blots and quantification of 3 independent experiments. (**B**) Treatment with 10 μM NF449 reverts the anti-atrophic activity of AG and UnAG on myotubes diameter upon dexamethasone treatment. (**C**) Treatment for 5 min with 1 μM AG or UnAG increases intracellular cAMP concentration. CGS, an agonist of AdoraA2A receptors, was used as positive control of Gα$_s$ agonist. (**D** and **E**) Anti-atrophic activity of AG and UnAG on myotubes diameter upon dexamethasone treatment is abolished by the treatment with 2.5 μg/ml H89, a PKA inhibitor (**D**), but unaffected by 100 nM pertussis toxin (PTX), a Gα$_i$ inhibitor (**E**). (**F**) Treatment with 25 nM PIK-75, an inhibitor of PI3Kα, blunts the anti-atrophic effect of IGF-1 on myotubes diameter upon dexamethasone treatment, without affecting AG and UnAG activity. Conversely, the anti-atrophic effect of AG and UnAG is abrogated by treatment with 200 nM TGX-221, an inhibitor of PI3Kβ. (**G**) Atrogin-1 expression analysis upon dexamethasone treatment with AG, UnAG, and IGF-1 in the presence or absence of 200 nM TGX-221. In experiments with NF449, H89, PIK-75, and TGX-221, control myotubes in differentiation medium were treated with DMSO, a vehicle for all these compounds. #P < 0.05, §P < 0.01 vs. DM control; *P < 0.05, **P < 0.01 vs. DEXA treatment.

All these data demonstrate that AG and UnAG, by activating a novel common receptor distinct to GHSR-1a, herein referred as "GhrlR2", stimulate an anti-atrophic signaling pathway in C2C12 myotubes, without inducing hypertrophy and protein synthesis, thus only partially overlapping with IGF-1 pathway (Fig. 15).

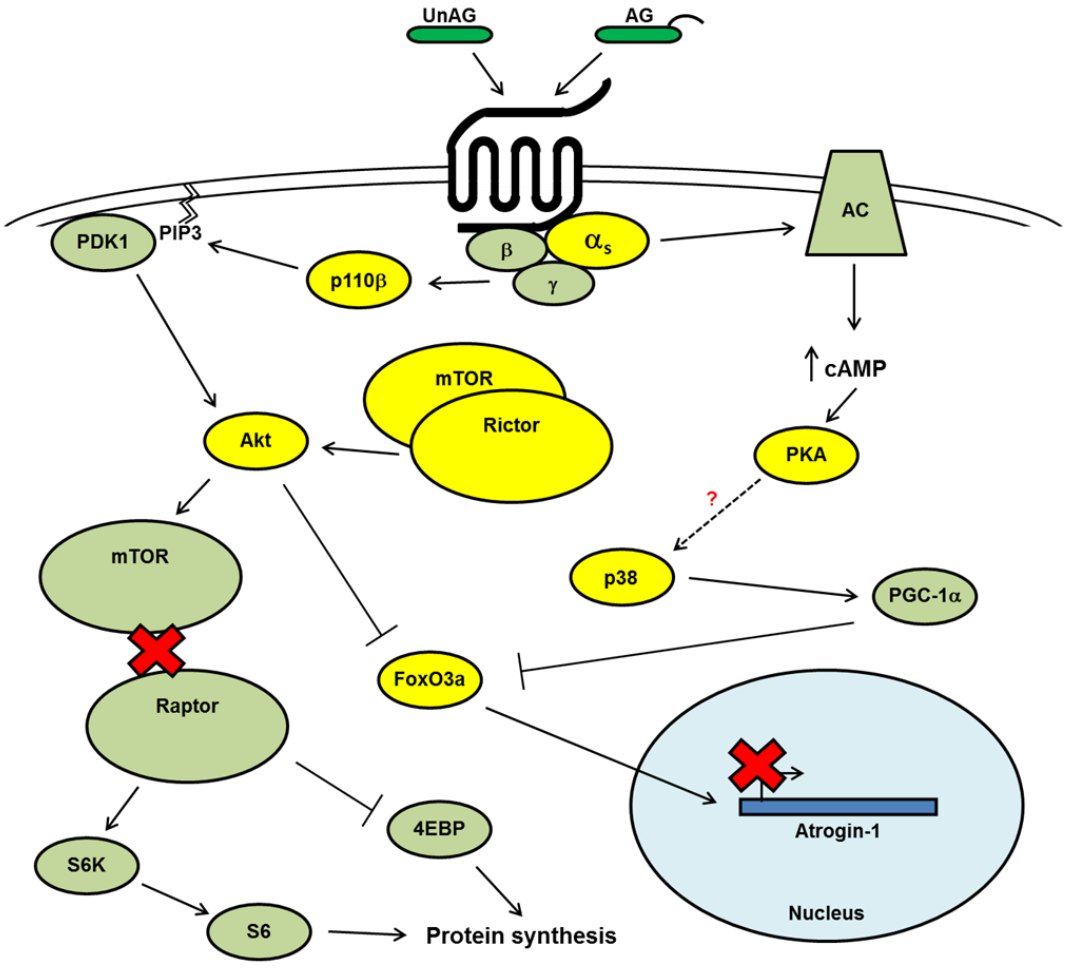

Figure 15: Signaling pathway of AG and UnAG mediating their anti-atrophic activity in skeletal muscle. Representative cartoon of the anti-atrophic pathway triggered by AG and UnAG summarizing the results obtained in C2C12 myotubes. Ghrelin peptides counteract skeletal muscle atrophy activating a novel common receptor, that, in turn, induces cAMP/PKA, PI3Kβ/mTORC2/Akt, and p38 signaling pathways, leading to the inhibition of protein degradation, without affecting mTORC1 and protein synthesis.

UnAG impairs denervation- and starvation-induced skeletal muscle atrophy

To investigate the ability of ghrelin to impair muscle wasting *in vivo*, by acting directly on skeletal muscle, we utilized UnAG to avoid the confounding effect of the GHSR-1a/GH/IGF-1 axis triggered by AG. We generated a transgenic mice line (Tg) overexpressing the *Ghrl* gene under a specific cardiac promoter (*Myh6/Ghrl*). Ghrelin expressed in the heart is released in the blood. These mice are characterized by 50-fold increase in circulating UnAG, without affecting AG concentration (for a detailed description of *Myh6/Ghrl* mice phenotype refer to the attached paper Porporato, 2013). Notably, these mice do not feature hypertrophy in skeletal muscle, consistently with the inability of UnAG to induce hypertrophy in C2C12 myotubes (Fig. 12A). We demonstrated that *Myh6/Ghrl* mice are protected from muscle wasting induced by both 48-hour of food deprivation (Fig. 16, A-E) and sciatic nerve resection (Fig. 16, F-K).

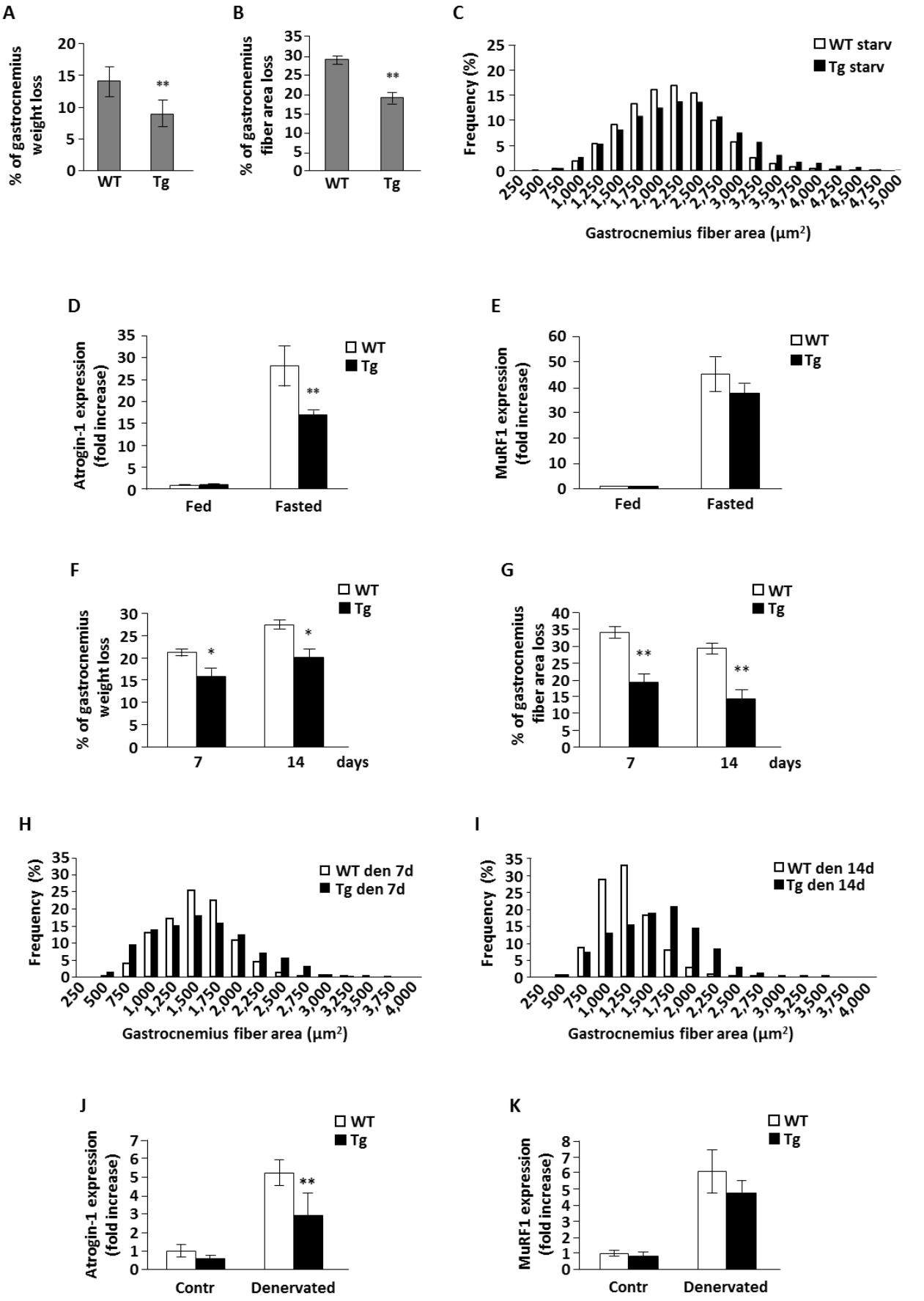
A
% of gastrocnemius weight loss
WT
Tg
B
% of gastrocnemius fiber area loss
C
Frequency (%)
WT starv
Tg starv
Gastrocnemius fiber area (µm²)
D
Atrogin-1 expression (fold increase)
Fed
Fasted
E
MuRF1 expression (fold increase)
F
% of gastrocnemius weight loss
7
14
days
G
% of gastrocnemius fiber area loss
H
Frequency (%)
WT den 7d
Tg den 7d
Gastrocnemius fiber area (µm²)
I
WT den 14d
Tg den 14d
J
Atrogin-1 expression (fold increase)
Contr
Denervated
K
MuRF1 expression (fold increase)

Figure 16 (from Porporato, 2013): *Myh6/Ghrl* mice are protected from skeletal muscle atrophy induced by either 48 hours of fasting or sciatic nerve resection. (**A**-**E**) Effect of fasting on gastrocnemii. Mean percentage of gastrocnemius weight loss (**A**) and cross-sectional area (CSA) reduction (**B**) of fasted *Myh6/Ghrl* (Tg) mice and WT littermates compared with fed animals. (**C**) Frequency distribution of gastrocnemii CSA of fasted *Myh6/Ghrl* and WT mice. (**D** and **E**) Atrogin-1 and MuRF1 expression in gastrocnemii of fed and fasted *Myh6/Ghrl* mice and their WT littermates, determined by real-time RT-PCR. N = 7 (fed WT and *Myh6/Ghrl*), 5 (fasted WT), 6 (fasted *Myh6/Ghrl*), and 3 (CSA loss and distribution, WT and *Myh6/Ghrl*). (**F**-**K**) Effect of denervation on gastrocnemii. Mean percentage of weight loss (**F**) and CSA reduction (**G**) of denervated gastrocnemius at 7 and 14 days after denervation, compared with the unperturbed side. (**H** and **I**) Frequency distribution of gastrocnemii CSA at 7 and 14 days after denervation in *Myh6/Ghrl* and WT littermates. (**J** and **K**) Atrogin-1 and MuRF1 expression in denervated gastrocnemii at 7 days after denervation, compared with the unperturbed side. N = 6 (WT), 5 (*Myh6/Ghrl*), and 3 (CSA loss and distribution, WT and *Myh6/Ghrl*). $^{**}P < 0.01$, $^{*}P < 0.05$ vs. WT.

Furthermore, subcutaneous injection of 100 μg/Kg UnAG triggers Akt^{S473}, FoxO3a^{T32}, and p38$^{T180/Y182}$ phosphorylation in gastrocnemii (Fig. 17, A-C). Importantly, at that concentration AG protects from heart failure-associated cachexia [213]. The repeated injection of 100 μg/Kg UnAG (twice a day) is sufficient to counteract skeletal muscle atrophy induced by starvation (Fig. 17, D-F) and denervation (Fig. 17, G-I). These data demonstrate that UnAG rapidly activates anti-atrophic signaling pathways in skeletal muscle, thus protecting from muscle wasting, without involving the GHSR-1a/GH/IGF-1 axis.

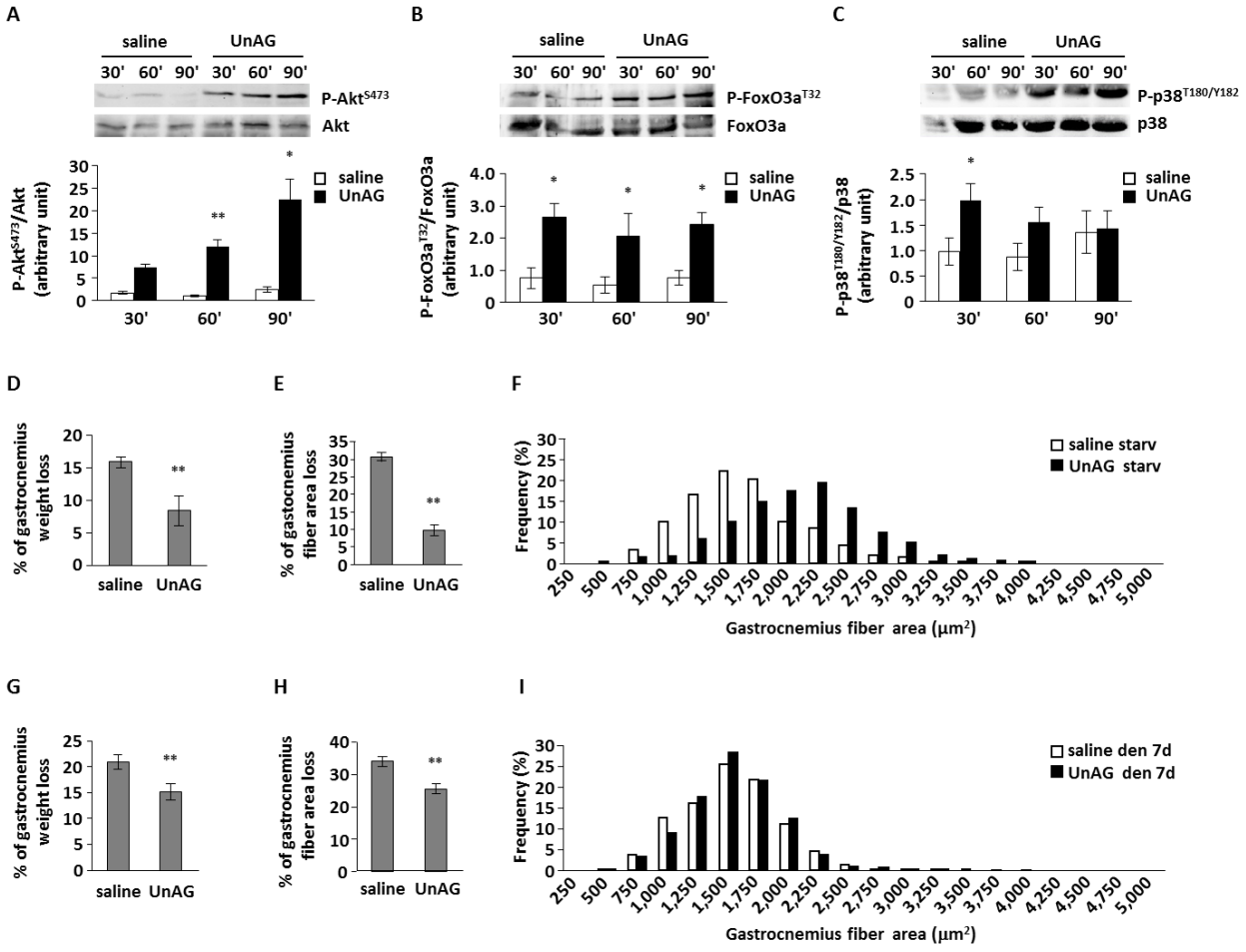

Figure 17 (from Porporato, 2013): UnAG pharmacological treatment protects skeletal muscle from fasting- and denervation-induced atrophy in WT mice. (**A**-**C**) Phosphorylation of Akt^{S473}, $FoxO3a^{T32}$, and $p38^{T180/Y182}$ in gastrocnemii of WT mice treated with 100 μg/Kg UnAG or saline. At the indicated time points, gastrocnemii were removed and processed for Western blot analysis. Shown are representative blots and densitometric analysis of 3 independent experiments, normalized to untreated animals (not shown). (**D**-**F**) Effect of fasting on gastrocnemii. Mean percent weight loss (**D**), CSA reduction (**E**), and CSA frequency distribution (**F**) of gastrocnemii from 48-hour fasted mice treated twice daily with 100 μg/Kg UnAG or saline (N = 5 per group). Frequency distribution was measured in 3 mice per group. In D and E, percent reduction shown is between fasted and fed mice. (**G**-**I**) Effect of denervation on gastrocnemii. Mean percent weight loss (**G**), CSA reduction (**H**), and CSA frequency distribution (**I**) of gastrocnemii from mice treated with 100 μg/Kg UnAG or saline twice daily for 7 days after sciatic nerve resection (N = 5 per group). CSA frequency distribution was measured in 3 mice per group. In G and H, percent reduction shown is between denervated gastrocnemii and gastrocnemii from the unperturbed side. **P* < 0.05, ***P* < 0.01 vs. saline treatment.

Both AG and UnAG impair muscle wasting in $Ghsr^{-/-}$ but not in WT mice

To confirm the existence of a novel receptor, distinct from GHSR-1a, mediating the activity of ghrelin peptides directly in skeletal muscle, we injected subcutaneously 100 μg/Kg of either AG or UnAG in $Ghsr^{-/-}$ mice, and we demonstrated that in those mice both peptides trigger Akt^{S473} phosphorylation in gastrocnemii (Fig. 18A). Moreover, the pharmacological treatment of either AG or UnAG protects from fasting-induced skeletal muscle atrophy (Fig. 18, B-D). These results are the first genetic proof of the existence of a novel receptor distinct from GHSR-1a, mediating activities of both AG and UnAG.

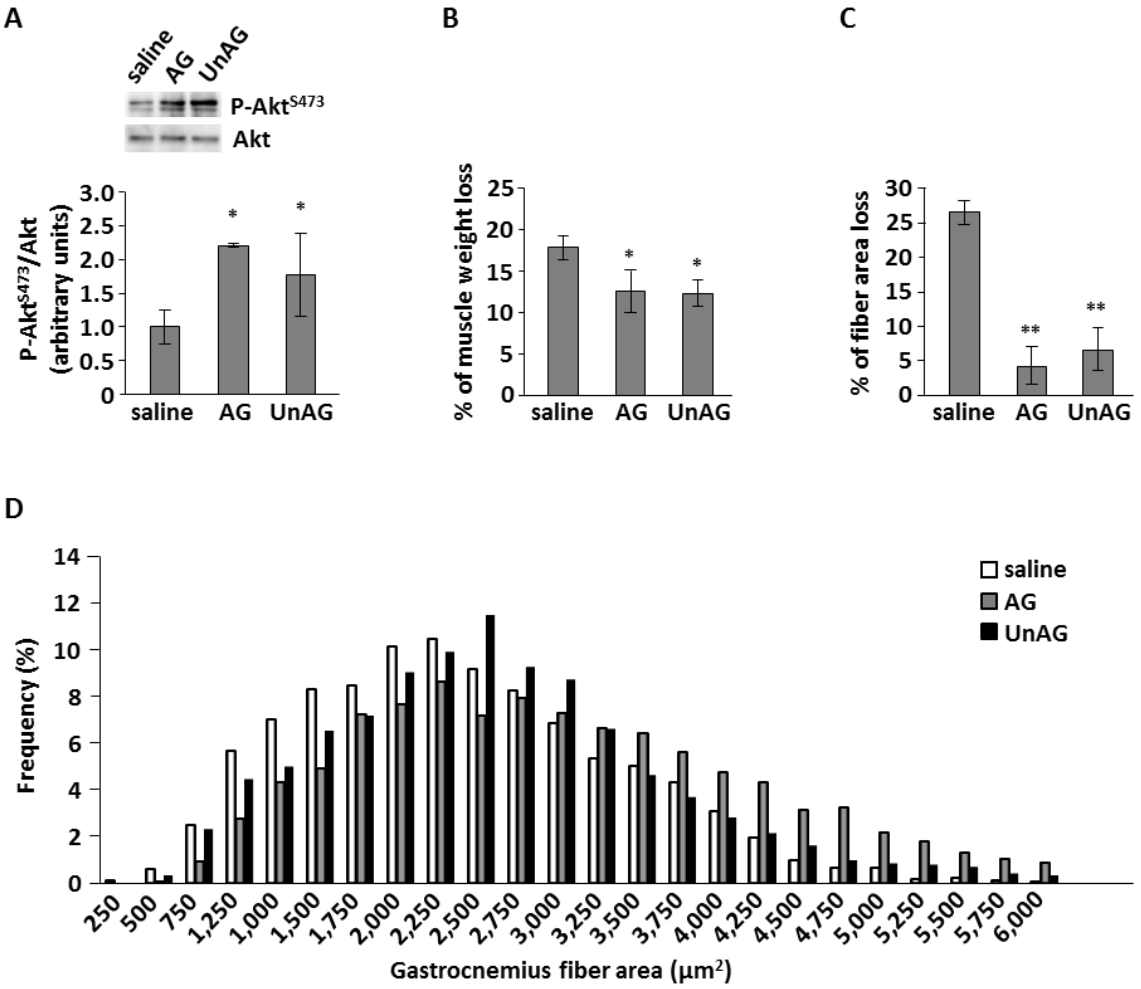

Figure 18 (from Porporato, 2013): AG and UnAG pharmacological treatment of Ghsr$^{-/-}$ mice induces anti-atrophic signaling and protects from fasting-induced skeletal muscle atrophy. (**A**) Phosphorylation of Akt^{S473} in gastrocnemii of Ghsr$^{-/-}$ mice injected with 100 µg/Kg AG or UnAG or with saline. 60 min after treatment, gastrocnemii were removed and processed for Western blot analysis. Shown are representative blots and densitometric analysis of 3 independent experiments. (**B**-**D**) Mean percentage weight loss (**B**), CSA reduction (**C**), and CSA frequency distribution (**D**) of gastrocnemii from fed or 48-hour fasted Ghsr$^{-/-}$ mice injected s.c. twice daily with 100 µg/Kg AG or UnAG or with saline (N = 5 per group). Frequency distribution was measured in 3 mice per group. In B and C percent reduction is between fasted and fed mice. *$P < 0.05$, **$P < 0.01$ vs. saline treatment.

Furthermore, we wanted to test the contribution of the GHSR-1a/GH/IGF-1 axis on the anti-atrophic activity of ghrelin peptides, comparing AG and UnAG pharmacological treatment in WT mice. Surprisingly, we observed that in WT mice AG is very inefficient to counteract muscle wasting induced by 48-hour of food deprivation compared to UnAG (Fig. 19A), although AG-treated mice show a moderate reduction of weight loss compared to saline- and UnAG-injected mice (Fig. 19B). Hence, although AG was biological active in WT mice, its treatment seems to not affect skeletal muscle mass, unlike UnAG. These results point out biological differences between

AG and UnAG, that may have crucial therapeutic implications. To further investigate this issue, we treated with AG, twice a day for 7 days after sciatic nerve resection, Ghsr$^{-/-}$ mice compared to WT. We confirmed that, indeed, AG exerts its beneficial effects on skeletal muscle only in Ghsr$^{-/-}$ mice, but not in WT mice (Fig. 19, C and D). These surprising results suggest that GHSR-1a signaling may negatively affect GhrlR2 activity in skeletal muscle, but this issue needs further investigations.

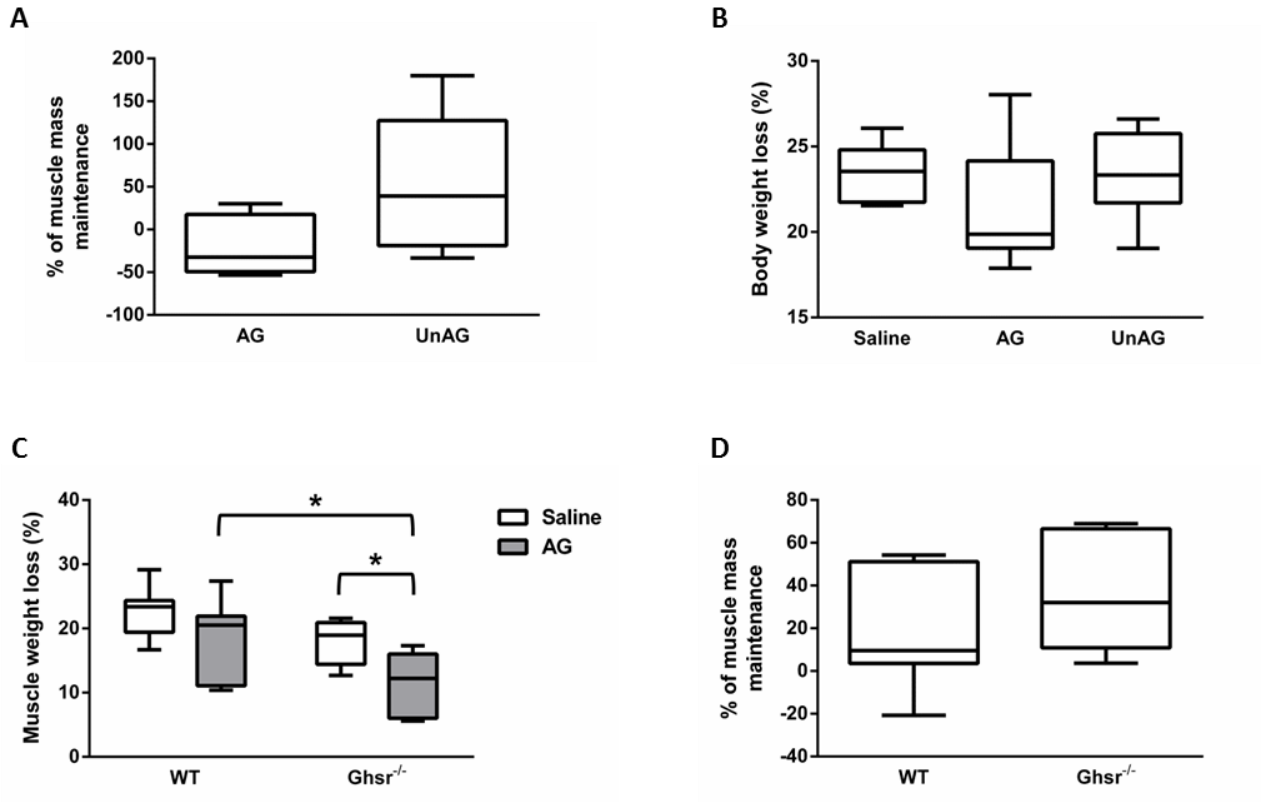

Figure 19 (unpublished): The anti-atrophic activity of AG is reduced in WT mice. (**A**-**B**) Effect of AG in fasting. Percentage of maintenance of gastrocnemii mass (**A**) and body weight loss (**B**) induced by s.c. injection of 100 µg/Kg AG or UnAG twice daily during 48-hour of food deprivation (N = 7 per group). In A percent maintenance is between AG- or UnAG- and saline-treated mice. In B percent reduction is calculated between initial and final body weight. (**C**-**D**) Effect of AG in denervation. (**C**) Percentage of gastrocnemii weight loss after 7 days from sciatic nerve resection, compared with the unperturbed side. (**D**) Percentage of AG ability to preserve gastrocnemius mass in WT compared to Ghsr$^{-/-}$ mice (N = 7 per group). *P < 0.05.

UnAG shows reduced anti-atrophic activity in cancer cachexia

The finding that AG is unable to counteract skeletal muscle wasting in WT mice has important translational implication. Indeed, it has been demonstrated that AG counteracts cachexia both in animal models and in patients [213-220], therefore it is the promising first drug against this critical medical need. It has been just concluded a phase III clinical trial for anamorelin, an AG analog, in non-small-cell lung carcinoma (NSCLC) patients. The results have not been published yet, but it has been reported that anamorelin improved body weight, lean body mass, but not handgrip strength (ESMO 27/09/2014 Press Release: Anamorelin Shown to Improve Appetite and Body Mass in Patients with Cancer Anorexia-Cachexia). Moreover, some patients displayed side effects, such as gastrointestinal and metabolic disorders, hyperglycemia, and diabetes mellitus. Similar results have been published from two Phase II clinical trial evaluating the treatment of anamorelin for cancer cachexia [267]. Since anamorelin is an AG analog, it is likely that it binds also the novel receptor GhrlR2, although there are no data about this. However, it is reasonable assume that the results obtained with anamorelin depend on GHSR-1a-mediated orexigenic, GH-releasing, and anti-inflammatory activities. Thus, anamorelin may affect directly skeletal muscle mass only in a lesser extent, as pointed out by our results on AG inability to counteract muscle wasting in WT mice. In addition, AG owns relevant diabetogenic effects [210], and a potential cancer risk associated with IGF-1 release [225]. For these reasons, the anti-atrophic activity of UnAG, which does not bind to GHSR-1a, has relevant therapeutic perspectives, and thus we decided to test the ability of UnAG to preserve skeletal muscle mass during cancer cachexia. We injected subcutaneously 5 millions of Lewis lung carcinoma (LLC) cells in *Myh6/Ghrl* mice. Globally, we observed that cachectic *Myh6/Ghrl* mice are slightly better than WT, and present low grade of skin ulceration around the tumor mass. Consistently, we found that *Myh6/Ghrl* mice show a lesser extent of anorexia in the severe cachexia stages (Fig. 20A), while body weight loss is similar (Fig. 20B). Notably, upregulation of circulating UnAG do not affect tumor mass (Fig. 20C). Surprisingly, we observed no significant differences, between WT and *Myh6/Ghrl* mice, in both epididymal fat weight (Fig. 20D), and gastrocnemii (GAS) and extensor digitorum longus (EDL) weight loss (Fig. 20, E and F), while only a modest improvement in tibialis anterior (TA) and quadriceps (QUAD) muscle mass (Fig. 20, G and H). The expression of Atrogin-1 and MuRF1 in GAS and TA further confirm the weak differences between WT and *Myh6/Ghrl* mice observed in muscles mass (Fig. 20, I-L). Consistently, frequency distribution of the minimal Feret's diameter of cachectic TA myofibers shows a little shift of *Myh6/Ghrl* myofibers, compared to WT, towards bigger diameters (Fig. 20,M

and N). In conclusion, these data unveil a modest efficacy of UnAG in counteracting cancer cachexia.

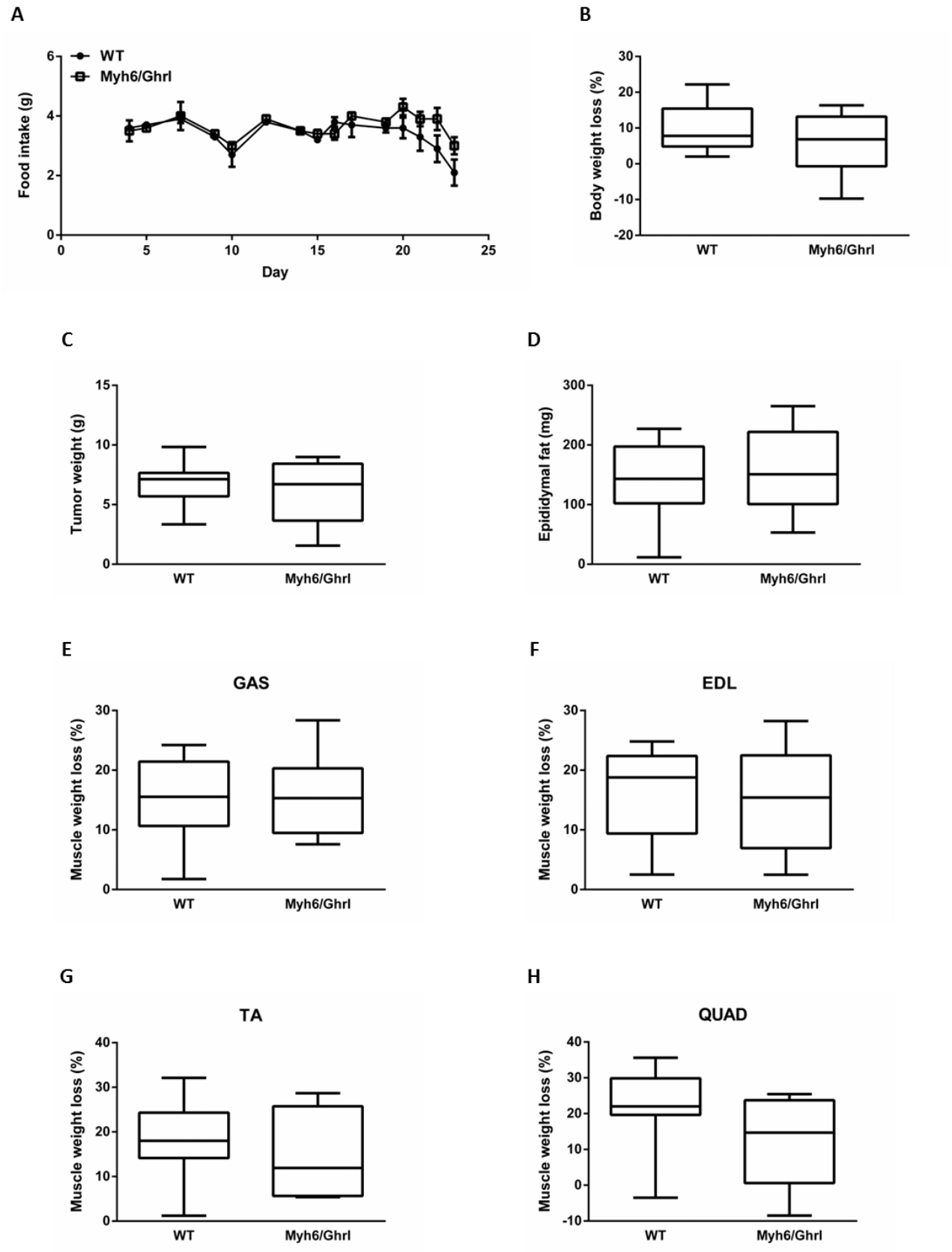

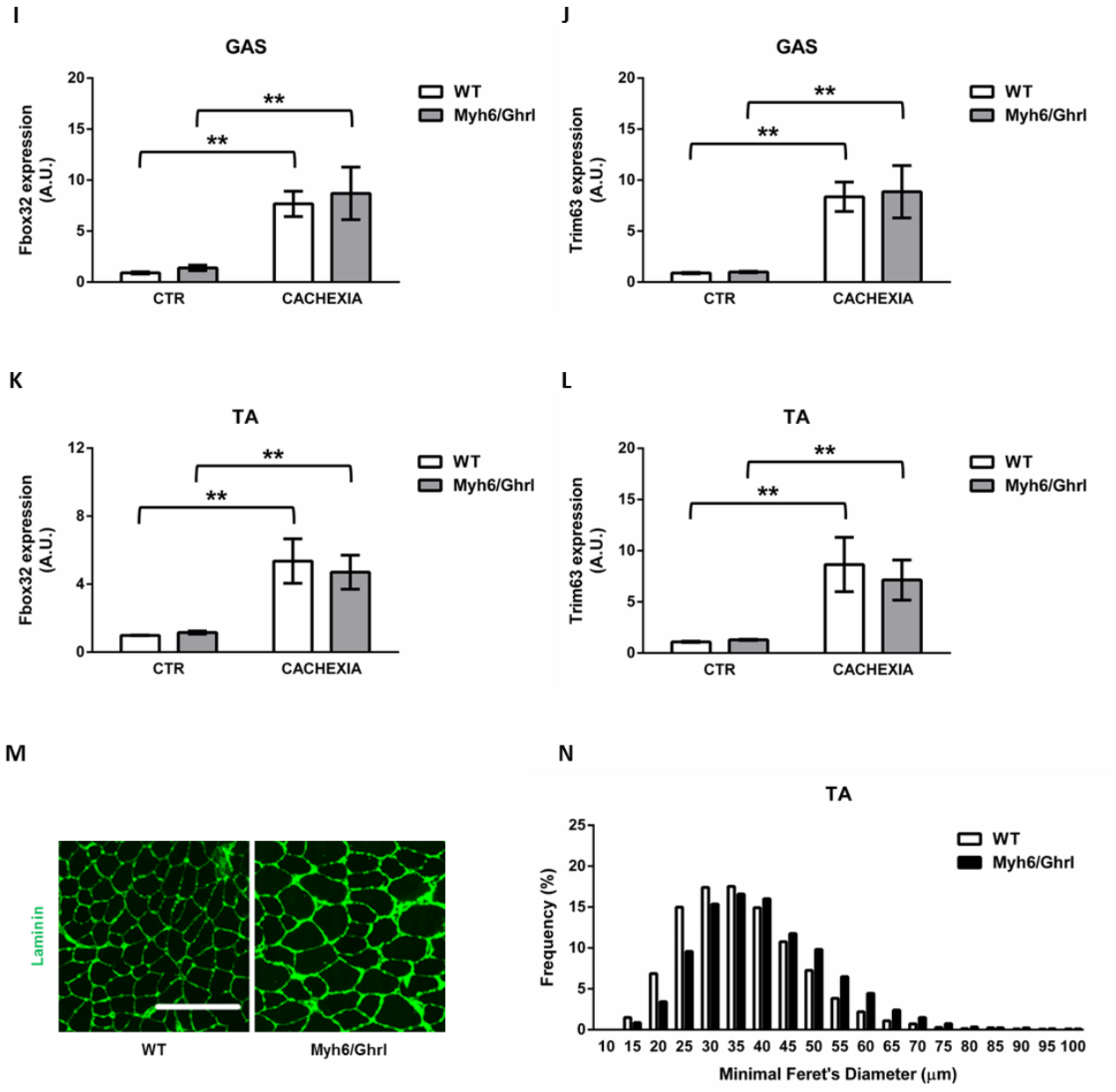

Figure 20 (unpublished): *Myh6/Ghrl* mice are weakly protected from LLC-induced cachexia. (**A**) Daily food intake during cancer cachexia progression. (**B**-**G**) Comparison between WT and *Myh6/Ghrl* mice, at 23 days after Lewis lung carcinoma (LLC) cells s.c. injection, of percentage of body weight loss (**B**), tumor weight (**C**), epididymal fat weight (**D**), and percentage of gastrocnemius (**E**), extensor digitorum longus (**F**), tibialis anterior (**G**), and quadricep (**H**) weight loss. N = 9 (WT) and 8 (*Myh/Ghrl*). In E-H percent reduction shown is between non-tumor-bearing and cachectic mice. (**I**-**L**) Atrogin-1 (*Fbox32*) and MuRF1 (*Trim63*) expression in gastrocnemii (**I** and **J**) and tibialis anterior (**K** and **L**) of non-tumor-bearing (CTR) and cachectic (CACHEXIA) mice. N = 3 (CTR), 6 (CACHEXIA GAS), 4 (CACHEXIA TA WT), and 8 (CACHEXIA TA *Myh6/Ghrl*). (**M**) Representative image of laminin staining of tibialis anterior of LLC-bearing mice, for measurement of minimal Feret's diameter of myofibers. (**N**) Frequency distribution of minimal Feret's diameter of tibialis anterior myofibers of cachectic mice, automatically quantified with ImageProPlus (Media Cybernetics). N = 4 (WT) and 5 (*Myh6/Ghrl*). ***P* < 0.01.

Circulating UnAG increases during cancer cachexia

Our data suggest that the anti-cachectic activities exerted by AG may dependent mainly by GHSR-1a-mediated orexigenic and GH-releasing effects. Moreover, AG has strong anti-inflammatory properties, through the activation of GHSR-1a, although it has been demonstrated that also UnAG downregulates inflammatory states [222-224]. However, it has been demonstrated that circulating AG and total ghrelin increase during cachexia, independently from the underlying pathology [226-232]. This evidence leads to the hypothesis that in cachexia there is the establishment of an AG resistance, as previously reported [233-235], and that only a higher concentration of AG may restore its effects GHSR-1a-mediated [234]. Since these studies reported concentration of circulating AG or total ghrelin, we wanted to specifically investigate UnAG concentration in cancer cachexia models. We observed, indeed, that circulating UnAG is up-regulated in adenocarcinoma C26- (Filigheddu and Coletti, unpublished results) and LLC-bearing mice (Fig. 21, A and B). Furthermore, it has been demonstrated that ghrelin may be relevant in physiologic muscle repair. Indeed, at 24h from intramuscular treatment with cardiotoxin (CTX), a necrotic agent stimulating skeletal muscle regeneration, ghrelin precursor preproghrelin, strongly increases in injured muscles [268]. Moreover, UnAG induces skeletal muscle regeneration upon ischemic damage [195]. Since the impairment of muscle regeneration is a crucial point in the eziopathogenesis of muscle decay in cancer cachexia [57-61], we tested whether cachectic muscles show increased ghrelin expression. We observed that in cachectic TA ghrelin expression is increased, although not statistically significant, mainly in C26- (Filigheddu and Coletti, unpublished results) than in LLC-bearing mice (Fig. 21, C and D). However, this finding points out the critical role of a particular cytokines combination regulating ghrelin expression in skeletal muscle, as an adaptive response to severe muscle injury.

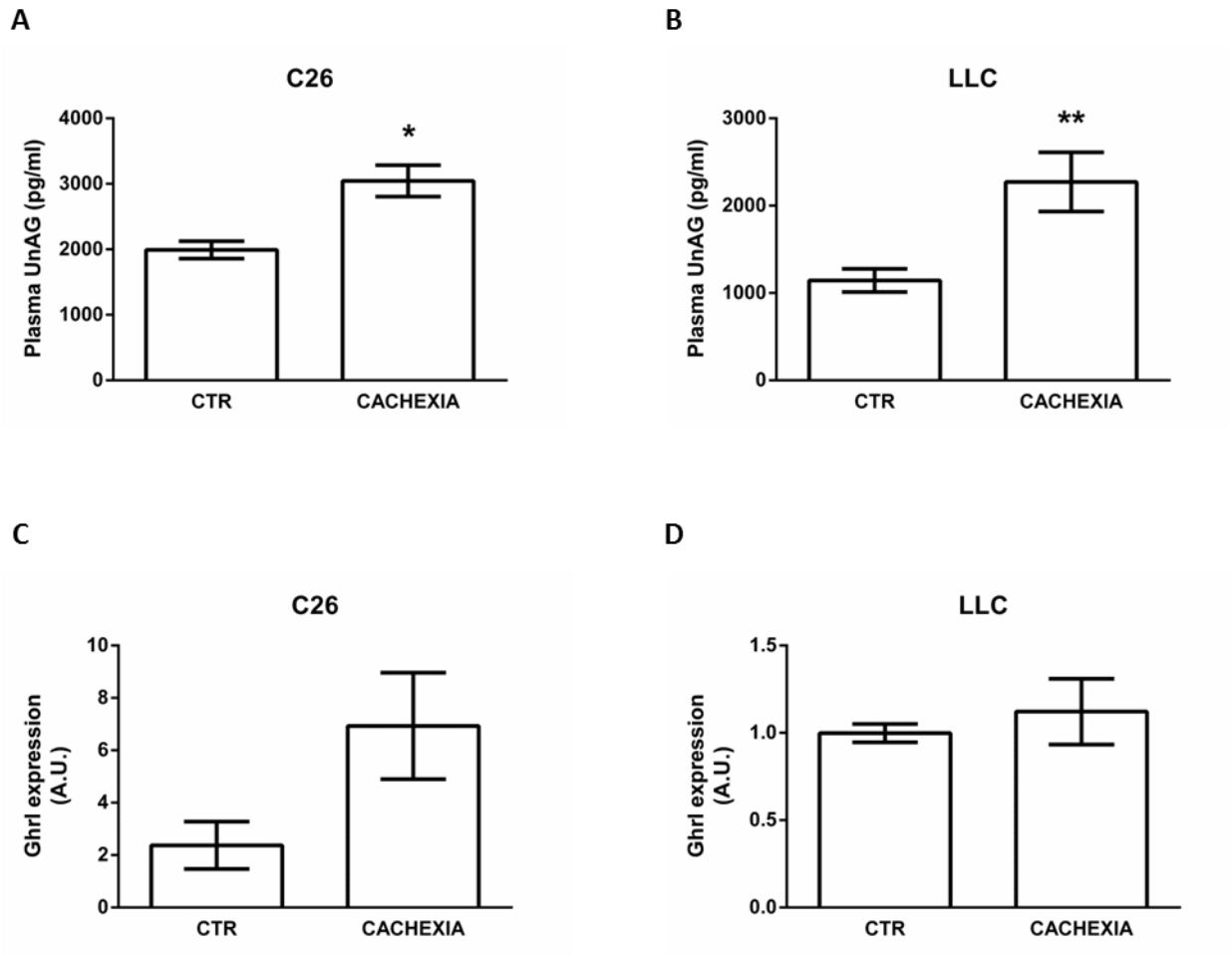

Figure 21 (unpublished): Ghrelin is upregulated in cancer cachexia. (**A** and **B**) Circulating levels of UnAG in non-tumor-bearing mice (CTR) and cachectic mice bearing C26 adenocarcinoma (**A**) or Lewis lung carcinoma (**B**). N = 8 (CTR C26, CACHEXIA LLC) and 10 (CTR LLC and CACHEXIA C26). (**C** and **D**) Ghrelin expression in tibialis anterior of C26- (**C**) and LLC- (**D**) induced cachectic mice. In N = 6 (CTR C26), 10 (CACHEXIA C26), 5 (CTR LLC), and 8 (CACHEXIA C26). **P* < 0.05, ***P* < 0.01 vs. CTR.

The increase in circulating ghrelin peptides may be the establishment of either a ghrelin resistance, or a compensatory mechanism, or both. Interestingly, also the tumor might release AG and UnAG to support its growth, similar to other factors. To investigate the physiological role of the upregulation of ghrelin peptides during cachexia, we studied the cachectic phenotype in $Ghrl^{-/-}$ mice. Interestingly, our results suggest that the ablation of *Ghrl* gene impacts only marginally cachexia progression. Indeed, we didn't observed any differences in food intake (Fig. 22A), body weight loss (Fig. 22B), epididymal fat weight (Fig. 22C), weight loss of GAS, TA, EDL and QUAD muscles (Fig. 22, D-G), and forelimb force (Fig. 22H). Importantly, not only the lacking of *Ghrl* gene do not affect tumor growth (Fig. 22I), but also tumor cells do not release UnAG in the circulation, at least in LLC-model. Indeed, circulating UnAG remains undetectable in $Ghrl^{-/-}$ mice also after LLC

transplantation (data not shown). Although these findings do not reveal the physiological role of the circulating AG and UnAG upregulation, they strongly suggest that ghrelin response, mediated not only by GHSR-1a but also by GhrlR2, is reduced or impaired during cancer cachexia.

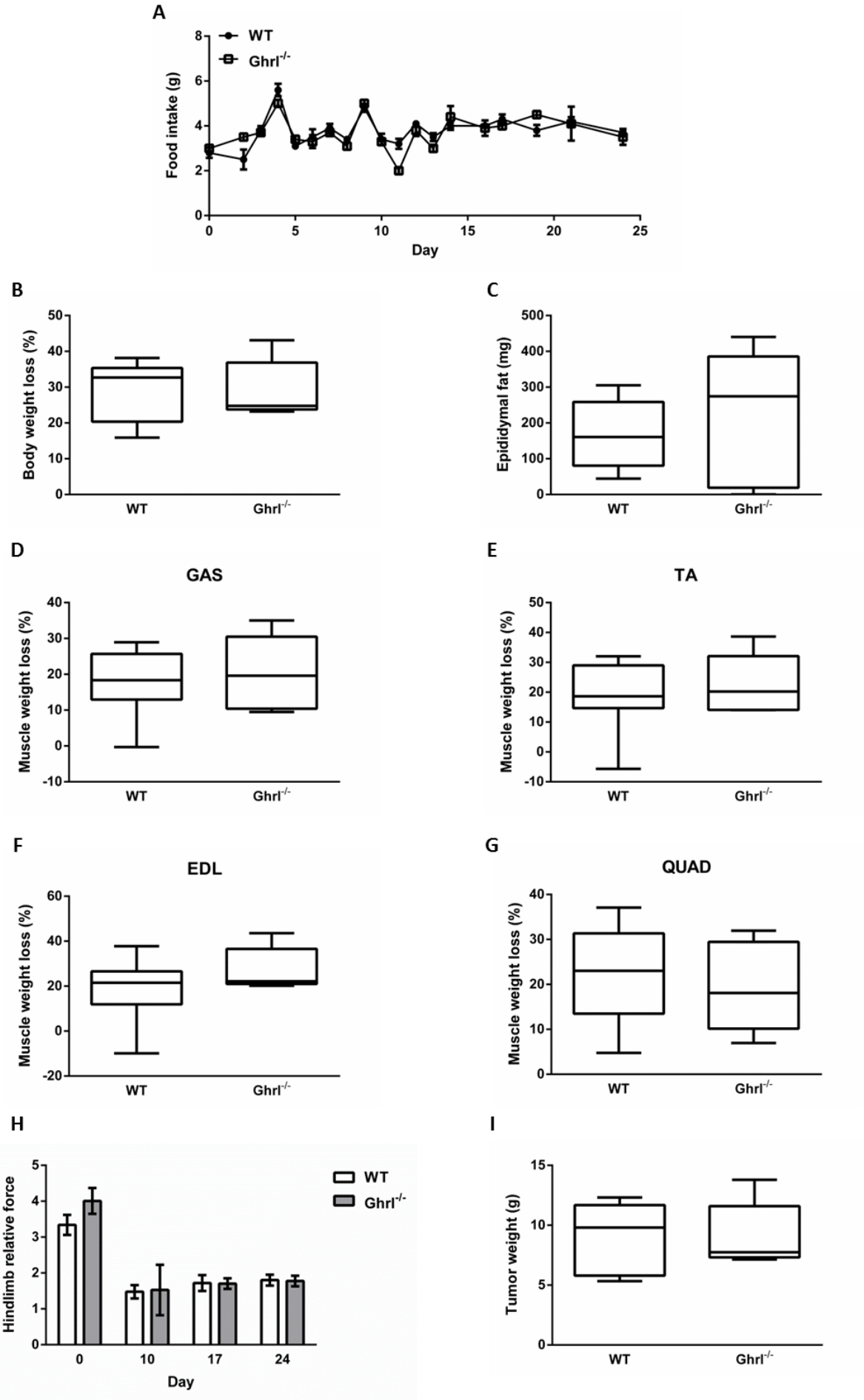
A
WT
Ghrl-/-
Food intake (g)
Day
B
Body weight loss (%)
WT
Ghrl-/-
C
Epididymal fat (mg)
WT
Ghrl-/-
D
GAS
Muscle weight loss (%)
WT
Ghrl-/-
E
TA
Muscle weight loss (%)
WT
Ghrl-/-
F
EDL
Muscle weight loss (%)
WT
Ghrl-/-
G
QUAD
Muscle weight loss (%)
WT
Ghrl-/-
H
Hindlimb relative force
WT
Ghrl-/-
Day
I
Tumor weight (g)
WT
Ghrl-/-

Figure 22 (unpublished): Ablation of *Ghrl* gene does not affect cancer cachexia progression. (**A**) Daily food intake during cancer cachexia progression. (**B**-**G**) Comparison between WT and Ghrl$^{-/-}$ mice, at 24 days after LLC injection, of percentage of body weight loss (**B**), epididymal fat weight (**C**), and percentage of gastrocnemius (**D**), tibialis anterior (**E**), extensor digitorum longus (**F**), and quadricep (**G**) weight loss. In D-G percent reduction shown is between non-tumor-bearing and cachectic mice. (**H**) Hindlimb relative force was measured with grasping test during cancer cachexia progression. (**I**) Tumor weight at 24 days after LLC cells inoculation. N = 9 (WT) and 5 (Ghrl$^{-/-}$).

PI3Kγ and PI3Kβ inversely affect ghrelin signaling

We have demonstrated that GhrlR2 is *bona fide* a Gα_s-coupled receptor triggering PI3Kβ/mTORC2, p38, and cAMP/PKA pathways. It has been demonstrated that β-ARs, which are also Gα_s-coupled receptors, activate two distinct PI3K isoforms: PI3Kβ, accountable for Akt activation, and PI3Kγ, necessary to internalization of β-ARs upon stimulation [236, 250]. Since the anti-atrophic activity of AG and UnAG is mediated by PI3Kβ activation, similar to β-ARs, and, in contrast, it has been shown that PI3Kγ mediates, through Akt activation, the anti-lipolytic actions of both peptides in adipocytes [269], we decided to investigate the role of PI3Kγ in the GhrlR2-triggered signaling in skeletal myotubes. Surprisingly, we observed that the ability of both peptides to counteract dexamethasone-induced atrophy seems enhanced in the presence of AS605240, a specific inhibitor of PI3Kγ (Fig. 23A). Moreover, in absence of dexamethasone, the inhibitor of PI3Kγ makes AG and UnAG hypertrophic factors, increasing the size of myotubes diameter over the basal level, like IGF-1 (Fig. 23B). Indeed, although AG and UnAG are unable to induce S6K^{T389} phosphorylation (Fig. 12G and 23C), both peptides increase S6K^{T389} phosphorylation when PI3Kγ is inhibited (Fig. 23D), indicating mTORC1 activation, consistently with the observed hypertrophic phenotype. In conclusion, we showed that PI3Kγ activity regulates AG/UnAG response, and inversely affects ghrelin signaling compared to PI3Kβ, as demonstrated for β-ARs.

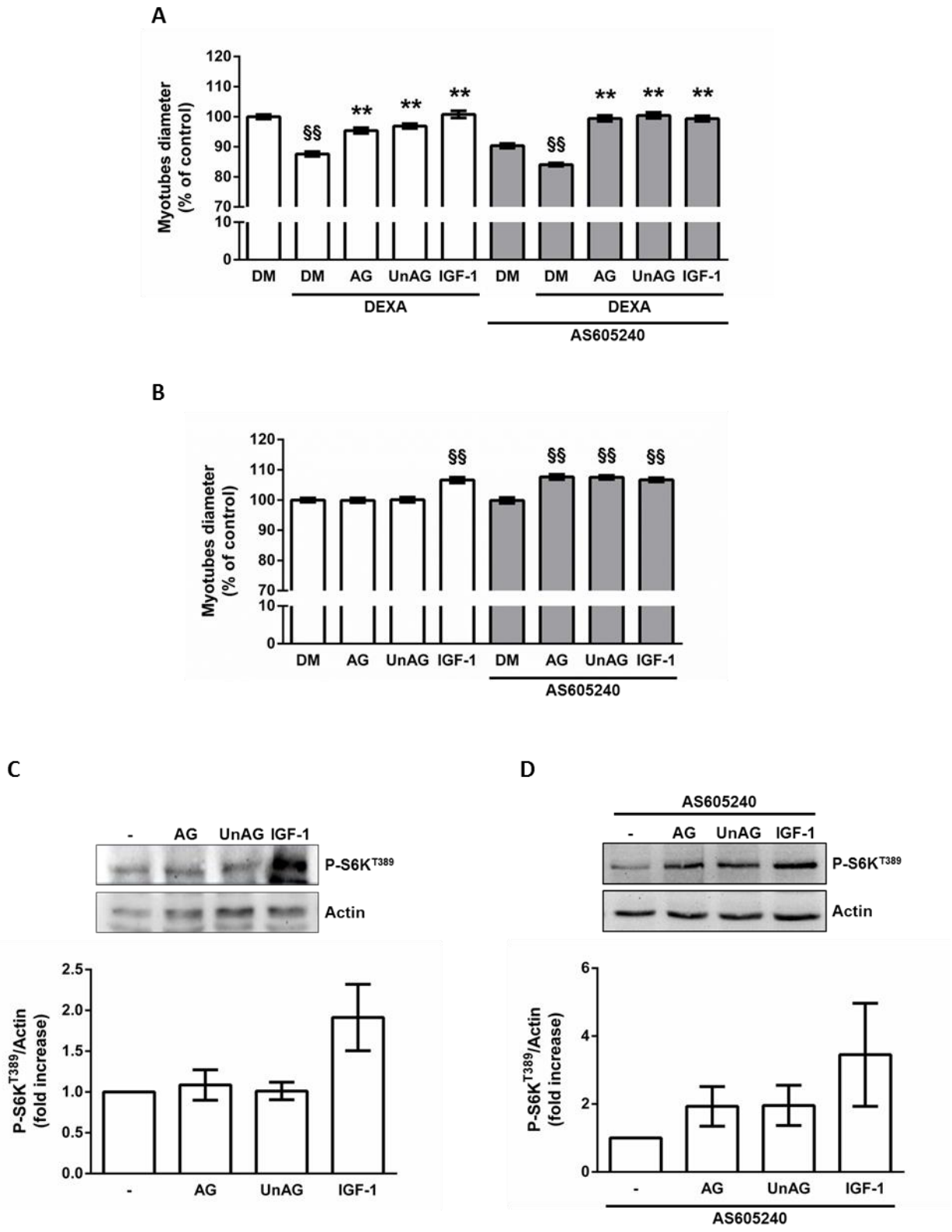

Figure 23 (unpublished): PI3Kγ inhibition enhances AG and UnAG signaling *in vitro*. (**A**) C2C12 myotubes diameter was measured after 24-hour of dexamethasone treatment, in the presence or absence of 40 nM AS605240, a PI3Kγ inhibitor, with 10 nM AG or UnAG, or 10 ng/ml IGF-1. (**B**) Treatment with 40 nM AS605240 makes AG and UnAG hypertrophic factors. (**C** and **D**) Phosphorylation of S6K^{T389}, detected by Western blotting, upon 20-min treatment with 1 µM AG or UnAG, or 10 ng/ml IGF-1, in the presence or absence of 40 nM AS605240. Shown are representative blots and quantification of 3 independent experiments. §§$P < 0.01$ vs. DM control; **$P < 0.01$ vs. DEXA treatment.

The expression of p101 increases in cancer cachexia

Based on our findings in C2C12 myotubes, we hypothesized that a deregulation in PI3Kγ activity may affect the AG/UnAG response through GhrlR2. Indeed, it has been demonstrated for β-ARs in heart failure that an upregulation of the PI3Kγ regulatory subunit p101 leads to an enhanced PI3Kγ activity, resulting in a strong downregulation of β-ARs density at the plasma membrane [236]. Consistently, the catalytic inhibition of PI3Kγ restores β-ARs density [236]. Therefore, we hypothesized that in cancer cachexia p101 expression might increase in skeletal muscle, negatively affecting the density of different receptors at the plasma membrane, including GhrlR2. In LLC-bearing mice we found, both in GAS and in TA, a tendency of p110γ expression to decrease, but not statistically significant (Fig. 24A), and, importantly, an upregulation of p101 expression (Fig. 24B), in contrast to that of p84/87 (Fig. 24C), leading to more than two-folds in p101/p87 ratio compared to controls (Fig. 24D). Interestingly, p101 expression in GAS correlates with tumor weight (Fig. 24E) and GAS weight loss (Fig. 24F), indicating a close connection between p101 expression and severity of cachexia. Indeed, we found an increase in p101 expression in a time dependent manner from LLC-inoculation (data not shown). In conclusion, these data demonstrate that in cachectic muscle there are a deregulation in PI3Kγ subunits expression, similar to that shown in heart failure. Hence, we hypothesized that the increased expression of p101 instead p84/87 in cancer cachexia leads to a downregulation of GhrlR2 at the plasma membrane, reducing the responsiveness to ghrelin peptides (Fig. 24G).

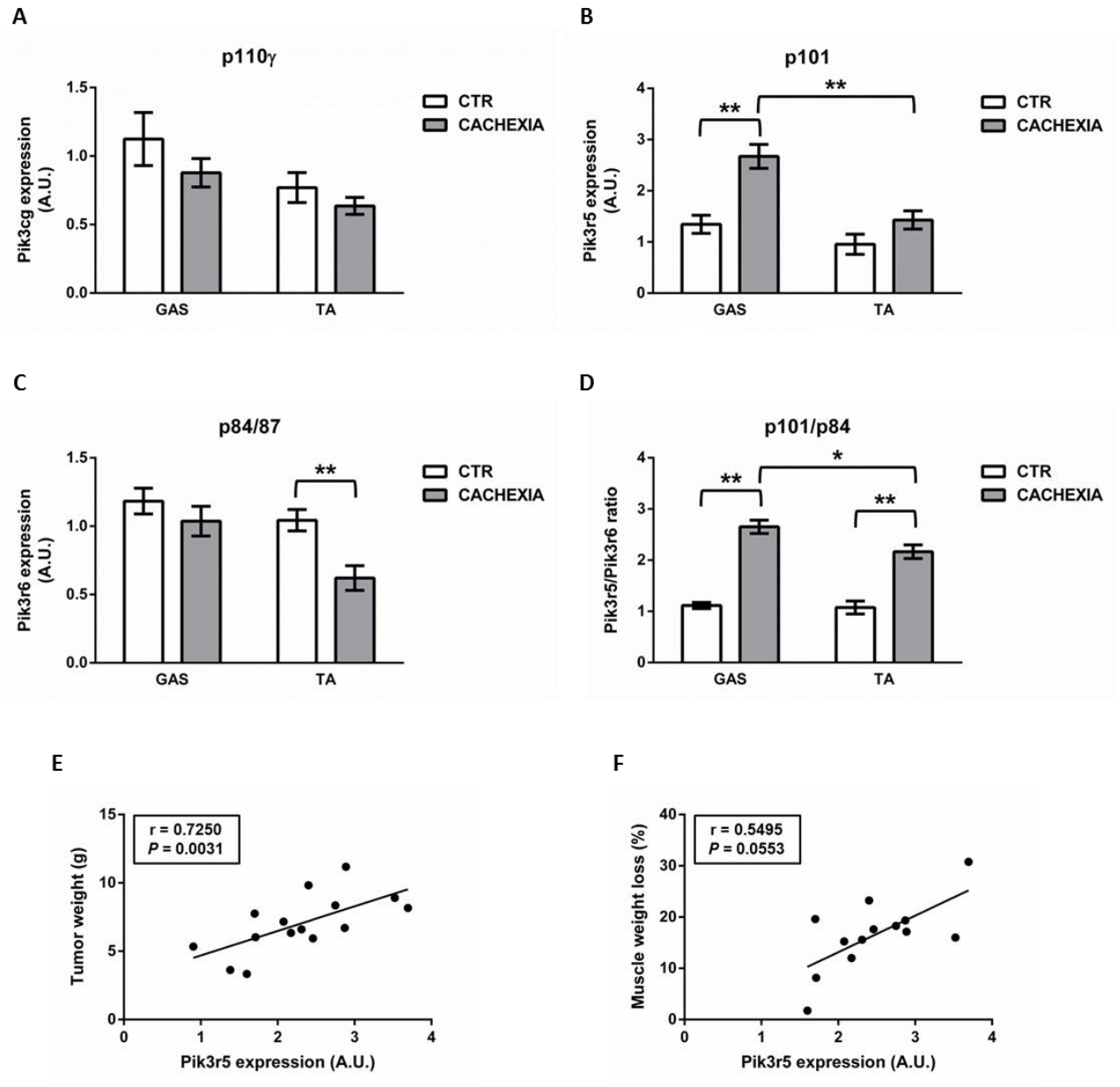

Figure 24 (unpublished): The p101 expression increases in cachectic muscles proportionally to cachexia grade. (**A**-**D**) PI3Kγ subunits expression in gastrocnemii, detected by real-time RT-PCR. Comparison between non-tumor-bearing and cachectic mice of the expression of p110γ (**A**), p101 (**B**), p84/87 (**C**). (**D**) Ratio between the expression of p101 and p84/87 regulatory subunits. (**E** and **F**) Correlation between p101 expression and tumor weight (**E**) or gastrocnemii weight loss (**F**). $^{**}P < 0.01$.

The AG and UnAG response inversely correlates with p101 expression

A key feature of cancer cachexia is the presence of chronic inflammatory state. Among others, TNFα, IFNγ, IL-6, and IL-1β are the pro-inflammatory cytokines mainly involved in cancer cachexia [51]. We investigated the modulation of p101 expression in C2C12 myotubes upon 24-hour treatment with either TNFα/IFNγ combination or IL-6. We observed that p101 expression significantly increases in TNFα/IFNγ-treated C2C12 myotubes, but not in those treated with IL-6 (Fig. 25A). Preliminary observations showed that AG and UnAG anti-atrophic activity is blunted or reduced after 24- or 48-hour treatment with LLC-conditioned medium, while is unaffected by C26-conditioned medium (Fig. 25, B and C). Since C26- and LLC-induced cachexia is mainly due by IL-6 and TNFα, respectively, we investigated the AG and UnAG ability to impair IL-6 and TNFa effects in C2C12 myotubes. We demonstrated that both IL-6 and TNFα/IFNγ treatment reduces myotubes size, but AG and UnAG is unable to counteract TNFα/IFNγ-induced atrophy (Fig. 25D), while they impair IL-6-mediated wasting (Fig. 25E). Accordingly, the ability of AG and UnAG to induce Akt^{S473} phosphorylation is blunted in TNFα/IFNγ- but not in IL-6-treated C2C12 myotubes (Fig. 25F). Finally, by co-transfecting in C2C12 myoblasts pcDNA3-myc-p110γ and pcDNA3-HA-p101 plasmids we observed an inhibition of the ability of ghrelin peptides to induce Akt^{S473} phosphorylation, compared to empty vector (Fig. 25G). These data demonstrate that the upregulation of p101 expression reduces AG and UnAG response.

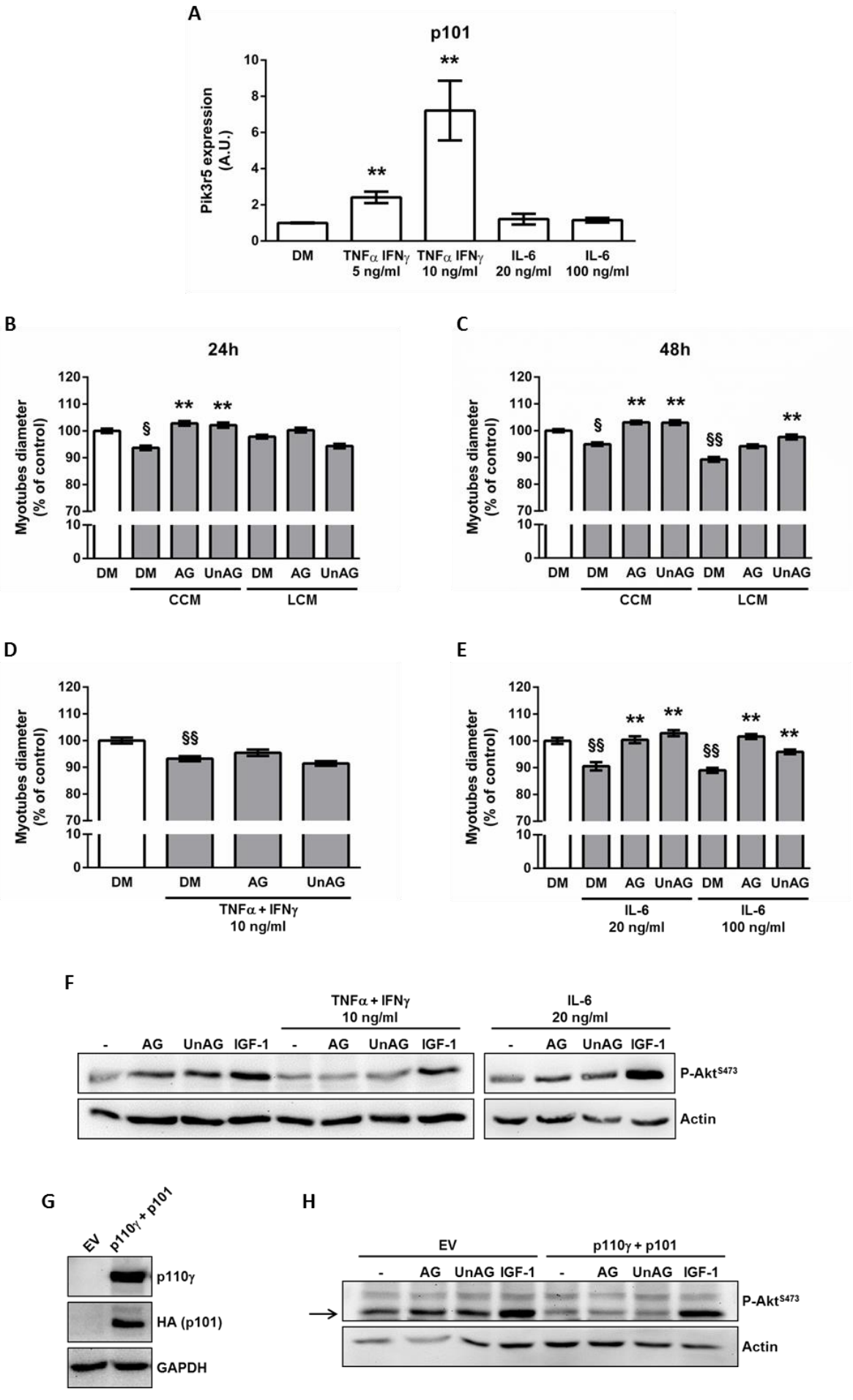
A
p101
Pik3r5 expression (A.U.)
DM
TNFα IFNγ 5 ng/ml
TNFα IFNγ 10 ng/ml
IL-6 20 ng/ml
IL-6 100 ng/ml
B
24h
Myotubes diameter (% of control)
DM
AG
UnAG
CCM
LCM
C
48h
D
TNFα + IFNγ 10 ng/ml
E
IL-6 20 ng/ml
IL-6 100 ng/ml
F
TNFα + IFNγ 10 ng/ml
IL-6 20 ng/ml
IGF-1
P-Akt S473
Actin
G
EV
p110γ + p101
p110γ
HA (p101)
GAPDH
H
EV
p110γ + p101
P-Akt S473
Actin

Figure 25 (unpublished): The expression of p101 negatively affects ghrelin signaling. (**A**) Expression of p101 in C2C12 myotubes upon treatment with 5 ng/ml or 10 ng/ml TNFα/IFNγ combination, and with 20 ng/ml or 100 ng/ml IL-6. (**B** and **C**) C2C12 myotubes diameter was measured after 24- or 48-hour treatment with conditioned media obtained by supernatant of C26 (CCM) or LLC (LCM) cells. (**D** and **E**) Treatment with TNFα/IFNγ (**D**), but not with IL-6 (**E**), blunts the anti-atrophic activity of AG and UnAG. (**F**) Phosphorylation of Akt^{S473}, detected by Western blotting, upon 5-min treatment with 1 μM AG or UnAG, or 10 ng/ml IGF-1, in the presence or absence of 10 ng/ml TNFα/IFNγ or 20 ng/ml IL-6. (**G**) Effect on protein levels of C2C12 myotubes transfection with empty vector (EV), pcDNA3-myc-p110γ and pcDNA3-HA-p101 (p110γ + p101), detected by Western blotting. (**H**) Phosphorylation of Akt^{S473}, detected by Western blotting, upon 5-min treatment with 1 μM AG or UnAG, or 10 ng/ml IGF-1 in C2C12 myotubes transfected as in G. §P < 0.05 vs. DM control; §§P < 0.01 vs. DM control; **P < 0.01 vs. CCM/LCM/IL-6 treatment.

Catalytic inhibition of PI3Kγ slightly improves cancer cachexia

Based on our findings that inhibition of PI3Kγ activity enhances AG/UnAG activity both in basal conditions and upon dexamethasone-treatment, and that the p101 expression inversely correlates with AG and UnAG response, we hypothesized that inhibition of PI3Kγ may restore the GhrlR2 response to the high levels of circulating ghrelin peptides. Indeed, accordingly to our hypothesis, PI3Kγ inhibition should increase GhrlR2 density sufficiently to restore AG/UnAG activities. Therefore, we induced cancer cachexia injecting LLC cells in $PI3K\gamma^{KD/KD}$ mice, characterized by a kinase dead mutation in p110γ [252]. Although PI3Kγ is highly expressed in immune system cells [239], its catalytic inactivation do not affect circulating cytokines (data not shown) and tumor growth (Fig. 26A), in contrast to what observed in orthotopic growth of LLC [241]. We observed that the percentage of body weight and skeletal muscle mass loss in GAS, TA, and EDL is comparable between WT and (Fig. 26, B-E), and the atrogenes expression analysis confirms the data on muscle weight (Fig. 26, F and G). The frequency distribution of minimal Feret's diameter of TA muscles show a shift of myofibers of $PI3K\gamma^{KD/KD}$ mice towards bigger diameters (Fig. 26H), as observed in *Myh6/Ghrl* mice (Fig. 20N). Nevertheless, food intake is improved in $PI3K\gamma^{KD/KD}$ mice at the last stages of cancer cachexia (Fig. 26I), indicating a global benefit induced by PI3Kγ inhibition, as observed in *Myh6/Ghrl* mice (Fig. 20A). Importantly, we observed a delayed increase in circulating UnAG concentration in $PI3K\gamma^{KD/KD}$ mice, compared to WT (Fig. 26J), while circulating AG is comparable (Fig. 26K), suggesting that these mice have either a reduced negative energy balance, or a reduced UnAG-resistance, or both. However, the weak improvement of symptoms in tumor-bearing $PI3K\gamma^{KD/KD}$ mice reveals that the only PI3Kγ inhibition is not sufficient to counteract or slow cancer cachexia.

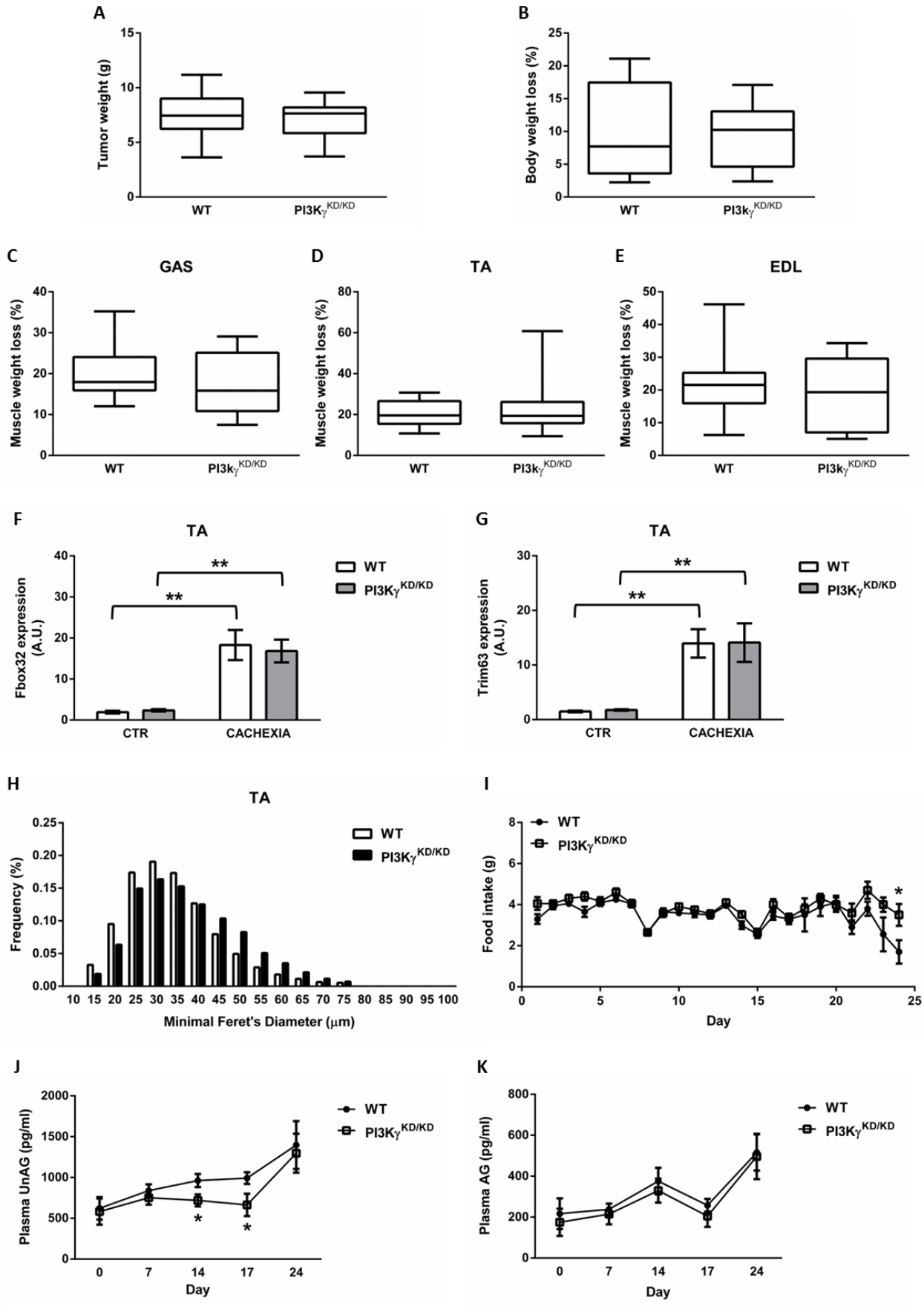
A
Tumor weight (g)
WT
PI3Kγ KD/KD
B
Body weight loss (%)
C
GAS
Muscle weight loss (%)
D
TA
E
EDL
F
Fbox32 expression (A.U.)
CTR
CACHEXIA
G
Trim63 expression (A.U.)
H
Frequency (%)
Minimal Feret's Diameter (μm)
I
Food intake (g)
Day
J
Plasma UnAG (pg/ml)
K
Plasma AG (pg/ml)

Figure 26 (unpublished): The inhibition of PI3Kγ slightly improves muscle wasting in cancer cachexia. (**A**-**F**) Comparison between WT and PI3K$\gamma^{KD/KD}$ mice, at 24 days after LLC injection, of tumor weight (**A**), and percentage of body (**B**), gastrocnemius (**C**), tibialis anterior (**D**), and extensor digitorum longus (**E**) weight loss (N = 10 per group). In C-E percent reduction shown is between non-tumor-bearing and cachectic mice. (**F** and **G**) Atrogin-1 (Fbox32) and MuRF1 (Trim63) expression in tibialis anterior of non-tumor-bearing (CTR) and cachectic (CACHEXIA) mice. N = 5 (CTR) and 9 (CACHEXIA). (**H**) Frequency distribution of minimal Feret's diameter of myofibers of cachectic mice, automatically quantified with ImageProPlus (N = 3 per group). (**I**-**K**) Daily food intake (**I**), and circulating UnAG (**J**) and AG (**K**) levels during cancer cachexia progression (N = 10 per group). **P* < 0.05; ***P* < 0.01.

PI3K$\gamma^{KD/KD}$ mice show skeletal muscle mass preservation in starvation but not in denervation

Although we investigated the role of PI3Kγ in the regulation of AG and UnAG response mainly in cancer cachexia models, we asked whether the induction of the expression of p101 instead p84/87 could be a more general response to stress induced by different stimuli, as previously suggested in other systems [239]. Indeed, we observed that the p101/p84 expression ratio is induced in skeletal muscle during denervation, fasting, and after CTX injection (Fig. 27, A-C). Although in CTX-injected muscles we cannot rule out exactly the contribution of infiltrating inflammatory cells, basally expressing high level of PI3Kγ, these results suggest that an increase in p101/p84 ratio may be a specific response of skeletal muscle to stress. However, PI3Kγ inhibition do not affect skeletal muscle mass in denervation (Fig. 27, D and E). In contrast, muscular mass of PI3K$\gamma^{KD/KD}$ mice is preserved during fasting (Fig. 27, F and G), although body weight is unaffected (Fig. 27H). Although the explanation of these data needs further investigations, it was surprising to find an induction of p101/p84 ratio in skeletal muscle damaged by denervation or fasting, in which we demonstrated a protective activity of UnAG (Porporato 2013). However, based on our hypothesis, the reason could rely on the different fold-increase of p101/p84 ratio observed in denervation, fasting, and cancer cachexia models, negatively correlating with the ability of UnAG to maintain muscle mass, as shown *in vitro*.

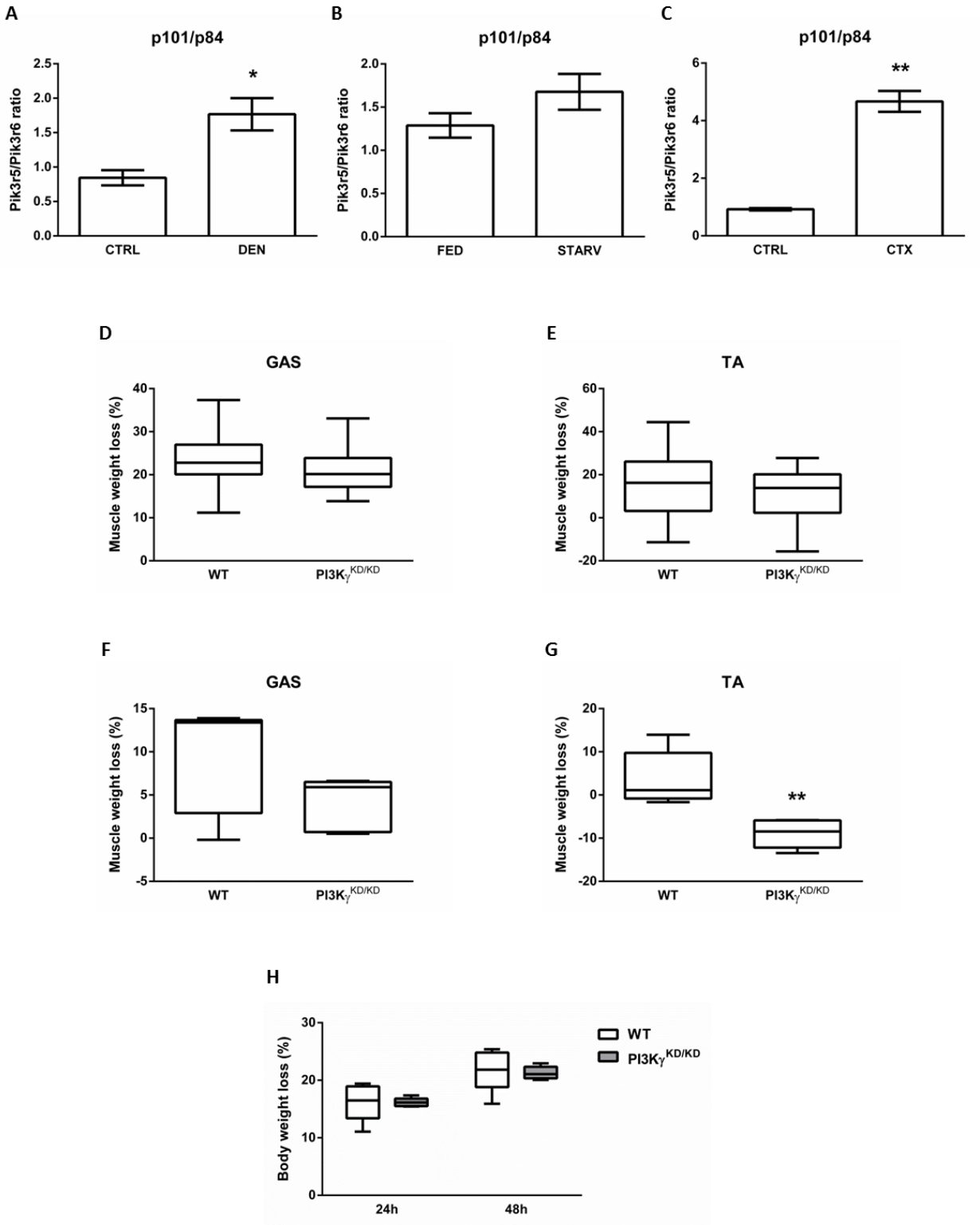

Figure 27 (unpublished): PI3Kγ$^{KD/KD}$ mice are protected from fasting-induced skeletal muscle wasting. (**A**-**C**) Ratio between p101 and p84/87 expression comparing gastrocnemii of controlateral (CTRL) and denervated (DEN) mice after 7 days from sciatic nerve resection (**A**), gastrocnemii of fed and starved (**STARV**) mice after 48-hour of food deprivation (**B**), tibialis anterior of controlateral (CTRL), and CTX-injected (CTX) mice at 24h from inoculation (**C**). N = 4 (Panel A) and N = 5 (Panel B and C). (**D** and **E**) Weight loss of gastrocnemius (**D**) and tibialis anterior (**E**) after 7 days from sciatic nerve resection. In D and E percent reduction shown is between denervated and unperturbed side. N = 10 (WT) and 11 (PI3Kγ$^{KD/KD}$). (**F**-**H**) Effect of 48-hour of fasting. Weight loss of gastrocnemius (**F**) and tibialis anterior (**G**). (**H**) Body weight loss after 24- and 48-hour of food deprivation. In F and G percent reduction shown is between fasted and fed mice. N = 5 per group. *$P < 0.05$; **$P < 0.01$.

DISCUSSION

We demonstrated that AG and UnAG counteract skeletal muscle atrophy both *in vitro*, induced by glucocorticoids treatment, and *in vivo*, induced by either denervation or fasting (Porporato, 2013). Moreover, we provided the first genetic proof for the existence of a second ghrelin receptor distinct by GHSR-1a, herein referred as "GhrlR2". Both AG and UnAG affect directly skeletal muscle, through GhrlR2 activation, without the involvement of the GHSR-1a/GH/IGF-1 axis (Porporato, 2013). Consistently, the anti-atrophic activity of AG and UnAG is distinct with that of IGF-1. Indeed, IGF-1 actions involve both mTORC1 and mTORC2 activation, depend on PI3Kα and do not require the activity of p38 (Porporato, 2013). Interestingly, the physiological role of ghrelin in the coordination of fasting and negative energy balance response is consistent with the inability of both AG and UnAG to induce protein synthesis and hypertrophy, a main feature of IGF-1 anti-atrophic activity.

Surprisingly, we observed that AG lacks anti-atrophic activity in WT mice, while it counteracts atrophy in $Ghsr^{-/-}$ mice. Conversely, UnAG treatment impairs muscle wasting both in WT and in $Ghsr^{-/-}$ mice. Although we would have expected that GHSR-1a/GH/IGF-1 axis would contribute to AG, but not UnAG, anti-atrophic activity, our finding indicates that not only GHSR-1a/GH/IGF-1 axis does not contribute, but impairs the GhrlR2-mediated anti-atrophic activity. Thus, we may raise the hypothesis that, *in vivo*, AG treatment by activating GHSR-1a would result in the inhibition of GhrlR2 function. However, as GHSR-1a is not expressed in skeletal muscle [212], we need to postulate that such cross-regulation is not cell autonomous and would imply the release of a circulating factor from a GHSR-1a-expressing tissue acting on GhrlR2 in the skeletal muscle. Consistently, it has been recently shown that local administration of AG in the skeletal muscle improves insulin sensitivity [211], while systemic administration of AG is diabetogenic and impairs insulin sensitivity in skeletal muscle [210]. These findings support the hypothesis that a circulating factor mediates GHSR-1a and GhrlR2 cross-talk. Although this hypothesis has not proved yet, these findings underscore the different biological significance of AG and UnAG, as indicated by the differences observed in body weight loss of starved mice treated with either AG or UnAG (Fig. 19). In addition, ghrelin and GOAT genes are regulated by distinct transcriptional factors [151], and

circulating levels of AG and UnAG are differently affected during fasting [148], enforcing the concept that UnAG features physiological roles partially distinct from AG. Consistently, it has been reported that only UnAG promotes muscle regeneration upon ischemic damage, further supporting different roles of ghrelin peptides [195]. Although mice carrying ablation of either *Ghrl*, or *Ghsr*, or *GOAT* show no substantial differences in basal conditions compared to WT mice, studies of the response of these mice to either calorie restriction or high-fat diet revealed that ghrelin system is particularly relevant for glucose homeostasis and regulation of body weight [175, 176]. Notably, the double knockout mice lacking both *Ghrl* and *Ghsr* genes show reduced body weight and increased energy expenditure also during a standard diet [270], suggesting that other components, still unidentified, are involved in the ghrelin system. However, the biological significance of the differences between AG and UnAG is still elusive.

A critical point undermining the understanding of AG and UnAG physiology is that the identity of GhrlR2 is still unknown. To address this issue, we are now testing a short list of candidate receptors obtained through two different approaches: i) we tested the ability of UnAG to recruit β-arrestin to the activated GPCR in a multiple screening covering the global portfolio of GPCRs developed by DiscoveRx Corporation; ii) on the other hand, in collaboration with Mauro Giacca at ICGEB in Trieste, we performed a high-throughput-screening (HTS) based on the loss of UnAG anti-apoptotic activity upon transfection of a siRNA library of mouse GPCRs. The discovery of the identity of GhrlR2, and/or other receptors, will help our understanding of ghrelin peptides-receptors interactions and regulation.

The finding that both AG and UnAG impair skeletal muscle atrophy, acting directly on skeletal muscle independently of GHSR-1a activity, prompted us to investigate their ability to improve lean body mass in cancer cachexia. So far, there are no specific drugs counteracting cancer cachexia, in particular targeting skeletal muscle. Indeed, although the loss of skeletal muscle mass and function is the primary cause of death for respiratory failure in cancer patients [51], all the drugs used in clinical practice against cancer cachexia are based on the reduction of anorexia and inflammation. In fact, the two most utilized drugs for cancer cachexia are megestrol acetate, stimulating appetite, and glucocorticoids, inhibiting inflammation, but both of them are ineffective in the long term [50]. Interestingly, it has been recently concluded a phase III clinical trial assessing the efficacy of anamorelin, a GHSR-1a agonist, in counteracting cachexia in NSCLC patients. Although results have not been published yet, clinical data revealed an improvement in lean body

mass and body weight, but few benefits in muscle strength (ESMO 27/09/2014 Press Release: Anamorelin Shown to Improve Appetite and Body Mass in Patients with Cancer Anorexia-Cachexia). Though the ability of anamorelin to activate GhrlR2 has not been proved yet, it is possible that this drug binds also to the novel receptor in the skeletal muscle, thus affecting cancer cachexia through multiple mechanisms. However, it is reasonable to assume that the efficacy of anamorelin resides on its GHSR-1a-mediated orexigenic, GH-releasing, and anti-inflammatory activities, and to a lesser extent on a direct anti-atrophic activity in skeletal muscle. In addition, our finding that AG treatment of WT mice fails to protect from denervation-induced muscle wasting, while it does protect in $Ghsr^{-/-}$ mice, indicating that its anti-atrophic activity is independent from anorexia and/or inflammation, lead us to doubt on the AG ability to directly affect skeletal muscle mass in physiological GHSR-1a-active systems. Moreover, AG-triggered GHSR-1a activation may be detrimental, as it leads to GH-dependent induction of IGF-1, which may enhance tumorigenesis [225], and it is diabetogenic by reducing insulin sensitivity [210]. For these reasons, UnAG, which does not bind to GHSR-1a, might be a promising novel approach for cancer cachexia. Surprisingly, UnAG featured a weak efficacy in counteracting cancer cachexia, suggesting that the GHSR-1a-mediated orexigenic, GH-releasing, and anti-inflammatory activities are indeed the key AG actions underlying its role as anti-cachectic treatment.

However, the weak anti-cachectic efficacy of UnAG observed in LLC-bearing mice may depend on the deregulation of GhrlR2 signaling. Indeed, we demonstrated that GhrlR2 is *bona fide* a $G\alpha_s$-coupled receptor like β-ARs: both induce cAMP pathway, and activate PI3Kβ and PI3Kγ, which reciprocally regulate ligand-triggered signaling. When this fine reciprocal regulation is impaired, the consequence could be a pathologic modulation of agonist response. Indeed, as demonstrated for β-ARs in heart failure [236], we showed that in cancer cachexia p101/p84 expression ratio increases in skeletal muscle. Moreover, we observed a negative correlation between p101 expression and ghrelin response, both *in vitro* and *in vivo*. Our results support the hypothesis that the upregulation of p101, instead p84/87, leads, as previously described [236], to a diminished density of receptors regulated by this mechanism, including GhrlR2. We are currently addressing whether cachectic muscle features a reduced GhrlR2 density at the plasma membrane. Importantly, based on our findings about the ability of different cytokines to finely modulate p101 expression, we can assume that in different genetic backgrounds, cancer types and stages, we will observe different UnAG responses, as suggested by results with conditioned media obtained by C26 and LLC cells. Hence, it is likely that in cachectic patients the modulation of PI3Kγ subunits

expression may be not very linear as we found in LLC cachexia model. Indeed, microarray analysis of muscle biopsies from cachectic patients, did not reveal a clear modulation of p101 and p84/87 expression compared to samples of non-cachectic patients [271]. However, the elucidation of the mechanisms affecting UnAG activity and receptor(s) regulation is crucial to increase our knowledge on cancer cachexia, to better design therapeutics, and to stratify cancer patients.

Interestingly, during cachexia the concentration of circulating AG and total ghrelin is upregulated, independently from the underlying pathology [226-232]. Consistently, we showed that both circulating AG and UnAG are elevated in LLC-bearing mice, and that UnAG is also upregulated in C26 model. This increase may be due by either a compensatory mechanism, in response to reduced food intake and negative energy balance, or an impaired tissues response to ghrelin peptides, or both. The hypothesis of an AG resistance related to GHSR-1a has been already reported [233-235]. Since GHSR-1a is a highly complex receptor that can dimerize with several other receptors, modulating its signaling [128], the mechanism underlying its desensitization may be indirect, but there are no data about it. In contrast, here we showed a GhrlR2-associated resistance in cancer cachexia, due, at least in part, to a deregulation of PI3Kγ. Consistently, we hypothesized that PI3Kγ inhibition could restore, at least in the early stages of cancer cachexia, a physiologic ghrelin response and/or energy balance. However, we found that the only inhibition of PI3Kγ weakly ameliorates cachexia symptoms, but, importantly, induces a delay in circulating UnAG upregulation, suggesting either an improvement in energy balance or in UnAG response. However, these data demonstrate that the postulated increase in the density of PI3Kγ-regulated receptors, including GhrlR2, is not sufficient to significantly counteract cancer cachexia. Otherwise, another explanation may rely on a balanced upregulation of both positive and negative signaling regulating skeletal muscle mass. Indeed, since the internalization mediated by PI3Kγ seems particularly related to $G\alpha_s$-coupled receptors, it has been recently demonstrated that PTH-related hormone, derived from tumor, promotes cancer cachexia [72], and its receptor is a $G\alpha_s$-coupled receptor [272], hence likely regulated by PI3Kγ. However, it needs further investigations to address this issue.

The demonstration that the inhibition of PI3Kγ enhances AG and UnAG actions in both atrophic and basal C2C12 myotubes indicates the crucial role of signal strength. Indeed, cAMP signaling impairs atrophy and induces hypertrophy in skeletal muscle, as revealed by the ability of β2-AR agonists to counteract muscle wasting in several diseases [25]. In particular, it has been

demonstrated that β2-AR agonists improve skeletal muscle mass and functions in cancer cachexia [273-281]. In contrast, the inability of AG and UnAG to induce hypertrophy and to significantly affect skeletal muscle mass in cancer cachexia suggests that the cAMP signal strength is crucial to determine AG/UnAG activity on skeletal muscle mass. Indeed, a possible explanation may rely on the amount of receptors in the plasma membrane. In fact, GhrlR2 is expressed at very low abundance in cardiomyocytes and C2C12 myoblasts, as compared to β2-ARs [184, 189]. The ability of AG and UnAG to induce hypertrophy *in vitro* only in the presence of PI3Kγ inhibitor suggests that the amount of cAMP signaling determines the balance between catabolic and anabolic functions, assuming that the inhibition of PI3Kγ increases GhrlR2 density at the plasma membrane, thus enhancing cAMP signaling triggered by AG and UnAG. In addition to cAMP, another crucial second messenger likely involved in the balance between anti-atrophic/hypertrophic pathways is PIP3, produced by PI3Ks, although this issue needs further investigation. However, to evaluate *in vivo* if UnAG ability to counteract muscle wasting is improved when PI3Kγ is inhibited, we generated *Myh6/Ghrl* X PI3K$\gamma^{KD/KD}$ mice, in which we will assess UnAG protective activity in models of cancer cachexia, denervation, and starvation.

Interestingly, we showed that UnAG enhances satellite cells (SCs) ability to regenerate skeletal muscle and to maintain the stem cells pool (Reano and Angelino, unpublished). It is relevant to note that UnAG pharmacological treatment of $Ghsr^{-/-}$ mice upregulates the Wnt pathway in skeletal muscle (data from [282] analyzed with Panther - http://www.pantherdb.org/), which is crucial in the regulation of SCs and myofibers activities, supporting the concept of an active role of ghrelin peptides in muscle regeneration and mass regulation [26, 27, 283, 284]. AG and UnAG induce C2C12 myoblasts differentiation and fusion into multinucleated myotubes, through activation of p38 [189]. Since p38 is a multi-functional protein, orchestrating different pathway in different conditions [265], it is likely that the ability of ghrelin peptides to induce p38 activation in both myoblasts [189] and myotubes (Porporato 2013) could explain the apparent conflict about the UnAG ability to promote both SCs self-renewal and differentiation. The UnAG unique feature to stimulate the whole SCs-driven repair of damaged skeletal muscle is particular relevant in a cancer cachexia context. Indeed, although the contribution of SCs in the context of skeletal muscle atrophy is poorly understood, it has been demonstrated that in cancer cachexia the regenerative process is deregulated and impaired [57-61]. In particular, although SCs are activated during cancer cachexia, they fail to differentiate into mature myotubes, due by a persistent upregulation

of Pax7 induced by a serum factor(s) still unknown. On one hand, this evidence supports that the high levels of circulating ghrelin peptides do not improve neither muscle mass nor SCs functions. However, on the other hand, it suggests further investigation on the perspective to enhance UnAG signaling in cachexia by inhibition of PI3Kγ. Although we have not still checked, in our models, SCs function and muscle regeneration, we hypothesize that cachectic *Myh6/Ghrl* mice will show an impairment in skeletal muscle regeneration process, despite the high concentration of circulating UnAG, and that cachectic PI3K$\gamma^{KD/KD}$ mice will show a partial restoration in SCs activities, likely affecting also other pro-regenerative factors, including, among others, Wnt-Fzd pathway. Indeed, beyond the UnAG ability to stimulate Wnt pathway, it is likely that, in both SCs and post-mitotic cells, the non-canonical Wnt pathway itself, mediated by a $G\alpha_s$-coupled signaling [26, 285], may be directly affected by PI3Kγ inhibition. Nevertheless, we believe that only the combination of UnAG treatment with PI3Kγ inhibition will significantly affect regeneration process in cancer cachexia.

Although the serum factor(s) impairing regenerative process in cancer cachexia is still elusive [61], it has been shown that TNFα stimulates myogenesis at low concentration (0.05 ng/ml), but, at higher concentration (from 0.5 to 100 ng/ml), TNFα impairs myogenesis [57, 74, 89], suggesting that elevated doses of TNFα, or prolonged exposure to it, lead to a deregulation of regenerative process. Consistently, it has been shown that long-treatment with TNFα induces a biphasic activation of NF-kB, and the second (and persistent) activation results in skeletal muscle decay [88]. Since we demonstrated that p101 is specifically affected by TNFα in a dose-dependent manner, we hypothesize that AG and UnAG response through GhrlR2, should be inversely correlated to TNFα concentration. In fact, it has been demonstrated that UnAG inhibits NF-kB activation triggered by 5 ng/ml TNFα/IFNγ treatment [222], but we showed that UnAG is totally ineffective to impair muscle wasting induced by 10 ng/ml TNFα/IFNγ, inversely reflecting p101 expression. These evidences point out the great relevance of chronic inflammation in regulating tissue pathways, and tissue response to several factors. Since several pathologies are associated with a persistent inflammatory state, such as cancer cachexia, muscle dystrophy, and aging, the study of molecular adaptation to chronic inflammation has strong translational perspectives.

Based on these data, the elevation of ghrelin peptides in cancer cachexia seems rely on a compensation to a ghrelin resistance, through both GHSR-1a and GhrlR2. However, it is likely that other mechanisms contribute to the upregulation of circulating AG and UnAG. Indeed, it may be a consequence of alterations in metabolic, neural, and endocrine pathways, induced as a

physiological response to maintain homeostasis during cancer cachexia. Indeed, several stressors induce changes in the circulating concentration of both AG and UnAG [286]: on one hand, physical stressors, such as exercise, abdominal surgery and endotoxin injection, decrease circulating AG and UnAG concentration; on the other hand, metabolic and psychological inducers of stress, such as caloric restriction, acute fasting, and cold exposure, increase plasma ghrelin peptides [286]. The release of ghrelin peptides from the stomach is the result of multiple simultaneous signals, coming from neural, endocrine, and metabolic systems, as elucidated by the identification of a repertoire of GPCRs regulating ghrelin release [287]. Since it has been recently reported that in cancer cachexia the autonomic nervous system, in particular the sympathetic branch, appears deregulated [115, 116], the increase in plasma ghrelin peptides may reflect this alterations. Indeed, both cholinergic and adrenergic agonists induce ghrelin release from stomach, indicating that the control of circulating ghrelin levels is regulated by both vagal and sympathetic systems [171, 194, 288-290]. Moreover, AG treatment increases muscle sympathetic activity in unperturbed conditions, while AG strongly inhibits it during experimental stress [291], suggesting a fine cross-talk between ghrelin and autonomic nervous system. Hence, circulating ghrelin in cancer cachexia may be, at least in part, the result of stress-related activation/deregulation of the autonomic nervous system, being the main player to maintain homeostasis during stress [292]. Moreover, it has been demonstrated that mTOR activity in the stomach regulates the expression of both ghrelin and GOAT [293]. Since mTOR is activated by positive energy balance, being a sensor of intracellular ATP/AMP ratio [294], it is likely that also this mechanism may be involved in the increase of circulating ghrelin peptides in cancer cachexia. Indeed, the nutritional state is a potent regulator of plasma ghrelin peptides concentration, reciprocally affected by positive and negative energy balance [295], and, in turn, ghrelin is involved in the adaptive response to weight loss [296]. Finally, although the role of insulin in the regulation of circulating ghrelin peptides is not completely understood [165-171], it is likely that the insulin resistance, associated with cancer cachexia [118, 119, 297], contributes to the elevation of plasma ghrelin. In conclusion, all of these physiological responses to cancer, alone or together with the adaptation to ghrelin resistance, may lead to the increase in circulating ghrelin peptides observed in cancer cachexia, and further investigations are needed to assess this issue.

Finally, although tumor-bearing PI3K$\gamma^{KD/KD}$ mice showed weak improvements compared to WT, the inhibition of PI3Kγ preserves skeletal muscle mass during fasting. Indeed, after 48-hour of food deprivation PI3K$\gamma^{KD/KD}$ mice present a significantly reduction of muscle weight loss than WT mice,

while after 7 days from sciatic denervation the are no significant differences in muscle mass between PI3K$\gamma^{KD/KD}$ and WT mice. These findings point out the importance of a systemic response, as in fasting, in the regulation of PI3Kγ. Although these data need further investigations, we can speculate that the reduction of skeletal muscle atrophy observed in starved PI3K$\gamma^{KD/KD}$ mice may be due by an increase of beneficial signaling mediated by Gα_s-coupled receptors, directly in skeletal muscle or in other tissues affecting skeletal muscle.

In conclusion, these data demonstrate that AG and UnAG counteract skeletal muscle atrophy acting directly in skeletal muscle through a still unknown receptor, GhrlR2. Moreover, we showed that cancer cachexia may be associated with a ghrelin resistance related not only to GHSR-1a, but also to the novel GhrlR2. The mechanism of the reduced ghrelin response through the GhrlR2 seems to rely on an upregulation of PI3Kγ, likely leading to a massive internalization of GhrlR2, thus decreasing responsiveness to ghrelin peptides. Finally, we demonstrated that the only inhibition of PI3Kγ in cancer cachexia does not strongly affect lean body mass, but, in contrast, preserves skeletal muscle in fasting. These findings improve our knowledge on ghrelin and PI3Kγ physiology, regulating skeletal muscle mass in both physiological and pathological conditions.

The main forthcoming investigations will be the identification of GhrlR2 receptor, and therefore the evaluation of its expression and regulation in physiological and pathological conditions. The discovery of GhrlR2 receptor will allow not only to better characterize both the ghrelin resistance observed in cancer cachexia and its functions in other physiological systems, but also to design agonists that will have relevant therapeutic implications. Moreover, we will assess if the simultaneous upregulation of UnAG and inhibition of PI3Kγ, obtained either in *Myh6/Ghrl* X PI3K$\gamma^{KD/KD}$ mice or by treating *Myh6/Ghrl* mice with AS605240, as reported [236], improve muscle mass and regenerative potential in cancer cachexia, as well as in denervation and in fasting. Finally, we will evaluate the role of inflammation and other stress in the regulation of PI3Kγ activity in skeletal muscle, and, in turn, we will assess if the increase of p101 expression leads to a downregulation of GhrlR2 density at plasma membrane, thus affecting ghrelin response. Besides the relevance of these investigations to increase our knowledge on the molecular mechanisms underlying cancer cachexia progression, and ghrelin and PI3Kγ physiology, the results obtained will have strong therapeutic and translational implications.

BIBLIOGRAPHY

1. Sandri M. Signaling in muscle atrophy and hypertrophy. Physiology (Bethesda). 2008 Jun;23:160-70. doi: 10.1152/physiol.00041.2007.

2. Schiaffino S, Dyar KA, Ciciliot S, Blaauw B, Sandri M. Mechanisms regulating skeletal muscle growth and atrophy. FEBS J. 2013 Sep;280(17):4294-314. doi: 10.1111/febs.12253.

3. Schiaffino S, Mammucari C. Regulation of skeletal muscle growth by the IGF1-Akt/PKB pathway: insights from genetic models. Skelet Muscle. 2011 Jan 24;1(1):4. doi: 10.1186/2044-5040-1-4.

4. Egerman MA, Glass DJ. Signaling pathways controlling skeletal muscle mass. Crit Rev Biochem Mol Biol. 2014 Jan-Feb;49(1):59-68. doi: 10.3109/10409238.2013.857291.

5. Rui L, Yuan M, Frantz D, Shoelson S, White MF. SOCS-1 and SOCS-3 block insulin signaling by ubiquitin-mediated degradation of IRS1 and IRS2. J Biol Chem. 2002 Nov 1;277(44):42394-8.

6. Shi J, Luo L, Eash J, Ibebunjo C, Glass DJ. The SCF-Fbxo40 complex induces IRS1 ubiquitination in skeletal muscle, limiting IGF1 signaling. Dev Cell. 2011 Nov 15;21(5):835-47. doi: 10.1016/j.devcel.2011.09.011.

7. Murgia M, Serrano AL, Calabria E, Pallafacchina G, Lomo T, Schiaffino S. Ras is involved in nerve-activity-dependent regulation of muscle genes. Nat Cell Biol. 2000 Mar;2(3):142-7.

8. Rommel C, Bodine SC, Clarke BA, Rossman R, Nunez L, Stitt TN, Yancopoulos GD, Glass DJ. Mediation of IGF-1-induced skeletal myotube hypertrophy by PI(3)K/Akt/mTOR and PI(3)K/Akt/GSK3 pathways. Nat Cell Biol. 2001 Nov;3(11):1009-13.

9. Inoki K, Li Y, Zhu T, Wu J, Guan KL. TSC2 is phosphorylated and inhibited by Akt and suppresses mTOR signalling. Nat Cell Biol. 2002 Sep;4(9):648-57.

10. Manning BD, Cantley LC. United at last: the tuberous sclerosis complex gene products connect the phosphoinositide 3-kinase/Akt pathway to mammalian target of rapamycin (mTOR) signalling. Biochem Soc Trans. 2003 Jun;31(Pt 3):573-8.

11. Laplante M, Sabatini DM. mTOR signaling in growth control and disease. Cell. 2012 Apr 13;149(2):274-93. doi: 10.1016/j.cell.2012.03.017.

12. Foster KG, Fingar DC. Mammalian target of rapamycin (mTOR): conducting the cellular signaling symphony. J Biol Chem. 2010 May 7;285(19):14071-7. doi: 10.1074/jbc.R109.094003.

13. Bentzinger CF, Romanino K, Cloëtta D, Lin S, Mascarenhas JB, Oliveri F, Xia J, Casanova E, Costa CF, Brink M, Zorzato F, Hall MN, Rüegg MA. Skeletal muscle-specific ablation of raptor, but not of rictor, causes metabolic changes and results in muscle dystrophy. Cell Metab. 2008 Nov;8(5):411-24. doi: 10.1016/j.cmet.2008.10.002.

14. Bodine SC, Stitt TN, Gonzalez M, Kline WO, Stover GL, Bauerlein R, Zlotchenko E, Scrimgeour A, Lawrence JC, Glass DJ, Yancopoulos GD. Akt/mTOR pathway is a crucial regulator of skeletal muscle hypertrophy and can prevent muscle atrophy in vivo. Nat Cell Biol. 2001 Nov;3(11):1014-9.

15. Pallafacchina G, Calabria E, Serrano AL, Kalhovde JM, Schiaffino S. A protein kinase B-dependent and rapamycin-sensitive pathway controls skeletal muscle growth but not fiber type specification. Proc Natl Acad Sci U S A. 2002 Jul 9;99(14):9213-8.

16. Bodine SC. mTOR signaling and the molecular adaptation to resistance exercise. Med Sci Sports Exerc. 2006 Nov;38(11):1950-7.

17. Taylor WE, Bhasin S, Artaza J, Byhower F, Azam M, Willard DH Jr, Kull FC Jr, Gonzalez-Cadavid N. Myostatin inhibits cell proliferation and protein synthesis in C2C12 muscle cells. Am J Physiol Endocrinol Metab. 2001 Feb;280(2):E221-8.

18. Lee SJ. Regulation of muscle mass by myostatin. Annu Rev Cell Dev Biol.2004;20:61-86.

19. Sartori R, Milan G, Patron M, Mammucari C, Blaauw B, Abraham R, Sandri M. Smad2 and 3 transcription factors control muscle mass in adulthood. Am J Physiol Cell Physiol. 2009 Jun;296(6):C1248-57. doi: 10.1152/ajpcell.00104.2009.

20. McFarlane C, Plummer E, Thomas M, Hennebry A, Ashby M, Ling N, Smith H, Sharma M, Kambadur R. Myostatin induces cachexia by activating the ubiquitin proteolytic system through an NF-kappaB-independent, FoxO1-dependent mechanism. J Cell Physiol. 2006 Nov;209(2):501-14.

21. Trendelenburg AU, Meyer A, Rohner D, Boyle J, Hatakeyama S, Glass DJ. Myostatin reduces Akt/TORC1/p70S6K signaling, inhibiting myoblast differentiation and myotube size. Am J Physiol Cell Physiol. 2009 Jun;296(6):C1258-70. doi: 10.1152/ajpcell.00105.2009.

22. Navegantes LC, Migliorini RH, do Carmo Kettelhut I. Adrenergic control of protein metabolism in skeletal muscle. Curr Opin Clin Nutr Metab Care. 2002 May;5(3):281-6.

23. Lynch GS, Ryall JG. Role of beta-adrenoceptor signaling in skeletal muscle: implications for muscle wasting and disease. Physiol Rev. 2008 Apr;88(2):729-67. doi: 10.1152/physrev.00028.2007.

24. Koopman R, Gehrig SM, Léger B, Trieu J, Walrand S, Murphy KT, Lynch GS. Cellular mechanisms underlying temporal changes in skeletal muscle protein synthesis and breakdown during chronic {beta}-adrenoceptor stimulation in mice. J Physiol. 2010 Dec 1;588(Pt 23):4811-23. doi: 10.1113/jphysiol.2010.196725.

25. Joassard OR, Durieux AC, Freyssenet DG. β2-Adrenergic agonists and the treatment of skeletal muscle wasting disorders. Int J Biochem Cell Biol. 2013 Oct;45(10):2309-21. doi: 10.1016/j.biocel.2013.06.025.

26. von Maltzahn J, Bentzinger CF, Rudnicki MA. Wnt7a-Fzd7 signalling directly activates the Akt/mTOR anabolic growth pathway in skeletal muscle. Nat Cell Biol. 2011 Dec 18;14(2):186-91. doi: 10.1038/ncb2404.

27. Le Grand F, Jones AE, Seale V, Scimè A, Rudnicki MA. Wnt7a activates the planar cell polarity pathway to drive the symmetric expansion of satellite stem cells. Cell Stem Cell. 2009 Jun 5;4(6):535-47. doi: 10.1016/j.stem.2009.03.013.

28. Berdeaux R, Stewart R. cAMP signaling in skeletal muscle adaptation: hypertrophy, metabolism, and regeneration. Am J Physiol Endocrinol Metab. 2012 Jul 1;303(1):E1-17. doi: 10.1152/ajpendo.00555.2011.

29. Minetti GC, Feige JN, Rosenstiel A, Bombard F, Meier V, Werner A, Bassilana F, Sailer AW, Kahle P, Lambert C, Glass DJ, Fornaro M. Gαi2 signaling promotes skeletal muscle hypertrophy, myoblast differentiation, and muscle regeneration. Sci Signal. 2011 Nov 29;4(201):ra80. doi: 10.1126/scisignal.2002038.

30. Cohen S, Nathan JA, Goldberg AL. Muscle wasting in disease: molecular mechanisms and promising therapies. Nat Rev Drug Discov. 2015 Jan;14(1):58-74. doi: 10.1038/nrd4467.

31. Sandri M. Autophagy in skeletal muscle. FEBS Lett. 2010 Apr;584(7):1411-6. doi: 10.1016/j.febslet.2010.01.056.

32. Lecker SH, Goldberg AL, Mitch WE. Protein degradation by the ubiquitin-proteasome pathway in normal and disease states. J Am Soc Nephrol. 2006 Jul;17(7):1807-19.

33. Jagoe RT, Goldberg AL. What do we really know about the ubiquitin-proteasome pathway in muscle atrophy? Curr Opin Clin Nutr Metab Care. 2001 May;4(3):183-90.

34. Gomes MD, Lecker SH, Jagoe RT, Navon A, Goldberg AL. Atrogin-1, a muscle-specific F-box protein highly expressed during muscle atrophy. Proc Natl Acad Sci U S A. 2001 Dec 4;98(25):14440-5.

35. Lecker SH, Jagoe RT, Gilbert A, Gomes M, Baracos V, Bailey J, Price SR, Mitch WE, Goldberg AL. Multiple types of skeletal muscle atrophy involve a common program of changes in gene expression. FASEB J. 2004 Jan;18(1):39-51.

36. Sacheck JM, Hyatt JP, Raffaello A, Jagoe RT, Roy RR, Edgerton VR, Lecker SH, Goldberg AL. Rapid disuse and denervation atrophy involve transcriptional changes similar to those of muscle wasting during systemic diseases. FASEB J. 2007 Jan;21(1):140-55.

37. Kandarian SC, Jackman RW. Intracellular signaling during skeletal muscle atrophy. Muscle Nerve. 2006 Feb;33(2):155-65.

38. Zhao J, Brault JJ, Schild A, Cao P, Sandri M, Schiaffino S, Lecker SH, Goldberg AL. FoxO3 coordinately activates protein degradation by the autophagic/lysosomal and proteasomal pathways in atrophying muscle cells. Cell Metab. 2007 Dec;6(6):472-83.

39. Mammucari C, Milan G, Romanello V, Masiero E, Rudolf R, Del Piccolo P, Burden SJ, Di Lisi R, Sandri C, Zhao J, Goldberg AL, Schiaffino S, Sandri M. FoxO3 controls autophagy in skeletal muscle in vivo. Cell Metab. 2007 Dec;6(6):458-71.

40. Bodine SC, Latres E, Baumhueter S, Lai VK, Nunez L, Clarke BA, Poueymirou WT, Panaro FJ, Na E, Dharmarajan K, Pan ZQ, Valenzuela DM, DeChiara TM, Stitt TN, Yancopoulos GD, Glass DJ. Identification of ubiquitin ligases required for skeletal muscle atrophy. Science. 2001 Nov 23;294(5547):1704-8.

41. Cohen S, Brault JJ, Gygi SP, Glass DJ, Valenzuela DM, Gartner C, Latres E,Goldberg AL. During muscle atrophy, thick, but not thin, filament components are degraded by MuRF1-dependent ubiquitylation. J Cell Biol. 2009 Jun 15;185(6):1083-95. doi: 10.1083/jcb.200901052.

42. Latres E, Amini AR, Amini AA, Griffiths J, Martin FJ, Wei Y, Lin HC, Yancopoulos GD, Glass DJ. Insulin-like growth factor-1 (IGF-1) inversely regulates atrophy-induced genes via the phosphatidylinositol 3-kinase/Akt/mammalian target of rapamycin (PI3K/Akt/mTOR) pathway. J Biol Chem. 2005 Jan 28;280(4):2737-44.

43. Shimizu N, Yoshikawa N, Ito N, Maruyama T, Suzuki Y, Takeda S, Nakae J, Tagata Y, Nishitani S, Takehana K, Sano M, Fukuda K, Suematsu M, Morimoto C, Tanaka H. Crosstalk between glucocorticoid receptor and nutritional sensor mTOR in skeletal muscle. Cell Metab. 2011 Feb 2;13(2):170-82. doi: 10.1016/j.cmet.2011.01.001.

44. Sarbassov DD, Ali SM, Sabatini DM. Growing roles for the mTOR pathway. Curr Opin Cell Biol. 2005 Dec;17(6):596-603.

45. Sandri M, Sandri C, Gilbert A, Skurk C, Calabria E, Picard A, Walsh K, Schiaffino S, Lecker SH, Goldberg AL. Foxo transcription factors induce the atrophy-related ubiquitin ligase atrogin-1 and cause skeletal muscle atrophy. Cell. 2004 Apr 30;117(3):399-412.

46. Kwak KS, Zhou X, Solomon V, Baracos VE, Davis J, Bannon AW, Boyle WJ, Lacey DL, Han HQ. Regulation of protein catabolism by muscle-specific and cytokine-inducible ubiquitin ligase E3alpha-II during cancer cachexia. Cancer Res. 2004 Nov 15;64(22):8193-8.

47. Lokireddy S, Wijesoma IW, Teng S, Bonala S, Gluckman PD, McFarlane C, Sharma M, Kambadur R. The ubiquitin ligase Mul1 induces mitophagy in skeletal muscle in response to muscle-wasting stimuli. Cell Metab. 2012 Nov 7;16(5):613-24. doi: 10.1016/j.cmet.2012.10.005.

48. Sartori R, Schirwis E, Blaauw B, Bortolanza S, Zhao J, Enzo E, Stantzou A, Mouisel E, Toniolo L, Ferry A, Stricker S, Goldberg AL, Dupont S, Piccolo S, Amthor H, Sandri M. BMP signaling controls muscle mass. Nat Genet. 2013 Nov;45(11):1309-18. doi: 10.1038/ng.2772.

49. Tisdale MJ. Cachexia in cancer patients. Nat Rev Cancer. 2002 Nov;2(11):862-71.

50. Argilés JM, Busquets S, Stemmler B, López-Soriano FJ. Cancer cachexia: understanding the molecular basis. Nat Rev Cancer. 2014 Nov;14(11):754-62. doi: 10.1038/nrc3829.

51. Tisdale MJ. Mechanisms of cancer cachexia. Physiol Rev. 2009 Apr;89(2):381-410. doi: 10.1152/physrev.00016.2008.

52. Fearon K, Strasser F, Anker SD, Bosaeus I, Bruera E, Fainsinger RL, Jatoi A, Loprinzi C, MacDonald N, Mantovani G, Davis M, Muscaritoli M, Ottery F, Radbruch L, Ravasco P, Walsh D, Wilcock A, Kaasa S, Baracos VE. Definition and classification of cancer cachexia: an international consensus. Lancet Oncol. 2011 May;12(5):489-95. doi: 10.1016/S1470-2045(10)70218-7.

53. Fearon KC, Glass DJ, Guttridge DC. Cancer cachexia: mediators, signaling, and metabolic pathways. Cell Metab. 2012 Aug 8;16(2):153-66. doi: 10.1016/j.cmet.2012.06.011.

54. Penna F, Baccino FM, Costelli P. Coming back: autophagy in cachexia. Curr Opin Clin Nutr Metab Care. 2014 May;17(3):241-6. doi: 10.1097/MCO.0000000000000048.

55. Acharyya S, Butchbach ME, Sahenk Z, Wang H, Saji M, Carathers M, Ringel MD, Skipworth RJ, Fearon KC, Hollingsworth MA, Muscarella P, Burghes AH, Rafael-Fortney JA, Guttridge DC. Dystrophin glycoprotein complex dysfunction: a regulatory link between muscular dystrophy and cancer cachexia. Cancer Cell. 2005 Nov;8(5):421-32.

56. Suzuki N, Motohashi N, Uezumi A, Fukada S, Yoshimura T, Itoyama Y, Aoki M, Miyagoe-Suzuki Y, Takeda S. NO production results in suspension-induced muscle atrophy through dislocation of neuronal NOS. J Clin Invest. 2007 Sep;117(9):2468-76.

57. Penna F, Costamagna D, Fanzani A, Bonelli G, Baccino FM, Costelli P. Muscle wasting and impaired myogenesis in tumor bearing mice are prevented by ERK inhibition. PLoS One. 2010 Oct 27;5(10):e13604. doi: 10.1371/journal.pone.0013604.

58. Costelli P, Muscaritoli M, Bossola M, Moore-Carrasco R, Crepaldi S, Grieco G, Autelli R, Bonelli G, Pacelli F, Lopez-Soriano FJ, Argilés JM, Doglietto GB, Baccino FM, Rossi Fanelli F. Skeletal muscle wasting in tumor-bearing rats is associated with MyoD down-regulation. Int J Oncol. 2005 Jun;26(6):1663-8.

59. Coletti D, Moresi V, Adamo S, Molinaro M, Sassoon D. Tumor necrosis factor-alpha gene transfer induces cachexia and inhibits muscle regeneration. Genesis. 2005 Nov;43(3):120-8.

60. Schwarzkopf M, Coletti D, Sassoon D, Marazzi G. Muscle cachexia is regulated by a p53-PW1/Peg3-dependent pathway. Genes Dev. 2006 Dec 15;20(24):3440-52.

61. He WA, Berardi E, Cardillo VM, Acharyya S, Aulino P, Thomas-Ahner J, Wang J, Bloomston M, Muscarella P, Nau P, Shah N, Butchbach ME, Ladner K, Adamo S, Rudnicki MA, Keller C, Coletti D, Montanaro F, Guttridge DC. NF-κB-mediated Pax7 dysregulation in the muscle microenvironment promotes cancer cachexia. J Clin Invest. 2013 Nov;123(11):4821-35.

62. Olguin HC, Olwin BB. Pax-7 up-regulation inhibits myogenesis and cell cycle progression in satellite cells: a potential mechanism for self-renewal. Dev Biol. 2004 Nov 15;275(2):375-88.

63. Agustsson T, Rydén M, Hoffstedt J, van Harmelen V, Dicker A, Laurencikiene J, Isaksson B, Permert J, Arner P. Mechanism of increased lipolysis in cancer cachexia. Cancer Res. 2007 Jun 1;67(11):5531-7.

64. Krauss S, Zhang CY, Lowell BB. The mitochondrial uncoupling-protein homologues. Nat Rev Mol Cell Biol. 2005 Mar;6(3):248-61.

65. Beck SA, Mulligan HD, Tisdale MJ. Lipolytic factors associated with murine and human cancer cachexia. J Natl Cancer Inst. 1990 Dec 19;82(24):1922-6. PubMed PMID: 2250313.

66. Islam-Ali BS, Tisdale MJ. Effect of a tumour-produced lipid-mobilizing factor on protein synthesis and degradation. Br J Cancer. 2001 Jun 15;84(12):1648-55.

67. Todorov PT, McDevitt TM, Cariuk P, Coles B, Deacon M, Tisdale MJ. Induction of muscle protein degradation and weight loss by a tumor product. Cancer Res. 1996 Mar 15;56(6):1256-61.

68. Cariuk P, Lorite MJ, Todorov PT, Field WN, Wigmore SJ, Tisdale MJ. Induction of cachexia in mice by a product isolated from the urine of cachectic cancer patients. Br J Cancer. 1997;76(5):606-13.

69. Todorov PT, Wyke SM, Tisdale MJ. Identification and characterization of a membrane receptor for proteolysis-inducing factor on skeletal muscle. Cancer Res. 2007 Dec 1;67(23):11419-27.

70. Watchorn TM, Waddell I, Ross JA. Proteolysis-inducing factor differentially influences transcriptional regulation in endothelial subtypes. Am J Physiol Endocrinol Metab. 2002 Apr;282(4):E763-9.

71. Watchorn TM, Dowidar N, Dejong CH, Waddell ID, Garden OJ, Ross JA. The cachectic mediator proteolysis inducing factor activates NF-kappaB and STAT3 in human Kupffer cells and monocytes. Int J Oncol. 2005 Oct;27(4):1105-11.

72. Kir S, White JP, Kleiner S, Kazak L, Cohen P, Baracos VE, Spiegelman BM. Tumour-derived PTH-related protein triggers adipose tissue browning and cancer cachexia. Nature. 2014 Sep 4;513(7516):100-4. doi: 10.1038/nature13528.

73. Ruan H, Hacohen N, Golub TR, Van Parijs L, Lodish HF. Tumor necrosis factor-alpha suppresses adipocyte-specific genes and activates expression of preadipocyte genes in 3T3-L1 adipocytes: nuclear factor-kappaB activation by TNF-alpha is obligatory. Diabetes. 2002 May;51(5):1319-36.

74. Guttridge DC, Mayo MW, Madrid LV, Wang CY, Baldwin AS Jr. NF-kappaB-induced loss of MyoD messenger RNA: possible role in muscle decay and cachexia. Science. 2000 Sep 29;289(5488):2363-6.

75. Oliff A, Defeo-Jones D, Boyer M, Martinez D, Kiefer D, Vuocolo G, Wolfe A, Socher SH. Tumors secreting human TNF/cachectin induce cachexia in mice. Cell. 1987 Aug 14;50(4):555-63.

76. García-Martínez C, López-Soriano FJ, Argilés JM. Acute treatment with tumour necrosis factor-alpha induces changes in protein metabolism in rat skeletal muscle. Mol Cell Biochem. 1993 Aug 11;125(1):11-8.

77. Bhatnagar S, Panguluri SK, Gupta SK, Dahiya S, Lundy RF, Kumar A. Tumor necrosis factor-α regulates distinct molecular pathways and gene networks in cultured skeletal muscle cells. PLoS One. 2010 Oct 12;5(10):e13262. doi: 10.1371/journal.pone.0013262.

78. Li YP, Chen Y, John J, Moylan J, Jin B, Mann DL, Reid MB. TNF-alpha acts via p38 MAPK to stimulate expression of the ubiquitin ligase atrogin1/MAFbx in skeletal muscle. FASEB J. 2005 Mar;19(3):362-70.

79. Frost RA, Nystrom GJ, Jefferson LS, Lang CH. Hormone, cytokine, and nutritional regulation of sepsis-induced increases in atrogin-1 and MuRF1 in skeletal muscle. Am J Physiol Endocrinol Metab. 2007 Feb;292(2):E501-12.

80. Moylan JS, Smith JD, Chambers MA, McLoughlin TJ, Reid MB. TNF induction of atrogin-1/MAFbx mRNA depends on Foxo4 expression but not AKT-Foxo1/3 signaling. Am J Physiol Cell Physiol. 2008 Oct;295(4):C986-93. doi: 10.1152/ajpcell.00041.2008.

81. Sishi BJ, Engelbrecht AM. Tumor necrosis factor alpha (TNF-α) inactivates the PI3-kinase/PKB pathway and induces atrophy and apoptosis in L6 myotubes. Cytokine. 2011 May;54(2):173-84. doi: 10.1016/j.cyto.2011.01.009.

82. Buck M, Chojkier M. Muscle wasting and dedifferentiation induced by oxidative stress in a murine model of cachexia is prevented by inhibitors of nitric oxide synthesis and antioxidants. EMBO J. 1996 Apr 15;15(8):1753-65.

83. Li YP, Reid MB. NF-kappaB mediates the protein loss induced by TNF-alpha in differentiated skeletal muscle myotubes. Am J Physiol Regul Integr Comp Physiol. 2000 Oct;279(4):R1165-70.

84. de Alvaro C, Teruel T, Hernandez R, Lorenzo M. Tumor necrosis factor alpha produces insulin resistance in skeletal muscle by activation of inhibitor kappaB kinase in a p38 MAPK-dependent manner. J Biol Chem. 2004 Apr 23;279(17):17070-8.
85. Rydén M, Arvidsson E, Blomqvist L, Perbeck L, Dicker A, Arner P. Targets for TNF-alpha-induced lipolysis in human adipocytes. Biochem Biophys Res Commun. 2004 May 21;318(1):168-75.

86. Laurencikiene J, van Harmelen V, Arvidsson Nordström E, Dicker A, Blomqvist L, Näslund E, Langin D, Arner P, Rydén M. NF-kappaB is important for TNF-alpha-induced lipolysis in human adipocytes. J Lipid Res. 2007 May;48(5):1069-77.

87. Alvarez B, Quinn LS, Busquets S, López-Soriano FJ, Argilés JM. Direct effects of tumor necrosis factor alpha (TNF-alpha) on murine skeletal muscle cell lines. Bimodal effects on protein metabolism. Eur Cytokine Netw. 2001 Jul-Sep;12(3):399-410.

88. Ladner KJ, Caligiuri MA, Guttridge DC. Tumor necrosis factor-regulated biphasic activation of NF-kappa B is required for cytokine-induced loss of skeletal muscle gene products. J Biol Chem. 2003 Jan 24;278(4):2294-303.

89. Chen SE, Jin B, Li YP. TNF-alpha regulates myogenesis and muscle regeneration by activating p38 MAPK. Am J Physiol Cell Physiol. 2007 May;292(5):C1660-71.

90. Scott HR, McMillan DC, Crilly A, McArdle CS, Milroy R. The relationship between weight loss and interleukin 6 in non-small-cell lung cancer. Br J Cancer. 1996 Jun;73(12):1560-2.

91. Martín F, Santolaria F, Batista N, Milena A, González-Reimers E, Brito MJ, Oramas J. Cytokine levels (IL-6 and IFN-gamma), acute phase response and nutritional status as prognostic factors in lung cancer. Cytokine. 1999 Jan;11(1):80-6.

92. Moses AG, Maingay J, Sangster K, Fearon KC, Ross JA. Pro-inflammatory cytokine release by peripheral blood mononuclear cells from patients with advanced pancreatic cancer: relationship to acute phase response and survival. Oncol Rep. 2009 Apr;21(4):1091-5.

93. Iwase S, Murakami T, Saito Y, Nakagawa K. Steep elevation of blood interleukin-6 (IL-6) associated only with late stages of cachexia in cancer patients. Eur Cytokine Netw. 2004 Oct-Dec;15(4):312-6.

94. Narsale AA, Carson JA. Role of interleukin-6 in cachexia: therapeutic implications. Curr Opin Support Palliat Care. 2014 Dec;8(4):321-7. doi: 10.1097/SPC.0000000000000091.

95. Bonetto A, Aydogdu T, Kunzevitzky N, Guttridge DC, Khuri S, Koniaris LG, Zimmers TA. STAT3 activation in skeletal muscle links muscle wasting and the acute phase response in cancer cachexia. PLoS One. 2011;6(7):e22538. doi: 10.1371/journal.pone.0022538.

96. Petruzzelli M, Schweiger M, Schreiber R, Campos-Olivas R, Tsoli M, Allen J, Swarbrick M, Rose-John S, Rincon M, Robertson G, Zechner R, Wagner EF. A switch from white to brown fat increases energy expenditure in cancer-associated cachexia. Cell Metab. 2014 Sep 2;20(3):433-47. doi: 10.1016/j.cmet.2014.06.011.

97. Strassmann G, Fong M, Kenney JS, Jacob CO. Evidence for the involvement of interleukin 6 in experimental cancer cachexia. J Clin Invest. 1992 May;89(5):1681-4.

98. Bonetto A, Aydogdu T, Jin X, Zhang Z, Zhan R, Puzis L, Koniaris LG, Zimmers TA. JAK/STAT3 pathway inhibition blocks skeletal muscle wasting downstream of IL-6 and in experimental cancer cachexia. Am J Physiol Endocrinol Metab. 2012 Aug 1;303(3):E410-21. doi: 10.1152/ajpendo.00039.2012.

99. Muñoz-Cánoves P, Scheele C, Pedersen BK, Serrano AL. Interleukin-6 myokine signaling in skeletal muscle: a double-edged sword? FEBS J. 2013 Sep;280(17):4131-48. doi: 10.1111/febs.12338.

100. Costelli P, Muscaritoli M, Bonetto A, Penna F, Reffo P, Bossola M, Bonelli G, Doglietto GB, Baccino FM, Rossi Fanelli F. Muscle myostatin signalling is enhanced in experimental cancer cachexia. Eur J Clin Invest. 2008 Jul;38(7):531-8. doi: 10.1111/j.1365-2362.2008.01970.x.

101. Seder CW, Hartojo W, Lin L, Silvers AL, Wang Z, Thomas DG, Giordano TJ, Chen G, Chang AC, Orringer MB, Beer DG. Upregulated INHBA expression may promote cell proliferation and is associated with poor survival in lung adenocarcinoma. Neoplasia. 2009 Apr;11(4):388-96.

102. Thomas TZ, Wang H, Niclasen P, O'Bryan MK, Evans LW, Groome NP, Pedersen J, Risbridger GP. Expression and localization of activin subunits and follistatins in tissues from men with high grade prostate cancer. J Clin Endocrinol Metab. 1997 Nov;82(11):3851-8.

103. Wildi S, Kleeff J, Maruyama H, Maurer CA, Büchler MW, Korc M. Overexpression of activin A in stage IV colorectal cancer. Gut. 2001 Sep;49(3):409-17.

104. Zhou X, Wang JL, Lu J, Song Y, Kwak KS, Jiao Q, Rosenfeld R, Chen Q, Boone T, Simonet WS, Lacey DL, Goldberg AL, Han HQ. Reversal of cancer cachexia and muscle wasting by ActRIIB antagonism leads to prolonged survival. Cell. 2010 Aug 20;142(4):531-43. doi: 10.1016/j.cell.2010.07.011.

105. Brink M, Price SR, Chrast J, Bailey JL, Anwar A, Mitch WE, Delafontaine P. Angiotensin II induces skeletal muscle wasting through enhanced protein degradation and down-regulates autocrine insulin-like growth factor I. Endocrinology. 2001 Apr;142(4):1489-96.

106. Yoshida T, Tabony AM, Galvez S, Mitch WE, Higashi Y, Sukhanov S, Delafontaine P. Molecular mechanisms and signaling pathways of angiotensin II-induced muscle wasting: potential therapeutic targets for cardiac cachexia. Int J Biochem Cell Biol. 2013 Oct;45(10):2322-32. doi: 10.1016/j.biocel.2013.05.035.

107. Grossberg AJ, Scarlett JM, Marks DL. Hypothalamic mechanisms in cachexia. Physiol Behav. 2010 Jul 14;100(5):478-89. doi: 10.1016/j.physbeh.2010.03.011.

108. Hyltander A, Drott C, Körner U, Sandström R, Lundholm K. Elevated energy expenditure in cancer patients with solid tumours. Eur J Cancer. 1991;27(1):9-15.

109. Falconer JS, Fearon KC, Plester CE, Ross JA, Carter DC. Cytokines, the acute-phase response, and resting energy expenditure in cachectic patients with pancreatic cancer. Ann Surg. 1994 Apr;219(4):325-31.

110. Evans WK, Makuch R, Clamon GH, Feld R, Weiner RS, Moran E, Blum R, Shepherd FA, Jeejeebhoy KN, DeWys WD. Limited impact of total parenteral nutrition on nutritional status during treatment for small cell lung cancer. Cancer Res. 1985 Jul;45(7):3347-53.

111. Argilés JM, López-Soriano FJ, Busquets S. Muscle wasting in cancer: the role of mitochondria. Curr Opin Clin Nutr Metab Care. 2015 Mar 12.

112. Miura S, Tomitsuka E, Kamei Y, Yamazaki T, Kai Y, Tamura M, Kita K, Nishino I, Ezaki O. Overexpression of peroxisome proliferator-activated receptor gamma co-activator-1alpha leads to muscle atrophy with depletion of ATP. Am J Pathol. 2006 Oct;169(4):1129-39.

113. Bindels LB, Delzenne NM. Muscle wasting: the gut microbiota as a new therapeutic target? Int J Biochem Cell Biol. 2013 Oct;45(10):2186-90. doi: 10.1016/j.biocel.2013.06.021.

114. Menconi MJ, Arany ZP, Alamdari N, Aversa Z, Gonnella P, O'Neal P, Smith IJ, Tizio S, Hasselgren PO. Sepsis and glucocorticoids downregulate the expression of the nuclear cofactor PGC-1beta in skeletal muscle. Am J Physiol Endocrinol Metab. 2010 Oct;299(4):E533-43. doi: 10.1152/ajpendo.00596.2009.

115. Hundsberger T, Omlin A, Haegele-Link S, Vehoff J, Strasser F. Autonomic dysfunction in cancer cachexia coincides with large fiber polyneuropathy. J Pain Symptom Manage. 2014 Oct;48(4):611-8.e1. doi: 10.1016/j.jpainsymman.2013.11.018.

116. Chauhan A, Sequeria A, Manderson C, Maddocks M, Wasley D, Wilcock A. Exploring autonomic nervous system dysfunction in patients with cancer cachexia: a pilot study. Auton Neurosci. 2012 Jan 26;166(1-2):93-5. doi: 10.1016/j.autneu.2011.09.006.

117. Kovacheva EL, Hikim AP, Shen R, Sinha I, Sinha-Hikim I. Testosterone supplementation reverses sarcopenia in aging through regulation of myostatin, c-Jun NH2-terminal kinase, Notch, and Akt signaling pathways. Endocrinology. 2010 Feb;151(2):628-38. doi: 10.1210/en.2009-1177.

118. Asp ML, Tian M, Wendel AA, Belury MA. Evidence for the contribution of insulin resistance to the development of cachexia in tumor-bearing mice. Int J Cancer. 2010 Feb 1;126(3):756-63. doi: 10.1002/ijc.24784.

119. Agustsson T, D'souza MA, Nowak G, Isaksson B. Mechanisms for skeletal muscle insulin resistance in patients with pancreatic ductal adenocarcinoma. Nutrition. 2011 Jul-Aug;27(7-8):796-801. doi: 10.1016/j.nut.2010.08.022.

120. Zechner R, Zimmermann R, Eichmann TO, Kohlwein SD, Haemmerle G, Lass A, Madeo F. FAT SIGNALS--lipases and lipolysis in lipid metabolism and signaling. Cell Metab. 2012 Mar 7;15(3):279-91. doi: 10.1016/j.cmet.2011.12.018.

121. Das SK, Eder S, Schauer S, Diwoky C, Temmel H, Guertl B, Gorkiewicz G, Tamilarasan KP, Kumari P, Trauner M, Zimmermann R, Vesely P, Haemmerle G, Zechner R, Hoefler G. Adipose triglyceride lipase contributes to cancer-associated cachexia. Science. 2011 Jul 8;333(6039):233-8. doi: 10.1126/science.1198973.

122. Das SK, Hoefler G. The role of triglyceride lipases in cancer associated cachexia. Trends Mol Med. 2013 May;19(5):292-301. doi: 10.1016/j.molmed.2013.02.006.

123. Kojima M, Hosoda H, Date Y, Nakazato M, Matsuo H, Kangawa K. Ghrelin is a growth-hormone-releasing acylated peptide from stomach. Nature. 1999 Dec 9;402(6762):656-60.

124. Howard AD, Feighner SD, Cully DF, Arena JP, Liberator PA, Rosenblum CI, Hamelin M, Hreniuk DL, Palyha OC, Anderson J, Paress PS, Diaz C, Chou M, Liu KK, McKee KK, Pong SS, Chaung LY, Elbrecht A, Dashkevicz M, Heavens R, Rigby M, Sirinathsinghji DJ, Dean DC, Melillo DG, Patchett AA, Nargund R, Griffin PR, DeMartino JA, Gupta SK, Schaeffer JM, Smith RG, Van der Ploeg LH. A receptor in

pituitary and hypothalamus that functions in growth hormone release. Science. 1996 Aug 16;273(5277):974-7.

125. Nishi Y, Yoh J, Hiejima H, Kojima M. Structures and molecular forms of the ghrelin-family peptides. Peptides. 2011 Nov;32(11):2175-82. doi: 10.1016/j.peptides.2011.07.024.

126. Kanamoto N, Akamizu T, Tagami T, Hataya Y, Moriyama K, Takaya K, Hosoda H, Kojima M, Kangawa K, Nakao K. Genomic structure and characterization of the 5'-flanking region of the human ghrelin gene. Endocrinology. 2004 Sep;145(9):4144-53.

127. Soares JB, Leite-Moreira AF. Ghrelin, des-acyl ghrelin and obestatin: three pieces of the same puzzle. Peptides. 2008 Jul;29(7):1255-70. doi: 10.1016/j.peptides.2008.02.018.

128. Delporte C. Structure and physiological actions of ghrelin. Scientifica (Cairo). 2013;2013:518909. doi: 10.1155/2013/518909.

129. Zhu X, Cao Y, Voogd K, Steiner DF. On the processing of proghrelin to ghrelin. J Biol Chem. 2006 Dec 15;281(50):38867-70.

130. Taylor MS, Ruch TR, Hsiao PY, Hwang Y, Zhang P, Dai L, Huang CR, Berndsen CE, Kim MS, Pandey A, Wolberger C, Marmorstein R, Machamer C, Boeke JD, Cole PA. Architectural organization of the metabolic regulatory enzyme ghrelin O-acyltransferase. J Biol Chem. 2013 Nov 8;288(45):32211-28. doi: 10.1074/jbc.M113.510313.

131. Yang J, Brown MS, Liang G, Grishin NV, Goldstein JL. Identification of the acyltransferase that octanoylates ghrelin, an appetite-stimulating peptide hormone. Cell. 2008 Feb 8;132(3):387-96. doi: 10.1016/j.cell.2008.01.017.

132. Gutierrez JA, Solenberg PJ, Perkins DR, Willency JA, Knierman MD, Jin Z, Witcher DR, Luo S, Onyia JE, Hale JE. Ghrelin octanoylation mediated by an orphan lipid transferase. Proc Natl Acad Sci U S A. 2008 Apr 29;105(17):6320-5. doi: 10.1073/pnas.0800708105.

133. Gahete MD, Rincón-Fernández D, Villa-Osaba A, Hormaechea-Agulla D, Ibáñez-Costa A, Martínez-Fuentes AJ, Gracia-Navarro F, Castaño JP, Luque RM. Ghrelin gene products, receptors, and GOAT enzyme: biological and pathophysiological insight. J Endocrinol. 2013 Dec 2;220(1):R1-24. doi: 10.1530/JOE-13-0391.

134. Zhang JV, Ren PG, Avsian-Kretchmer O, Luo CW, Rauch R, Klein C, Hsueh AJ. Obestatin, a peptide encoded by the ghrelin gene, opposes ghrelin's effects on food intake. Science. 2005 Nov 11;310(5750):996-9.

135. Chartrel N, Alvear-Perez R, Leprince J, Iturrioz X, Reaux-Le Goazigo A, Audinot V, Chomarat P, Coge F, Nosjean O, Rodriguez M, Galizzi JP, Boutin JA, Vaudry H, Llorens-Cortes C. Comment on "Obestatin, a peptide encoded by the ghrelin gene, opposes ghrelin's effects on food intake". Science. 2007 Feb 9;315(5813):766; author reply 766.

136. Lauwers E, Landuyt B, Arckens L, Schoofs L, Luyten W. Obestatin does not activate orphan G protein-coupled receptor GPR39. Biochem Biophys Res Commun. 2006 Dec 8;351(1):21-5.

137. Trovato L, Gallo D, Settanni F, Gesmundo I, Ghigo E, Granata R. Obestatin: is it really doing something? Front Horm Res. 2014;42:175-85. doi: 10.1159/000358346.

138. Nishi Y, Mifune H, Yabuki A, Tajiri Y, Hirata R, Tanaka E, Hosoda H, Kangawa K, Kojima M. Changes in Subcellular Distribution of n-Octanoyl or n-Decanoyl Ghrelin in Ghrelin-Producing Cells. Front Endocrinol (Lausanne). 2013 Jul 9;4:84. doi: 10.3389/fendo.2013.00084.

139. Nishi Y, Hiejima H, Hosoda H, Kaiya H, Mori K, Fukue Y, Yanase T, Nawata H, Kangawa K, Kojima M. Ingested medium-chain fatty acids are directly utilized for the acyl modification of ghrelin. Endocrinology. 2005 May;146(5):2255-64.

140. Nishi Y, Mifune H, Kojima M. Ghrelin acylation by ingestion of medium-chain fatty acids. Methods Enzymol. 2012;514:303-15. doi: 10.1016/B978-0-12-381272-8.00019-2.

141. González CR, Vázquez MJ, López M, Diéguez C. Influence of chronic undernutrition and leptin on GOAT mRNA levels in rat stomach mucosa. J Mol Endocrinol. 2008 Dec;41(6):415-21. doi: 10.1677/JME-08-0102.

142. Soriano-Guillén L, Barrios V, Campos-Barros A, Argente J. Ghrelin levels in obesity and anorexia nervosa: effect of weight reduction or recuperation. J Pediatr. 2004 Jan;144(1):36-42.

143. Tschöp M, Smiley DL, Heiman ML. Ghrelin induces adiposity in rodents. Nature. 2000 Oct 19;407(6806):908-13.

144. Nakazato M, Murakami N, Date Y, Kojima M, Matsuo H, Kangawa K, Matsukura S. A role for ghrelin in the central regulation of feeding. Nature. 2001 Jan 11;409(6817):194-8.

145. Cummings DE. Ghrelin and the short- and long-term regulation of appetite and body weight. Physiol Behav. 2006 Aug 30;89(1):71-84.

146. van der Lely AJ, Tschöp M, Heiman ML, Ghigo E. Biological, physiological, pathophysiological, and pharmacological aspects of ghrelin. Endocr Rev. 2004 Jun;25(3):426-57.

147. Frecka JM, Mattes RD. Possible entrainment of ghrelin to habitual meal patterns in humans. Am J Physiol Gastrointest Liver Physiol. 2008 Mar;294(3):G699-707. doi: 10.1152/ajpgi.00448.2007.

148. Kirchner H, Gutierrez JA, Solenberg PJ, Pfluger PT, Czyzyk TA, Willency JA, Schürmann A, Joost HG, Jandacek RJ, Hale JE, Heiman ML, Tschöp MH. GOAT links dietary lipids with the endocrine control of energy balance. Nat Med. 2009 Jul;15(7):741-5. doi: 10.1038/nm.1997.

149. Date Y, Murakami N, Kojima M, Kuroiwa T, Matsukura S, Kangawa K, Nakazato M. Central effects of a novel acylated peptide, ghrelin, on growth hormone release in rats. Biochem Biophys Res Commun. 2000 Aug 28;275(2):477-80.

150. Liu J, Prudom CE, Nass R, Pezzoli SS, Oliveri MC, Johnson ML, Veldhuis P, Gordon DA, Howard AD, Witcher DR, Geysen HM, Gaylinn BD, Thorner MO. Novel ghrelin assays provide evidence for independent regulation of ghrelin acylation and secretion in healthy young men. J Clin Endocrinol Metab. 2008 May;93(5):1980-7. doi: 10.1210/jc.2007-2235.

151. Shiimura Y, Ohgusu H, Sato T, Kojima M. Regulation of the Human Ghrelin Promoter Activity by Transcription Factors, NF-κB and Nkx2.2. Int J Endocrinol. 2015;2015:580908. doi: 10.1155/2015/580908.

152. Sun Y, Wang P, Zheng H, Smith RG. Ghrelin stimulation of growth hormone release and appetite is mediated through the growth hormone secretagogue receptor. Proc Natl Acad Sci U S A. 2004 Mar 30;101(13):4679-84.

153. Sun Y, Ahmed S, Smith RG. Deletion of ghrelin impairs neither growth nor appetite. Mol Cell Biol. 2003 Nov;23(22):7973-81.

154. Prodam F, Filigheddu N. Ghrelin gene products in acute and chronic inflammation. Arch Immunol Ther Exp (Warsz). 2014 Oct;62(5):369-84. doi: 10.1007/s00005-014-0287-9.

155. Dixit VD, Schaffer EM, Pyle RS, Collins GD, Sakthivel SK, Palaniappan R, Lillard JW Jr, Taub DD. Ghrelin inhibits leptin- and activation-induced proinflammatory cytokine expression by human monocytes and T cells. J Clin Invest. 2004 Jul;114(1):57-66.

156. Dixit VD, Yang H, Cooper-Jenkins A, Giri BB, Patel K, Taub DD. Reduction of T cell-derived ghrelin enhances proinflammatory cytokine expression: implications for age-associated increases in inflammation. Blood. 2009 May 21;113(21):5202-5. doi: 10.1182/blood-2008-09-181255.

157. Dixit VD, Yang H, Sun Y, Weeraratna AT, Youm YH, Smith RG, Taub DD. Ghrelin promotes thymopoiesis during aging. J Clin Invest. 2007 Oct;117(10):2778-90.

158. Wierup N, Svensson H, Mulder H, Sundler F. The ghrelin cell: a novel developmentally regulated islet cell in the human pancreas. Regul Pept. 2002 Jul 15;107(1-3):63-9.

159. Date Y, Nakazato M, Hashiguchi S, Dezaki K, Mondal MS, Hosoda H, Kojima M, Kangawa K, Arima T, Matsuo H, Yada T, Matsukura S. Ghrelin is present in pancreatic alpha-cells of humans and rats and stimulates insulin secretion. Diabetes. 2002 Jan;51(1):124-9.

160. Dezaki K, Hosoda H, Kakei M, Hashiguchi S, Watanabe M, Kangawa K, Yada T. Endogenous ghrelin in pancreatic islets restricts insulin release by attenuating Ca2+ signaling in beta-cells: implication in the glycemic control in rodents. Diabetes. 2004 Dec;53(12):3142-51.

161. Granata R, Baragli A, Settanni F, Scarlatti F, Ghigo E. Unraveling the role of the ghrelin gene peptides in the endocrine pancreas. J Mol Endocrinol. 2010 Sep;45(3):107-18. doi: 10.1677/JME-10-0019.

162. Chuang JC, Sakata I, Kohno D, Perello M, Osborne-Lawrence S, Repa JJ, Zigman JM. Ghrelin directly stimulates glucagon secretion from pancreatic alpha-cells. Mol Endocrinol. 2011 Sep;25(9):1600-11. doi: 10.1210/me.2011-1001.

163. Damjanovic SS, Lalic NM, Pesko PM, Petakov MS, Jotic A, Miljic D, Lalic KS, Lukic L, Djurovic M, Djukic VB. Acute effects of ghrelin on insulin secretion and glucose disposal rate in gastrectomized patients. J Clin Endocrinol Metab. 2006 Jul;91(7):2574-81.

164. Vestergaard ET, Gormsen LC, Jessen N, Lund S, Hansen TK, Moller N, Jorgensen JO. Ghrelin infusion in humans induces acute insulin resistance and lipolysis independent of growth hormone signaling. Diabetes. 2008 Dec;57(12):3205-10. doi: 10.2337/db08-0025.

165. Saad MF, Bernaba B, Hwu CM, Jinagouda S, Fahmi S, Kogosov E, Boyadjian R. Insulin regulates plasma ghrelin concentration. J Clin Endocrinol Metab. 2002 Aug;87(8):3997-4000.

166. Briggs DI, Andrews ZB. A recent update on the role of ghrelin in glucose homeostasis. Curr Diabetes Rev. 2011 May;7(3):201-7.

167. Flanagan DE, Evans ML, Monsod TP, Rife F, Heptulla RA, Tamborlane WV, Sherwin RS. The influence of insulin on circulating ghrelin. Am J Physiol Endocrinol Metab. 2003 Feb;284(2):E313-6.

168. Möhlig M, Spranger J, Otto B, Ristow M, Tschöp M, Pfeiffer AF. Euglycemic hyperinsulinemia, but not lipid infusion, decreases circulating ghrelin levels in humans. J Endocrinol Invest. 2002 Dec;25(11):RC36-8.

169. Caixás A, Bashore C, Nash W, Pi-Sunyer F, Laferrère B. Insulin, unlike food intake, does not suppress ghrelin in human subjects. J Clin Endocrinol Metab. 2002 Apr;87(4):1902.

170. Schaller G, Schmidt A, Pleiner J, Woloszczuk W, Wolzt M, Luger A. Plasma ghrelin concentrations are not regulated by glucose or insulin: a double-blind, placebo-controlled crossover clamp study. Diabetes. 2003 Jan;52(1):16-20.

171. Mundinger TO, Cummings DE, Taborsky GJ Jr. Direct stimulation of ghrelin secretion by sympathetic nerves. Endocrinology. 2006 Jun;147(6):2893-901.

172. Gauna C, Delhanty PJ, Hofland LJ, Janssen JA, Broglio F, Ross RJ, Ghigo E, van der Lely AJ. Ghrelin stimulates, whereas des-octanoyl ghrelin inhibits, glucose output by primary hepatocytes. J Clin Endocrinol Metab. 2005 Feb;90(2):1055-60.

173. Broglio F, Prodam F, Me E, Riganti F, Lucatello B, Granata R, Benso A, Muccioli G, Ghigo E. Ghrelin: endocrine, metabolic and cardiovascular actions. J Endocrinol Invest. 2005;28(5 Suppl):23-5.

174. Murata M, Okimura Y, Iida K, Matsumoto M, Sowa H, Kaji H, Kojima M, Kangawa K, Chihara K. Ghrelin modulates the downstream molecules of insulin signaling in hepatoma cells. J Biol Chem. 2002 Feb 15;277(7):5667-74.

175. Kang K, Zmuda E, Sleeman MW. Physiological role of ghrelin as revealed by the ghrelin and GOAT knockout mice. Peptides. 2011 Nov;32(11):2236-41. doi: 10.1016/j.peptides.2011.04.028.

176. Albarran-Zeckler RG, Sun Y, Smith RG. Physiological roles revealed by ghrelin and ghrelin receptor deficient mice. Peptides. 2011 Nov;32(11):2229-35. doi: 10.1016/j.peptides.2011.07.003. Epub 2011 Jul 12.

177. Bednarek MA, Feighner SD, Pong SS, McKee KK, Hreniuk DL, Silva MV, Warren VA, Howard AD, Van Der Ploeg LH, Heck JV. Structure-function studies on the new growth hormone-releasing peptide, ghrelin: minimal sequence of ghrelin necessary for activation of growth hormone secretagogue receptor 1a. J Med Chem. 2000 Nov 16;43(23):4370-6.

178. Chen CY, Asakawa A, Fujimiya M, Lee SD, Inui A. Ghrelin gene products and the regulation of food intake and gut motility. Pharmacol Rev. 2009 Dec;61(4):430-81. doi: 10.1124/pr.109.001958.

179. Andrews ZB. The extra-hypothalamic actions of ghrelin on neuronal function. Trends Neurosci. 2011 Jan;34(1):31-40. doi: 10.1016/j.tins.2010.10.001.

180. Satou M, Nishi Y, Yoh J, Hattori Y, Sugimoto H. Identification and characterization of acyl-protein thioesterase 1/lysophospholipase I as a ghrelin deacylation/lysophospholipid hydrolyzing enzyme in

fetal bovine serum and conditioned medium. Endocrinology. 2010 Oct;151(10):4765-75. doi: 10.1210/en.2010-0412.

181. Mizutani M, Atsuchi K, Asakawa A, Matsuda N, Fujimura M, Inui A, Kato I, Fujimiya M. Localization of acyl ghrelin- and des-acyl ghrelin-immunoreactive cells in the rat stomach and their responses to intragastric pH. Am J Physiol Gastrointest Liver Physiol. 2009 Nov;297(5):G974-80.

182. Gauna C, van de Zande B, van Kerkwijk A, Themmen AP, van der Lely AJ, Delhanty PJ. Unacylated ghrelin is not a functional antagonist but a full agonist of the type 1a growth hormone secretagogue receptor (GHS-R). Mol Cell Endocrinol. 2007 Aug 15;274(1-2):30-4.

183. Heppner KM, Piechowski CL, Müller A, Ottaway N, Sisley S, Smiley DL, Habegger KM, Pfluger PT, Dimarchi R, Biebermann H, Tschöp MH, Sandoval DA, Perez-Tilve D. Both acyl and des-acyl ghrelin regulate adiposity and glucose metabolism via central nervous system ghrelin receptors. Diabetes. 2014 Jan;63(1):122-31. doi: 10.2337/db13-0414.

184. Baldanzi G, Filigheddu N, Cutrupi S, Catapano F, Bonissoni S, Fubini A, Malan D, Baj G, Granata R, Broglio F, Papotti M, Surico N, Bussolino F, Isgaard J, Deghenghi R, Sinigaglia F, Prat M, Muccioli G, Ghigo E, Graziani A. Ghrelin and des-acyl ghrelin inhibit cell death in cardiomyocytes and endothelial cells through ERK1/2 and PI 3-kinase/AKT. J Cell Biol. 2002 Dec 23;159(6):1029-37.

185. Thompson NM, Gill DA, Davies R, Loveridge N, Houston PA, Robinson IC, Wells T. Ghrelin and des-octanoyl ghrelin promote adipogenesis directly in vivo by a mechanism independent of the type 1a growth hormone secretagogue receptor. Endocrinology. 2004 Jan;145(1):234-42.

186. Delhanty PJ, van der Eerden BC, van der Velde M, Gauna C, Pols HA, Jahr H, Chiba H, van der Lely AJ, van Leeuwen JP. Ghrelin and unacylated ghrelin stimulate human osteoblast growth via mitogen-activated protein kinase (MAPK)/phosphoinositide 3-kinase (PI3K) pathways in the absence of GHS-R1a. J Endocrinol. 2006 Jan;188(1):37-47.

187. Cassoni P, Papotti M, Ghè C, Catapano F, Sapino A, Graziani A, Deghenghi R, Reissmann T, Ghigo E, Muccioli G. Identification, characterization, and biological activity of specific receptors for natural (ghrelin) and synthetic growth hormone secretagogues and analogs in human breast carcinomas and cell lines. J Clin Endocrinol Metab. 2001 Apr;86(4):1738-45.

188. Cassoni P, Ghé C, Marrocco T, Tarabra E, Allia E, Catapano F, Deghenghi R, Ghigo E, Papotti M, Muccioli G. Expression of ghrelin and biological activity of specific receptors for ghrelin and des-acyl ghrelin in human prostate neoplasms and related cell lines. Eur J Endocrinol. 2004 Feb;150(2):173-84.

189. Filigheddu N, Gnocchi VF, Coscia M, Cappelli M, Porporato PE, Taulli R, Traini S, Baldanzi G, Chianale F, Cutrupi S, Arnoletti E, Ghè C, Fubini A, Surico N, Sinigaglia F, Ponzetto C, Muccioli G, Crepaldi T, Graziani A. Ghrelin and des-acyl ghrelin promote differentiation and fusion of C2C12 skeletal muscle cells. Mol Biol Cell. 2007 Mar;18(3):986-94.

190. Granata R, Settanni F, Biancone L, Trovato L, Nano R, Bertuzzi F, Destefanis S, Annunziata M, Martinetti M, Catapano F, Ghè C, Isgaard J, Papotti M, Ghigo E, Muccioli G. Acylated and unacylated ghrelin promote proliferation and inhibit apoptosis of pancreatic beta-cells and human islets: involvement of 3',5'-cyclic adenosine monophosphate/protein kinase A, extracellular signal-regulated kinase 1/2, and phosphatidyl inositol 3-Kinase/Akt signaling. Endocrinology. 2007 Feb;148(2):512-29.

191. Jeffery PL, Herington AC, Chopin LK. Expression and action of the growth hormone releasing peptide ghrelin and its receptor in prostate cancer cell lines. J Endocrinol. 2002 Mar;172(3):R7-11.

192. Muccioli G, Pons N, Ghè C, Catapano F, Granata R, Ghigo E. Ghrelin and des-acyl ghrelin both inhibit isoproterenol-induced lipolysis in rat adipocytes via a non-type 1a growth hormone secretagogue receptor. Eur J Pharmacol. 2004 Sep 13;498(1-3):27-35.

193. Benso A, St-Pierre DH, Prodam F, Gramaglia E, Granata R, van der Lely AJ, Ghigo E, Broglio F. Metabolic effects of overnight continuous infusion of unacylated ghrelin in humans. Eur J Endocrinol. 2012 May;166(5):911-6. doi: 10.1530/EJE-11-0982.

194. Broglio F, Gottero C, Prodam F, Gauna C, Muccioli G, Papotti M, Abribat T, Van Der Lely AJ, Ghigo E. Non-acylated ghrelin counteracts the metabolic but not the neuroendocrine response to acylated ghrelin in humans. J Clin Endocrinol Metab. 2004 Jun;89(6):3062-5.

195. Togliatto G, Trombetta A, Dentelli P, Cotogni P, Rosso A, Tschöp MH, Granata R, Ghigo E, Brizzi MF. Unacylated ghrelin promotes skeletal muscle regeneration following hindlimb ischemia via SOD-2-mediated miR-221/222 expression. J Am Heart Assoc. 2013 Dec 5;2(6):e000376. doi: 10.1161/JAHA.113.000376.

196. Asakawa A, Inui A, Fujimiya M, Sakamaki R, Shinfuku N, Ueta Y, Meguid MM, Kasuga M. Stomach regulates energy balance via acylated ghrelin and desacyl ghrelin. Gut. 2005 Jan;54(1):18-24.

197. Inhoff T, Wiedenmann B, Klapp BF, Mönnikes H, Kobelt P. Is desacyl ghrelin a modulator of food intake? Peptides. 2009 May;30(5):991-4. doi: 10.1016/j.peptides.2009.01.019.

198. Toshinai K, Yamaguchi H, Sun Y, Smith RG, Yamanaka A, Sakurai T, Date Y, Mondal MS, Shimbara T, Kawagoe T, Murakami N, Miyazato M, Kangawa K, Nakazato M. Des-acyl ghrelin induces food intake by a mechanism independent of the growth hormone secretagogue receptor. Endocrinology. 2006 May;147(5):2306-14.

199. Gao M, Yang J, Liu G, Wei R, Zhang L, Wang H, Wang G, Gao H, Chen G, Hong T. Ghrelin promotes the differentiation of human embryonic stem cells in infarcted cardiac microenvironment. Peptides. 2012 Apr;34(2):373-9. doi: 10.1016/j.peptides.2012.02.006.

200. Gao M, Yang J, Wei R, Liu G, Zhang L, Wang H, Wang G, Gao H, Chen G, Hong T. Ghrelin induces cardiac lineage differentiation of human embryonic stem cells through ERK1/2 pathway. Int J Cardiol. 2013 Sep 10;167(6):2724-33. doi: 10.1016/j.ijcard.2012.06.106.

201. Giovambattista A, Gaillard RC, Spinedi E. Ghrelin gene-related peptides modulate rat white adiposity. Vitam Horm. 2008;77:171-205.

202. Miegueu P, St Pierre D, Broglio F, Cianflone K. Effect of desacyl ghrelin, obestatin and related peptides on triglyceride storage, metabolism and GHSR signaling in 3T3-L1 adipocytes. J Cell Biochem. 2011 Feb;112(2):704-14. doi: 10.1002/jcb.22983.

203. Delhanty PJ, van Koetsveld PM, Gauna C, van de Zande B, Vitale G, Hofland LJ, van der Lely AJ. Ghrelin and its unacylated isoform stimulate the growth of adrenocortical tumor cells via an anti-apoptotic pathway. Am J Physiol Endocrinol Metab. 2007 Jul;293(1):E302-9.

204. Favaro E, Granata R, Miceli I, Baragli A, Settanni F, Cavallo Perin P, Ghigo E, Camussi G, Zanone MM. The ghrelin gene products and exendin-4 promote survival of human pancreatic islet endothelial cells in hyperglycaemic conditions, through phosphoinositide 3-kinase/Akt, extracellular

signal-related kinase (ERK)1/2 and cAMP/protein kinase A (PKA) signalling pathways. Diabetologia. 2012 Apr;55(4):1058-70. doi: 10.1007/s00125-011-2423-y.

205. Sato M, Nakahara K, Goto S, Kaiya H, Miyazato M, Date Y, Nakazato M, Kangawa K, Murakami N. Effects of ghrelin and des-acyl ghrelin on neurogenesis of the rat fetal spinal cord. Biochem Biophys Res Commun. 2006 Nov 24;350(3):598-603.

206. Chung H, Seo S, Moon M, Park S. Phosphatidylinositol-3-kinase/Akt/glycogen synthase kinase-3 beta and ERK1/2 pathways mediate protective effects of acylated and unacylated ghrelin against oxygen-glucose deprivation-induced apoptosis in primary rat cortical neuronal cells. J Endocrinol. 2008 Sep;198(3):511-21. doi: 10.1677/JOE-08-0160.

207. Hwang S, Moon M, Kim S, Hwang L, Ahn KJ, Park S. Neuroprotective effect of ghrelin is associated with decreased expression of prostate apoptosis response-4. Endocr J. 2009;56(4):609-17.

208. Rodríguez A, Gómez-Ambrosi J, Catalán V, Rotellar F, Valentí V, Silva C, Mugueta C, Pulido MR, Vázquez R, Salvador J, Malagón MM, Colina I, Frühbeck G. The ghrelin O-acyltransferase-ghrelin system reduces TNF-α-induced apoptosis and autophagy in human visceral adipocytes. Diabetologia. 2012 Nov;55(11):3038-50. doi: 10.1007/s00125-012-2671-5.

209. Zhan M, Yuan F, Liu H, Chen H, Qiu X, Fang W. Inhibition of proliferation and apoptosis of vascular smooth muscle cells by ghrelin. Acta Biochim Biophys Sin (Shanghai). 2008 Sep;40(9):769-76.

210. Delhanty PJ, van der Lely AJ. Ghrelin and glucose homeostasis. Peptides. 2011 Nov;32(11):2309-18. doi: 10.1016/j.peptides.2011.03.001.

211. Vestergaard ET, Møller N, Jørgensen JO. Acute peripheral tissue effects of ghrelin on interstitial levels of glucose, glycerol, and lactate: a microdialysis study in healthy human subjects. Am J Physiol Endocrinol Metab. 2013 Jun 15;304(12):E1273-80. doi: 10.1152/ajpendo.00662.2012.

212. Sun Y, Garcia JM, Smith RG. Ghrelin and growth hormone secretagogue receptor expression in mice during aging. Endocrinology. 2007 Mar;148(3):1323-9.

213. Nagaya N, Uematsu M, Kojima M, Ikeda Y, Yoshihara F, Shimizu W, Hosoda H, Hirota Y, Ishida H, Mori H, Kangawa K. Chronic administration of ghrelin improves left ventricular dysfunction and attenuates development of cardiac cachexia in rats with heart failure. Circulation. 2001 Sep 18;104(12):1430-5

214. Nagaya N, Moriya J, Yasumura Y, Uematsu M, Ono F, Shimizu W, Ueno K, Kitakaze M, Miyatake K, Kangawa K. Effects of ghrelin administration on left ventricular function, exercise capacity, and muscle wasting in patients with chronic heart failure. Circulation. 2004 Dec 14;110(24):3674-9.

215. Nagaya N, Itoh T, Murakami S, Oya H, Uematsu M, Miyatake K, Kangawa K. Treatment of cachexia with ghrelin in patients with COPD. Chest. 2005 Sep;128(3):1187-93.

216. DeBoer MD, Zhu XX, Levasseur P, Meguid MM, Suzuki S, Inui A, Taylor JE, Halem HA, Dong JZ, Datta R, Culler MD, Marks DL. Ghrelin treatment causes increased food intake and retention of lean body mass in a rat model of cancer cachexia. Endocrinology. 2007 Jun;148(6):3004-12.

217. Deboer MD, Zhu X, Levasseur PR, Inui A, Hu Z, Han G, Mitch WE, Taylor JE, Halem HA, Dong JZ, Datta R, Culler MD, Marks DL. Ghrelin treatment of chronic kidney disease: improvements in lean body mass and cytokine profile. Endocrinology. 2008 Feb;149(2):827-35.

218. Hanada T, Toshinai K, Kajimura N, Nara-Ashizawa N, Tsukada T, Hayashi Y, Osuye K, Kangawa K, Matsukura S, Nakazato M. Anti-cachectic effect of ghrelin in nude mice bearing human melanoma cells. Biochem Biophys Res Commun. 2003 Feb 7;301(2):275-9.

219. Garcia JM, Cata JP, Dougherty PM, Smith RG. Ghrelin prevents cisplatin-induced mechanical hyperalgesia and cachexia. Endocrinology. 2008 Feb;149(2):455-60.

220. Garcia JM, Scherer T, Chen JA, Guillory B, Nassif A, Papusha V, Smiechowska J, Asnicar M, Buettner C, Smith RG. Inhibition of cisplatin-induced lipid catabolism and weight loss by ghrelin in male mice. Endocrinology. 2013 Sep;154(9):3118-29. doi: 10.1210/en.2013-1179.

221. Reano S, Graziani A, Filigheddu N. Acylated and unacylated ghrelin administration to blunt muscle wasting. Curr Opin Clin Nutr Metab Care. 2014 May;17(3):236-40. doi: 10.1097/MCO.0000000000000049.

222. Sheriff S, Kadeer N, Joshi R, Friend LA, James JH, Balasubramaniam A. Des-acyl ghrelin exhibits pro-anabolic and anti-catabolic effects on C2C12 myotubes exposed to cytokines and reduces burn-induced muscle proteolysis in rats. Mol Cell Endocrinol. 2012 Apr 4;351(2):286-95. doi: 10.1016/j.mce.2011.12.021.

223. Bulgarelli I, Tamiazzo L, Bresciani E, Rapetti D, Caporali S, Lattuada D, Locatelli V, Torsello A. Desacyl-ghrelin and synthetic GH-secretagogues modulate the production of inflammatory cytokines in mouse microglia cells stimulated by beta-amyloid fibrils. J Neurosci Res. 2009 Sep;87(12):2718-27. doi: 10.1002/jnr.22088.

224. Sibilia V, Pagani F, Mrak E, Dieci E, Tulipano G, Ferrucci F. Pharmacological characterization of the ghrelin receptor mediating its inhibitory action on inflammatory pain in rats. Amino Acids. 2012 Oct;43(4):1751-9.

225. Fürstenberger G, Senn HJ. Insulin-like growth factors and cancer. Lancet Oncol. 2002 May;3(5):298-302. Review. PubMed PMID: 12067807.

226. Nagaya N, Uematsu M, Kojima M, Date Y, Nakazato M, Okumura H, Hosoda H, Shimizu W, Yamagishi M, Oya H, Koh H, Yutani C, Kangawa K. Elevated circulating level of ghrelin in cachexia associated with chronic heart failure: relationships between ghrelin and anabolic/catabolic factors. Circulation. 2001 Oct 23;104(17):2034-8.

227. Shimizu Y, Nagaya N, Isobe T, Imazu M, Okumura H, Hosoda H, Kojima M, Kangawa K, Kohno N. Increased plasma ghrelin level in lung cancer cachexia. Clin Cancer Res. 2003 Feb;9(2):774-8.

228. Hanada T, Toshinai K, Date Y, Kajimura N, Tsukada T, Hayashi Y, Kangawa K, Nakazato M. Upregulation of ghrelin expression in cachectic nude mice bearing human melanoma cells. Metabolism. 2004 Jan;53(1):84-8.

229. Kerem M, Ferahkose Z, Yilmaz UT, Pasaoglu H, Ofluoglu E, Bedirli A, Salman B, Sahin TT, Akin M. Adipokines and ghrelin in gastric cancer cachexia. World J Gastroenterol. 2008 Jun 21;14(23):3633-41.

230. Takahashi M, Terashima M, Takagane A, Oyama K, Fujiwara H, Wakabayashi G. Ghrelin and leptin levels in cachectic patients with cancer of the digestive organs. Int J Clin Oncol. 2009 Aug;14(4):315-20. doi: 10.1007/s10147-008-0856-1.

231. Karapanagiotou EM, Polyzos A, Dilana KD, Gratsias I, Boura P, Gkiozos I, Syrigos KN. Increased serum levels of ghrelin at diagnosis mediate body weight loss in non-small cell lung cancer (NSCLC) patients. Lung Cancer. 2009 Dec;66(3):393-8. doi: 10.1016/j.lungcan.2009.02.006.

232. Wang HS, Oh DS, Ohning GV, Pisegna JR. Elevated serum ghrelin exerts an orexigenic effect that may maintain body mass index in patients with metastatic neuroendocrine tumors. J Mol Neurosci. 2007;33(3):225-31.

233. Garcia JM, Garcia-Touza M, Hijazi RA, Taffet G, Epner D, Mann D, Smith RG, Cunningham GR, Marcelli M. Active ghrelin levels and active to total ghrelin ratio in cancer-induced cachexia. J Clin Endocrinol Metab. 2005 May;90(5):2920-6.

234. Wang W, Andersson M, Iresjö BM, Lönnroth C, Lundholm K. Effects of ghrelin on anorexia in tumor-bearing mice with eicosanoid-related cachexia. Int J Oncol. 2006 Jun;28(6):1393-400.

235. Lund LH, Williams JJ, Freda P, LaManca JJ, LeJemtel TH, Mancini DM. Ghrelin resistance occurs in severe heart failure and resolves after heart transplantation. Eur J Heart Fail. 2009 Aug;11(8):789-94. doi: 10.1093/eurjhf/hfp088.

236. Perino A, Ghigo A, Ferrero E, Morello F, Santulli G, Baillie GS, Damilano F, Dunlop AJ, Pawson C, Walser R, Levi R, Altruda F, Silengo L, Langeberg LK, Neubauer G, Heymans S, Lembo G, Wymann MP, Wetzker R, Houslay MD, Iaccarino G, Scott JD, Hirsch E. Integrating cardiac PIP3 and cAMP signaling through a PKA anchoring function of p110γ. Mol Cell. 2011 Apr 8;42(1):84-95. doi: 10.1016/j.molcel.2011.01.030.

237. Vanhaesebroeck B, Stephens L, Hawkins P. PI3K signalling: the path to discovery and understanding. Nat Rev Mol Cell Biol. 2012 Feb 23;13(3):195-203. doi: 10.1038/nrm3290.

238. Vanhaesebroeck B, Guillermet-Guibert J, Graupera M, Bilanges B. The emerging mechanisms of isoform-specific PI3K signalling. Nat Rev Mol Cell Biol. 2010 May;11(5):329-41. doi: 10.1038/nrm2882.

239. Hirsch E, Lembo G, Montrucchio G, Rommel C, Costa C, Barberis L. Signaling through PI3Kgamma: a common platform for leukocyte, platelet and cardiovascular stress sensing. Thromb Haemost. 2006 Jan;95(1):29-35.

240. Guillermet-Guibert J, Bjorklof K, Salpekar A, Gonella C, Ramadani F, Bilancio A, Meek S, Smith AJ, Okkenhaug K, Vanhaesebroeck B. The p110beta isoform of phosphoinositide 3-kinase signals downstream of G protein-coupled receptors and is functionally redundant with p110gamma. Proc Natl Acad Sci U S A. 2008 Jun 17;105(24):8292-7. doi: 10.1073/pnas.0707761105.

241. Schmid MC, Avraamides CJ, Dippold HC, Franco I, Foubert P, Ellies LG, Acevedo LM, Manglicmot JR, Song X, Wrasidlo W, Blair SL, Ginsberg MH, Cheresh DA, Hirsch E, Field SJ, Varner JA. Receptor tyrosine kinases and TLR/IL1Rs unexpectedly activate myeloid cell PI3kγ, a single convergent point promoting tumor inflammation and progression. Cancer Cell. 2011 Jun 14;19(6):715-27. doi: 10.1016/j.ccr.2011.04.016.

242. Hirsch E, Katanaev VL, Garlanda C, Azzolino O, Pirola L, Silengo L, Sozzani S, Mantovani A, Altruda F, Wymann MP. Central role for G protein-coupled phosphoinositide 3-kinase gamma in inflammation. Science. 2000 Feb 11;287(5455):1049-53.

243. Sasaki T, Irie-Sasaki J, Jones RG, Oliveira-dos-Santos AJ, Stanford WL, Bolon B, Wakeham A, Itie A, Bouchard D, Kozieradzki I, Joza N, Mak TW, Ohashi PS, Suzuki A, Penninger JM. Function of PI3Kgamma in thymocyte development, T cell activation, and neutrophil migration. Science. 2000 Feb 11;287(5455):1040-6.

244. Li Z, Jiang H, Xie W, Zhang Z, Smrcka AV, Wu D. Roles of PLC-beta2 and -beta3 and PI3Kgamma in chemoattractant-mediated signal transduction. Science. 2000 Feb 11;287(5455):1046-9.

245. Lopez-Ilasaca M, Gutkind JS, Wetzker R. Phosphoinositide 3-kinase gamma is a mediator of Gbetagamma-dependent Jun kinase activation. J Biol Chem. 1998 Jan 30;273(5):2505-8.

246. Rubio I, Rodriguez-Viciana P, Downward J, Wetzker R. Interaction of Ras with phosphoinositide 3-kinase gamma. Biochem J. 1997 Sep 15;326 (Pt 3):891-5.

247. Bondeva T, Pirola L, Bulgarelli-Leva G, Rubio I, Wetzker R, Wymann MP. Bifurcation of lipid and protein kinase signals of PI3Kgamma to the protein kinases PKB and MAPK. Science. 1998 Oct 9;282(5387):293-6.

248. Vasudevan NT, Mohan ML, Gupta MK, Hussain AK, Naga Prasad SV. Inhibition of protein phosphatase 2A activity by PI3Kγ regulates β-adrenergic receptor function. Mol Cell. 2011 Mar 18;41(6):636-48. doi: 10.1016/j.molcel.2011.02.025.

249. Naga Prasad SV, Jayatilleke A, Madamanchi A, Rockman HA. Protein kinase activity of phosphoinositide 3-kinase regulates beta-adrenergic receptor endocytosis. Nat Cell Biol. 2005 Aug;7(8):785-96.

250. Naga Prasad SV, Laporte SA, Chamberlain D, Caron MG, Barak L, Rockman HA. Phosphoinositide 3-kinase regulates beta2-adrenergic receptor endocytosis by AP-2 recruitment to the receptor/beta-arrestin complex. J Cell Biol. 2002 Aug 5;158(3):563-75.

251. Naga Prasad SV, Barak LS, Rapacciuolo A, Caron MG, Rockman HA. Agonist-dependent recruitment of phosphoinositide 3-kinase to the membrane by beta-adrenergic receptor kinase 1. A role in receptor sequestration. J Biol Chem. 2001 Jun 1;276(22):18953-9.

252. Patrucco E, Notte A, Barberis L, Selvetella G, Maffei A, Brancaccio M, Marengo S, Russo G, Azzolino O, Rybalkin SD, Silengo L, Altruda F, Wetzker R, Wymann MP, Lembo G, Hirsch E. PI3Kgamma modulates the cardiac response to chronic pressure overload by distinct kinase-dependent and -independent effects. Cell. 2004 Aug 6;118(3):375-87.

253. Crackower MA, Oudit GY, Kozieradzki I, Sarao R, Sun H, Sasaki T, Hirsch E, Suzuki A, Shioi T, Irie-Sasaki J, Sah R, Cheng HY, Rybin VO, Lembo G, Fratta L, Oliveira-dos-Santos AJ, Benovic JL, Kahn CR, Izumo S, Steinberg SF, Wymann MP, Backx PH, Penninger JM. Regulation of myocardial contractility and cell size by distinct PI3K-PTEN signaling pathways. Cell. 2002 Sep 20;110(6):737-49.

254. Reed SA, Sandesara PB, Senf SM, Judge AR. Inhibition of FoxO transcriptional activity prevents muscle fiber atrophy during cachexia and induces hypertrophy. FASEB J. 2012 Mar;26(3):987-1000. doi: 10.1096/fj.11-189977.

255. Sandri M, Lin J, Handschin C, Yang W, Arany ZP, Lecker SH, Goldberg AL, Spiegelman BM. PGC-1alpha protects skeletal muscle from atrophy by suppressing FoxO3 action and atrophy-specific gene transcription. Proc Natl Acad Sci U S A. 2006 Oct 31;103(44):16260-5.

256. Stitt TN, Drujan D, Clarke BA, Panaro F, Timofeyva Y, Kline WO, Gonzalez M, Yancopoulos GD, Glass DJ. The IGF-1/PI3K/Akt pathway prevents expression of muscle atrophy-induced ubiquitin ligases by inhibiting FOXO transcription factors. Mol Cell. 2004 May 7;14(3):395-403.

257. Acharyya S, Ladner KJ, Nelsen LL, Damrauer J, Reiser PJ, Swoap S, Guttridge DC. Cancer cachexia is regulated by selective targeting of skeletal muscle gene products. J Clin Invest. 2004 Aug;114(3):370-8.

258. Lokireddy S, Wijesoma IW, Bonala S, Wei M, Sze SK, McFarlane C, Kambadur R, Sharma M. Myostatin is a novel tumoral factor that induces cancer cachexia. Biochem J. 2012 Aug 15;446(1):23-36. doi: 10.1042/BJ20112024.

259. White JP, Puppa MJ, Gao S, Sato S, Welle SL, Carson JA. Muscle mTORC1 suppression by IL-6 during cancer cachexia: a role for AMPK. Am J Physiol Endocrinol Metab. 2013 May 15;304(10):E1042-52. doi: 10.1152/ajpendo.00410.2012.

260. Briguet A, Courdier-Fruh I, Foster M, Meier T, Magyar JP. Histological parameters for the quantitative assessment of muscular dystrophy in the mdx-mouse. Neuromuscul Disord. 2004 Oct;14(10):675-82.

261. Sarbassov DD, Ali SM, Sengupta S, Sheen JH, Hsu PP, Bagley AF, Markhard AL, Sabatini DM. Prolonged rapamycin treatment inhibits mTORC2 assembly and Akt/PKB. Mol Cell. 2006 Apr 21;22(2):159-68.

262. Copp J, Manning G, Hunter T. TORC-specific phosphorylation of mammalian target of rapamycin (mTOR): phospho-Ser2481 is a marker for intact mTOR signaling complex 2. Cancer Res. 2009 Mar 1;69(5):1821-7. doi: 10.1158/0008-5472.CAN-08-3014.

263. Lamming DW, Ye L, Katajisto P, Goncalves MD, Saitoh M, Stevens DM, Davis JG, Salmon AB, Richardson A, Ahima RS, Guertin DA, Sabatini DM, Baur JA. Rapamycin-induced insulin resistance is mediated by mTORC2 loss and uncoupled from longevity. Science. 2012 Mar 30;335(6076):1638-43. doi: 10.1126/science.1215135.

264. Clavel S, Siffroi-Fernandez S, Coldefy AS, Boulukos K, Pisani DF, Dérijard B. Regulation of the intracellular localization of Foxo3a by stress-activated protein kinase signaling pathways in skeletal muscle cells. Mol Cell Biol. 2010 Jan;30(2):470-80. doi: 10.1128/MCB.00666-09.

265. Cuadrado A, Nebreda AR. Mechanisms and functions of p38 MAPK signalling. Biochem J. 2010 Aug 1;429(3):403-17. doi: 10.1042/BJ20100323.

266. McClung JM, Judge AR, Powers SK, Yan Z. p38 MAPK links oxidative stress to autophagy-related gene expression in cachectic muscle wasting. Am J Physiol Cell Physiol. 2010 Mar;298(3):C542-9. doi: 10.1152/ajpcell.00192.2009.

267. Garcia JM, Boccia RV, Graham CD, Yan Y, Duus EM, Allen S, Friend J. Anamorelin for patients with cancer cachexia: an integrated analysis of two phase 2, randomised, placebo-controlled, double-blind trials. Lancet Oncol. 2015 Jan;16(1):108-16. doi: 10.1016/S1470-2045(14)71154-4.

268. Gurriarán-Rodríguez U, Santos-Zas I, Al-Massadi O, Mosteiro CS, Beiroa D, Nogueiras R, Crujeiras AB, Seoane LM, Señarís J, García-Caballero T, Gallego R, Casanueva FF, Pazos Y, Camiña JP. The obestatin/GPR39 system is up-regulated by muscle injury and functions as an autocrine regenerative system. J Biol Chem. 2012 Nov 2;287(45):38379-89. doi: 10.1074/jbc.M112.374926.

269. Baragli A, Ghè C, Arnoletti E, Granata R, Ghigo E, Muccioli G. Acylated and unacylated ghrelin attenuate isoproterenol-induced lipolysis in isolated rat visceral adipocytes through activation of phosphoinositide 3-kinase γ and phosphodiesterase 3B. Biochim Biophys Acta. 2011 Jun;1811(6):386-96. doi: 10.1016/j.bbalip.2011.03.001.

270. Pfluger PT, Kirchner H, Günnel S, Schrott B, Perez-Tilve D, Fu S, Benoit SC, Horvath T, Joost HG, Wortley KE, Sleeman MW, Tschöp MH. Simultaneous deletion of ghrelin and its receptor increases motor activity and energy expenditure. Am J Physiol Gastrointest Liver Physiol. 2008 Mar;294(3):G610-8.

271. Gallagher IJ, Stephens NA, MacDonald AJ, Skipworth RJ, Husi H, Greig CA, Ross JA, Timmons JA, Fearon KC. Suppression of skeletal muscle turnover in cancer cachexia: evidence from the transcriptome in sequential human muscle biopsies. Clin Cancer Res. 2012 May 15;18(10):2817-27. doi: 10.1158/1078-0432.CCR-11-2133.

272. Vilardaga JP, Romero G, Friedman PA, Gardella TJ. Molecular basis of parathyroid hormone receptor signaling and trafficking: a family B GPCR paradigm. Cell Mol Life Sci. 2011 Jan;68(1):1-13. doi: 10.1007/s00018-010-0465-9.

273. Busquets S, Figueras MT, Fuster G, Almendro V, Moore-Carrasco R, Ametller E, Argilés JM, López-Soriano FJ. Anticachectic effects of formoterol: a drug for potential treatment of muscle wasting. Cancer Res. 2004 Sep 15;64(18):6725-31.

274. Busquets S, Toledo M, Sirisi S, Orpí M, Serpe R, Coutinho J, Martínez R, Argilés JM, López-Soriano FJ. Formoterol and cancer muscle wasting in rats: Effects on muscle force and total physical activity. Exp Ther Med. 2011 Jul;2(4):731-735.

275. Carbó N, López-Soriano J, Tarragó T, González O, Llovera M, López-Soriano FJ, Argilés JM. Comparative effects of beta2-adrenergic agonists on muscle waste associated with tumour growth. Cancer Lett. 1997 May 1;115(1):113-8.

276. Costelli P, Llovera M, García-Martínez C, Carbó N, López-Soriano FJ, Argilés JM. Enhanced leucine oxidation in rats bearing an ascites hepatoma (Yoshida AH-130) and its reversal by clenbuterol. Cancer Lett. 1995 May 4;91(1):73-8.

277. Costelli P, García-Martínez C, Llovera M, Carbó N, López-Soriano FJ, Agell N, Tessitore L, Baccino FM, Argilés JM. Muscle protein waste in tumor-bearing rats is effectively antagonized by a beta 2-adrenergic agonist (clenbuterol). Role of the ATP-ubiquitin-dependent proteolytic pathway. J Clin Invest. 1995 May;95(5):2367-72.

278. Fuster G, Busquets S, Ametller E, Olivan M, Almendro V, de Oliveira CC, Figueras M, López-Soriano FJ, Argilés JM. Are peroxisome proliferator-activated receptors involved in skeletal muscle wasting during experimental cancer cachexia? Role of beta2-adrenergic agonists. Cancer Res. 2007 Jul 1;67(13):6512-9.

279. Hyltander A, Svaninger G, Lundholm K. The effect of clenbuterol on body composition in spontaneously eating tumour-bearing mice. Biosci Rep. 1993 Dec;13(6):325-31.

280. Stallion A, Foley-Nelson T, Chance WT, Fischer JE. Effects of increased beta 2-agonist dose in tumor-bearing animals. Nutr Cancer. 1993;20(3):251-60.

281. Stallion A, Foley-Nelson T, Chance WT, James JH, Fischer JE. Anticatabolic effect of the beta 2-agonist cimaterol in vivo in tumor-bearing animals. J Surg Res. 1995 Sep;59(3):387-92.

282. Delhanty PJ, Sun Y, Visser JA, van Kerkwijk A, Huisman M, van Ijcken WF, Swagemakers S, Smith RG, Themmen AP, van der Lely AJ. Unacylated ghrelin rapidly modulates lipogenic and insulin signaling pathway gene expression in metabolically active tissues of GHSR deleted mice. PLoS One. 2010 Jul 26;5(7):e11749. doi: 10.1371/journal.pone.0011749.

283. Bentzinger CF, von Maltzahn J, Dumont NA, Stark DA, Wang YX, Nhan K, Frenette J, Cornelison DD, Rudnicki MA. Wnt7a stimulates myogenic stem cell motility and engraftment resulting in improved muscle strength. J Cell Biol. 2014 Apr 14;205(1):97-111. doi: 10.1083/jcb.201310035.

284. von Maltzahn J, Renaud JM, Parise G, Rudnicki MA. Wnt7a treatment ameliorates muscular dystrophy. Proc Natl Acad Sci U S A. 2012 Dec 11;109(50):20614-9. doi: 10.1073/pnas.1215765109.

285. Chen AE, Ginty DD, Fan CM. Protein kinase A signalling via CREB controls myogenesis induced by Wnt proteins. Nature. 2005 Jan 20;433(7023):317-22.

286. Stengel A, Wang L, Taché Y. Stress-related alterations of acyl and desacyl ghrelin circulating levels: mechanisms and functional implications. Peptides. 2011 Nov;32(11):2208-17. doi: 10.1016/j.peptides.2011.07.002.

287. Engelstoft MS, Park WM, Sakata I, Kristensen LV, Husted AS, Osborne-Lawrence S, Piper PK, Walker AK, Pedersen MH, Nøhr MK, Pan J, Sinz CJ, Carrington PE, Akiyama TE, Jones RM, Tang C, Ahmed K, Offermanns S, Egerod KL, Zigman JM, Schwartz TW. Seven transmembrane G protein-coupled receptor repertoire of gastric ghrelin cells. Mol Metab. 2013 Sep 4;2(4):376-92. doi: 10.1016/j.molmet.2013.08.006.

288. Hosoda H, Kangawa K. The autonomic nervous system regulates gastric ghrelin secretion in rats. Regul Pept. 2008 Feb 7;146(1-3):12-8.

289. de la Cour CD, Norlén P, Håkanson R. Secretion of ghrelin from rat stomach ghrelin cells in response to local microinfusion of candidate messenger compounds: a microdialysis study. Regul Pept. 2007 Oct 4;143(1-3):118-26.

290. Zhao TJ, Sakata I, Li RL, Liang G, Richardson JA, Brown MS, Goldstein JL, Zigman JM. Ghrelin secretion stimulated by {beta}1-adrenergic receptors in cultured ghrelinoma cells and in fasted mice. Proc Natl Acad Sci U S A. 2010 Sep 7;107(36):15868-73. doi: 10.1073/pnas.1011116107.

291. Lambert E, Lambert G, Ika-Sari C, Dawood T, Lee K, Chopra R, Straznicky N, Eikelis N, Drew S, Tilbrook A, Dixon J, Esler M, Schlaich MP. Ghrelin modulates sympathetic nervous system activity and stress response in lean and overweight men. Hypertension. 2011 Jul;58(1):43-50. doi: 10.1161/HYPERTENSIONAHA.111.171025.

292. Goldstein DS. Adrenal responses to stress. Cell Mol Neurobiol. 2010 Nov;30(8):1433-40. doi: 10.1007/s10571-010-9606-9.

293. Xu G, Li Y, An W, Li S, Guan Y, Wang N, Tang C, Wang X, Zhu Y, Li X, Mulholland MW, Zhang W. Gastric mammalian target of rapamycin signaling regulates ghrelin production and food intake. Endocrinology. 2009 Aug;150(8):3637-44. doi: 10.1210/en.2009-0372.

294. Dennis PB, Jaeschke A, Saitoh M, Fowler B, Kozma SC, Thomas G. Mammalian TOR: a homeostatic ATP sensor. Science. 2001 Nov 2;294(5544):1102-5.

295. Shiiya T, Nakazato M, Mizuta M, Date Y, Mondal MS, Tanaka M, Nozoe S, Hosoda H, Kangawa K, Matsukura S. Plasma ghrelin levels in lean and obese humans and the effect of glucose on ghrelin secretion. J Clin Endocrinol Metab. 2002 Jan;87(1):240-4.

296. Cummings DE, Weigle DS, Frayo RS, Breen PA, Ma MK, Dellinger EP, Purnell JQ. Plasma ghrelin levels after diet-induced weight loss or gastric bypass surgery. N Engl J Med. 2002 May 23;346(21):1623-30.

297. Yoshikawa T, Noguchi Y, Doi C, Makino T, Nomura K. Insulin resistance in patients with cancer: relationships with tumor site, tumor stage, body-weight loss, acute-phase response, and energy expenditure. Nutrition. 2001 Jul-Aug;17(7-8):590-3.

Acylated and unacylated ghrelin impair skeletal muscle atrophy in mice

Paolo E. Porporato,[1] Nicoletta Filigheddu,[1] Simone Reano,[1] Michele Ferrara,[1] Elia Angelino,[1] Viola F. Gnocchi,[1] Flavia Prodam,[2] Giulia Ronchi,[3] Sharmila Fagoonee,[4] Michele Fornaro,[3] Federica Chianale,[1] Gianluca Baldanzi,[1] Nicola Surico,[1] Fabiola Sinigaglia,[1] Isabelle Perroteau,[5] Roy G. Smith,[6] Yuxiang Sun,[7] Stefano Geuna,[3] and Andrea Graziani[1]

[1]Department of Translational Medicine, Interdisciplinary Research Center of Autoimmune Diseases (IRCAD), and Biotechnology Center for Applied Medical Research (BRMA), Università del Piemonte Orientale "Amedeo Avogadro" — Alessandria, Novara, Vercelli, Italy. [2]Department of Health Sciences, Università del Piemonte Orientale "Amedeo Avogadro" — Alessandria, Novara, Vercelli, Italy. [3]Neuroscience Institute "Cavalieri Ottolenghi" (NICO) and Department of Clinical and Biological Sciences, University of Torino, Orbassano (TO), Italy. [4]Molecular Biotechnology Center and Department of Genetics, Biology and Biochemistry, and [5]Department of Life Sciences and Systems Biology, University of Torino, Torino, Italy. [6]Department of Metabolism and Aging, The Scripps Research Institute, Scripps, Florida, USA. [7]USDA ARS Children's Nutrition Research Center, Departments of Pediatrics and Molecular and Cellular Biology, Baylor College of Medicine, Houston, Texas, USA.

Cachexia is a wasting syndrome associated with cancer, AIDS, multiple sclerosis, and several other disease states. It is characterized by weight loss, fatigue, loss of appetite, and skeletal muscle atrophy and is associated with poor patient prognosis, making it an important treatment target. Ghrelin is a peptide hormone that stimulates growth hormone (GH) release and positive energy balance through binding to the receptor GHSR-1a. Only acylated ghrelin (AG), but not the unacylated form (UnAG), can bind GHSR-1a; however, UnAG and AG share several GHSR-1a–independent biological activities. Here we investigated whether UnAG and AG could protect against skeletal muscle atrophy in a GHSR-1a–independent manner. We found that both AG and UnAG inhibited dexamethasone-induced skeletal muscle atrophy and atrogene expression through PI3Kβ-, mTORC2-, and p38-mediated pathways in myotubes. Upregulation of circulating UnAG in mice impaired skeletal muscle atrophy induced by either fasting or denervation without stimulating muscle hypertrophy and GHSR-1a–mediated activation of the GH/IGF-1 axis. In *Ghsr*-deficient mice, both AG and UnAG induced phosphorylation of Akt in skeletal muscle and impaired fasting-induced atrophy. These results demonstrate that AG and UnAG act on a common, unidentified receptor to block skeletal muscle atrophy in a GH-independent manner.

Introduction

Skeletal muscle atrophy involves massive loss of muscle structural proteins, which leads to muscle weight decrease and progressive loss of muscle function. Skeletal muscle atrophy is induced by muscle denervation and disuse, and it is also the key component of cachexia, a catabolic, debilitating response to several diseases. Cachectic patients not only sustain a decreased quality of life, but also face a worse prognosis of the underlying pathology, making cachexia an important target for treatment (1). Ghrelin is a circulating peptide hormone, octanoylated on Ser3, that is mainly produced by the stomach, which, by acting on the hypothalamus and the pituitary, induces GH secretion and stimulates food intake and adiposity through binding to its receptor, GHSR-1a (2–5). In addition to its endocrine activities, ghrelin protects cardiac function after heart damage (6, 7). In vitro, ghrelin inhibits the apoptosis of cardiomyocytes and other cell types by activating PI3K/Akt and ERK-1/2 pathways (8–10). Acylated ghrelin (AG) and unacylated ghrelin (UnAG) are generated from the same precursor, which can be acylated by the specific intracellular ghrelin-O-acyltransferase GOAT (11, 12). UnAG, which is far more abundant in plasma than AG, does not bind to GHSR-1a, lacks any GH-releasing activity (13), and has been considered for many years to be the inactive product of ghrelin catabolism. However, UnAG shares with AG common high-affinity binding sites on several cell types lacking GHSR-1a, including myocardial and skeletal myocytes, where they stimulate survival and differentiation, respectively (8, 9, 14–16). Furthermore, UnAG regulates gene expression in fat, muscle, and liver independently of GHSR-1a (17).

In both human patients and experimental models, AG ameliorates cachexia induced by several pathological conditions (6, 7, 13, 18–21). Although AG may inhibit cachexia by stimulating food intake, positive energy balance, and release of GH and IGF-1, the mechanisms underlying its anticachectic activity have not been fully elucidated.

Since we have previously shown that AG and UnAG, independently of GHSR-1a, inhibit apoptosis of cardiomyocytes by activating PI3K/Akt (8), a major antiatrophic signaling pathway (22, 23), and stimulate C2C12 skeletal myoblast differentiation (16), we investigated whether AG and UnAG could protect skeletal muscle from atrophy. Here, we provided evidence in vitro and in vivo that AG and UnAG, independently of GHSR-1a and activation of the GH/IGF-1 axis, trigger an antiatrophic signaling pathway by acting directly on the skeletal muscle, thereby protecting it from experimentally induced atrophy.

Results

AG and UnAG prevent dexamethasone-induced atrophy in C2C12-derived myotubes via mTORC2. C2C12 myotubes are a widely used model to study in vitro skeletal muscle atrophy induced by the synthetic glucocorticoid dexamethasone (24–26). Muscle atrophy was measured

Authorship note: Paolo E. Porporato and Nicoletta Filigheddu contributed equally to this work.

Conflict of interest: The authors have declared that no conflict of interest exists.

Citation for this article: *J Clin Invest.* doi:10.1172/JCI39920.

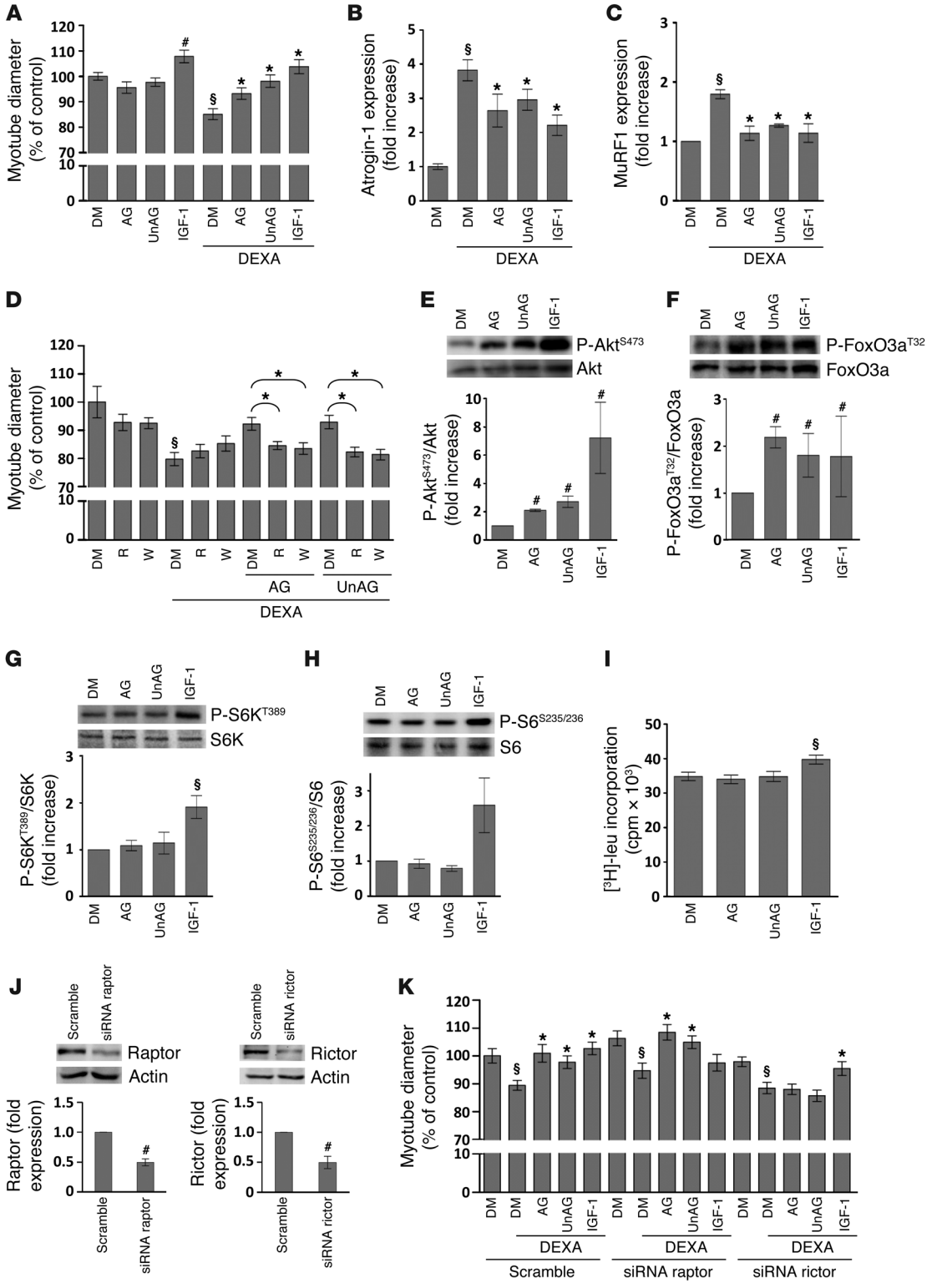
A
Myotube diameter (% of control)
DM
AG
UnAG
IGF-1
DEXA
B
Atrogin-1 expression (fold increase)
C
MuRF1 expression (fold increase)
D
Myotube diameter (% of control)
R
W
E
P-Akt^{S473}
Akt
P-Akt^{S473}/Akt (fold increase)
F
P-FoxO3a^{T32}
FoxO3a
P-FoxO3a^{T32}/FoxO3a (fold increase)
G
P-S6K^{T389}
S6K
P-S6K^{T389}/S6K (fold increase)
H
P-S6$^{S235/236}$
S6
P-S6$^{S235/236}$/S6 (fold increase)
I
[^{3}H]-leu incorporation (cpm x 10^3)
J
Scramble
siRNA raptor
Raptor
Actin
Raptor (fold expression)
siRNA rictor
Rictor
Rictor (fold expression)
K
Myotube diameter (% of control)
Scramble
siRNA raptor
siRNA rictor

Figure 1
AG and UnAG protect C2C12 myotubes from dexamethasone-induced atrophy without induction of protein synthesis or hypertrophy. (**A**) Myotube diameters were measured after 24-hour treatment in differentiation medium (DM) with 10 nM AG, 10 nM UnAG, and/or 1 μM dexamethasone (DEXA). In every experiment, 10 ng/ml IGF-1 was used as positive control for antiatrophic/hypertrophic activity. (**B** and **C**) Atrogin-1 and MuRF1 expression analysis upon dexamethasone treatment with or without AG and UnAG. (**D**) Treatment with 100 nM wortmannin (W) or 20 ng/ml rapamycin (R) reverted the antiatrophic activity of AG and UnAG on myotube diameter. Control myotubes in differentiation medium were treated with DMSO, a vehicle for both wortmannin and rapamycin. (**E** and **F**) Phosphorylation of Akt^{S473} and $FoxO3a^{T32}$, detected by Western blotting, upon treatment for 20 minutes with 1 μM AG or UnAG. Shown are representative blots and quantification of 3 independent experiments. (**G–I**) IGF-1, but not AG and UnAG, induced protein synthesis, as determined by phosphorylation of $S6K^{T389}$ (**G**) or $S6^{S235/236}$ (**H**) and by incorporation of [^{3}H]-leucine (**I**). (**J**) Effect of raptor and rictor silencing on protein levels, detected by Western blotting. (**K**) Silencing of rictor, but not of raptor, reverted the antiatrophic activity of AG and UnAG on the diameter of myotubes treated as in **A**. $^{\#}P < 0.05$, $^{\S}P < 0.01$ vs. DM control; $^{*}P < 0.01$ vs. DEXA treatment.

both as reduction of myotube diameter and as expression of the muscle-specific ubiquitin ligases Atrogin-1 (also known as MAFbx) and MuRF1, which drive muscle protein degradation in several models of muscle atrophy (24–27). Myotubes were treated with 1 μM dexamethasone for 24 hours in the presence or absence of 10 nM AG or UnAG, or with 10 ng/ml IGF-1 as a positive control of atrophy protection. Treatment with dexamethasone reduced myotube diameters by 20% and induced Atrogin-1 and MuRF1 expression. AG and UnAG impaired both these effects (Figure 1, A–C).

Skeletal muscle atrophy and atrogene expression can be opposed by the activation of mammalian target of rapamycin (mTOR), which, by forming 2 distinct protein complexes, mTORC1 and mTORC2, triggers distinct pathways that lead, respectively, to increased protein synthesis and to inhibited protein degradation (28, 29). To assess whether mTOR mediates the signaling triggered by AG/UnAG, myotubes were incubated with rapamycin, an inhibitor of mTORC1, which, upon prolonged treatment, also impairs the assembly of mTORC2 in several cell types, including C2C12 cells (refs. 30–32 and Supplemental Figure 1, A and B; supplemental material available online with this article; doi:10.1172/JCI39920DS1).

Upon 24-hour treatment of atrophying myotubes with 20 ng/ml rapamycin, the antiatrophic activity of AG/UnAG on myotube diameter was fully reverted (Figure 1D), which indicates that activation of mTOR is indeed required for the antiatrophic activity of AG and UnAG. Moreover, in the same assay, the antiatrophic activity of AG/UnAG was inhibited by 100 nM wortmannin, an inhibitor of PI3K, whose product $PI(3,4,5)P_3$ is essential for the activity of Akt, a substrate of mTORC2 that also mediates the activation of mTORC1 (29). These findings indicate that AG/UnAG antiatrophic activity requires both mTOR and Akt. Thus, we assayed the activity of both mTOR complexes. We evaluated mTORC2 activity as phosphorylation of Akt^{S473}, which, in turn, phosphorylates $FoxO3a^{T32}$, thus preventing Atrogin-1 transcription (24, 25). AG/UnAG, as well as IGF-1, induced phosphorylation of Akt^{S473} and $FoxO3a^{T32}$ (Figure 1, E and F), which indicates that they activate mTORC2-mediated pathways.

The activity of mTORC1 was assayed as phosphorylation of $S6K^{T389}$, a direct substrate of mTORC1, and of its substrate $S6^{S235/236}$, a ribosomal protein whose phosphorylation mediates protein synthesis (29). AG and UnAG did not induce phosphorylation of $S6K^{T389}$ and $S6^{S235/236}$ (Figure 1, G and H), nor protein synthesis (as measured by [^{3}H]-leucine incorporation; Figure 1I) or myotube hypertrophy (Figure 1A). Conversely, IGF-1 induced $S6K^{T389}$ and $S6^{S235/236}$ phosphorylation, [^{3}H]-leucine incorporation, and myotube diameter increase, as expected.

By silencing raptor and rictor, specific components of mTORC1 and mTORC2, respectively (Figure 1J), we observed that downregulation of rictor abrogated the protective effect of both peptides on dexamethasone-induced muscle atrophy, measured as myotube diameter, while it did not affect the antiatrophic activity of IGF-1 (Figure 1K). Conversely, raptor silencing impaired IGF-1 antiatrophic activity without affecting that of AG/UnAG. These results indicate that mTORC2 pathway mediates AG/UnAG antiatrophic activity in C2C12 myotubes, without involving mTORC1-mediated protein synthesis.

To identify the signaling pathways differently activated by AG/UnAG and IGF-1, we investigated the role of p38 serine kinase, whose activation by AG/UnAG mediates C2C12 myoblast differentiation (16). In C2C12 myotubes, AG/UnAG, as well as IGF-1, induced phosphorylation of $p38^{T180/Y182}$ (Figure 2A), and its pharmacological inhibition impaired the antiatrophic activity of AG/UnAG, but not of IGF-1 (Figure 2B).

Activation of p38 has been reported to downregulate Atrogin-1, thereby contributing to the protection of skeletal muscle from atrophy (33). On the other hand, p38 mediates induction of Atrogin-1 by TNF-α and oxidative stress and of MuRF1 by serum starvation (34–37). Inhibition of p38 with SB203580 reduced dexamethasone-induced expression of both Atrogin-1 and MuRF1; nevertheless, induction of Atrogin-1, but not MuRF1, was still significant (Figure 2, C and D). In the presence of SB203580, AG and UnAG, but not IGF-1, failed to further reduce the residual induction of Atrogin-1, which indicates that p38 mediates AG/UnAG signaling in regulating Atrogin-1 expression.

To further characterize AG/UnAG antiatrophic activity, we treated C2C12 myotubes with NF449, a compound uncoupling $G\alpha_s$ from GPCRs, which inhibits antiapoptotic activity of AG and UnAG in pancreatic β cells (9, 38). NF449 completely abrogated Akt^{S473} phosphorylation and antiatrophic activity of AG/UnAG without affecting IGF-1 activities (Figure 2, E and F), which supports the hypothesis that AG and UnAG act through a GPCR, as previously suggested (9).

PI3K α and β isoforms mediate Akt activation upon stimulation of tyrosine kinase receptors and GPCRs, respectively (39, 40). We dissected the contribution of PI3Kα and PI3Kβ to IGF-1 and AG/UnAG antiatrophic activity using isoform-specific PI3K inhibitors. Whereas inhibition of PI3Kα by PIK-75 abolished IGF-1 antiatrophic activity, it did not affect AG/UnAG protection. Conversely, inhibition of PI3Kβ by TGX-221 impaired AG/UnAG antiatrophic activity while not affecting IGF-1 protection (Figure 2G). The involvement of PI3Kβ in AG/UnAG antiatrophic activity was further supported by the finding that TGX-221 prevented AG/UnAG from reducing dexamethasone-induced Atrogin-1 expression (Figure 2H). Together, these data strongly suggest that AG/UnAG acts through GPCR-dependent signaling pathways involving a PI3K isoform distinct from that of IGF-1.

Glucocorticoids induce muscle mass reduction by also upregulating the expression of myostatin, a TGF-β family member that acts as a negative regulator of muscle mass. Myostatin reduces the

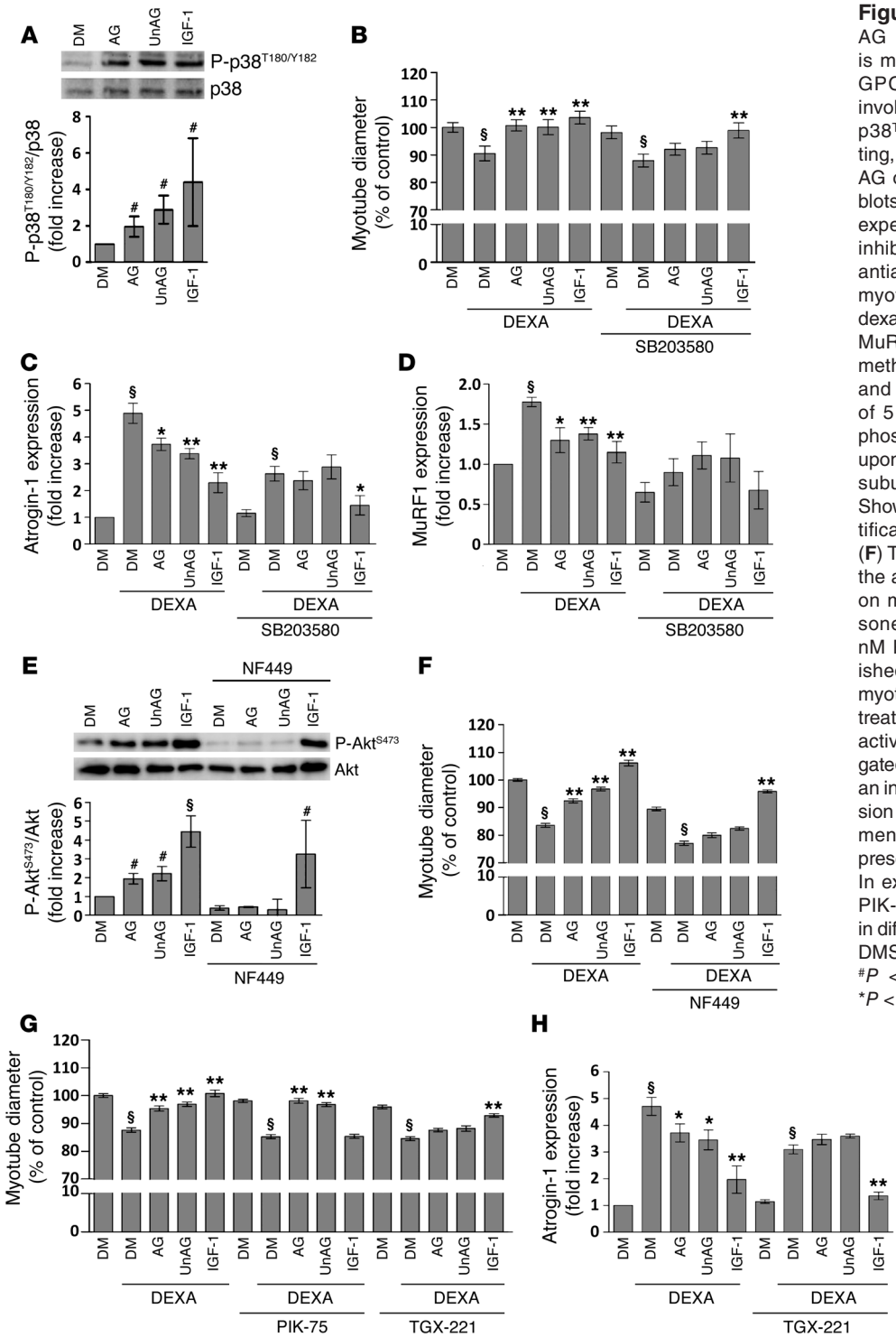

Figure 2

AG and UnAG antiatrophic signaling is mediated by p38 and acts through a GPCR-dependent signaling pathway involving PI3Kβ. (**A**) Phosphorylation of $p38^{T180/Y182}$, detected by Western blotting, after 20-minute treatment with 1 μM AG or UnAG. Shown are representative blots and quantification of 3 independent experiments. (**B**) Treatment with the p38 inhibitor SB203580 (5 μM) reverted the antiatrophic activity of AG and UnAG on myotube diameter upon treatment with dexamethasone. (**C** and **D**) Atrogin-1 and MuRF1 expression analysis upon dexamethasone treatment with or without AG and UnAG in the presence or absence of 5 μM SB203580. (**E**) AG and UnAG phosphorylation of Akt^{S473} was abolished upon treatment with 10 μM NF449, a $G\alpha_s$ subunit–selective G protein antagonist. Shown are representative blots and quantification of 3 independent experiments. (**F**) Treatment with 10 μM NF449 reverted the antiatrophic activity of AG and UnAG on myotube diameter upon dexamethasone treatment. (**G**) Treatment with 25 nM PIK-75, an inhibitor of PI3Kα, abolished the antiatrophic effect of IGF-1 on myotube diameter upon dexamethasone treatment, without affecting AG and UnAG activity. The antiatrophic effect was abrogated by treatment with 200 nM TGX-221, an inhibitor of PI3Kβ. (**H**) Atrogin-1 expression analysis upon dexamethasone treatment with AG, UnAG, and IGF-1 in the presence or absence of 200 nM TGX-221. In experiments with SB203580, NF449, PIK-75, and TGX-221, control myotubes in differentiation medium were treated with DMSO, a vehicle for all these compounds. $^{\#}P < 0.05$, $^{\S}P < 0.01$ vs. DM control; $^{*}P < 0.05$, $^{**}P < 0.01$ vs. DEXA treatment.

size of human skeletal muscle cell–derived myotubes by reducing mTOR/Akt/p70S6K signaling, while simultaneous treatment with IGF-1 restores myotube size, Akt phosphorylation, and protein synthesis (41, 42). In C2C12 myotubes, dexamethasone treatment actually induced the expression of myostatin, which was significantly reduced by IGF-1. However, AG/UnAG had no effect on myostatin expression (Supplemental Figure 1C), providing further evidence that ghrelin and IGF-1 inhibit muscle atrophy through distinct, partially overlapping, mechanisms.

Tg mice with high levels of circulating UnAG are protected from fasting- and denervation-induced atrophy. To verify in vivo the relevance of the findings described above, we used a strain of Tg mice with cardiac-specific ghrelin gene (*Ghrl*) expression. In these mice (referred to herein as *Myh6/Ghrl*), *Ghrl* overexpression in the heart results in

Table 1
Phenotypical characterization of *Myh6/Ghrl* mice

	WT	*Myh6/Ghrl*
UnAG (pg/ml)	445.4 ± 155	25,000.5 ± 360[A]
AG, fed (pg/ml)	41.7 ± 1.6	39.3 ± 1.5
AG, fasted (pg/ml)	75.7 ± 8.8	68.2 ± 9.5
IGF-1, fed (ng/ml)	748.5 ± 56	765.5 ± 120
IGF-1, fasted (ng/ml)	398 ± 93	328 ± 37
Insulin (pg/ml)	571 ± 58	631 ± 129
Tibial length (mm)	19.65 ± 0.11	19.62 ± 0.22
Nasoanal length (mm)	91.59 ± 0.51	90.61 ± 0.95
BMI, fed (g/cm^2)	3.32 ± 0.12	3.33 ± 0.08
BMI, fasted (g/cm^2)	2.93 ± 0.06	2.92 ± 0.09
Gastrocnemius weight, fed (mg)	134.86 ± 4.6	137.2 ± 5.62
Gastrocnemius weight, fasted (mg)	118 ± 4	124 ± 3.1
Gastrocnemius weight/tibial length, fed (mg/mm)	6.86 ± 0.22	6.99 ± 0.25
Gastrocnemius weight/tibial length, fasted (mg/mm)	5.89 ± 0.14	6.36 ± 0.15[B]
Heart weight, fed (mg)	117.5 ± 11.8	122 ± 6.8
Heart weight, fasted (mg)	103.0 ± 7.1	105 ± 3.3
Heart weight/nasoanal length, fed (mg/mm)	1.22 ± 0.12	1.28 ± 0.08
Heart weight/nasoanal length, fasted (mg/mm)	1.16 ± 0.07	1.16 ± 0.03
Daily food intake (g)	4.66 ± 0.17	4.73 ± 0.07
Daily food intake, denervated (g)	4.60 ± 0.17	4.60 ± 0.18

Measurements were performed as described in Methods. Muscle mass and tibial length were calculated as the mean of right and left hindlimbs. $n = 7$ per group (fed); 4 per group (fasted 48 hours); 5 per group (denervated). Data are mean ± SEM. [A]$P < 0.01$ vs. WT. [B]$P < 0.05$ vs. WT.

a 50-fold increase of circulating UnAG, without affecting AG levels (Table 1), as previously observed in other *Ghrl*-overexpressing Tg mice (43–45). *Ghrl* mRNA overexpression was restricted to the myocardium of *Myh6/Ghrl* mice, without leakage in the skeletal muscle (Supplemental Figure 2A). Moreover, consistent with the inability of UnAG to activate GHSR-1a and to promote GH release and adiposity, *Myh6/Ghrl* mice did not feature any change in circulating IGF-1 concentration, tibial and nasoanal length, BMI, or food intake compared with their WT littermates. In addition, fasting decreased IGF-1 and increased ghrelin circulating concentrations to the same extent in WT and *Myh6/Ghrl* mice (Table 1). These data strongly indicate that the upregulation of circulating UnAG in *Myh6/Ghrl* mice does not activate GHSR-1a in the pituitary and hypothalamus, stimulate the GH/IGF-1 axis, or affect endogenous ghrelin regulation. Moreover, tissue expression of IGF-1, which in skeletal muscle may act locally in a paracrine/autocrine manner (46), was not altered in *Myh6/Ghrl* mice, either in fed or in fasted animals (Supplemental Figure 2B).

Although AG and UnAG differently regulate insulin release and sensitivity (47), basal insulin level, glucose uptake, and insulin sensitivity were not affected in *Myh6/Ghrl* mice (Table 1 and Supplemental Figure 2, C and D).

Notably, compared with WT animals, fed *Myh6/Ghrl* mice did not feature any difference in heart and gastrocnemius muscle weight (Table 1), fiber cross-sectional area (CSA) distribution, or hindlimb force (as measured by grasping test; Supplemental Figure 2, E and F), which indicates that high levels of circulating UnAG do not induce skeletal muscle hypertrophy in vivo, consistent with the inability of UnAG to induce hypertrophy in C2C12-derived myotubes.

To investigate whether UnAG might protect from muscle wasting, we induced skeletal muscle atrophy by food deprivation. After 48 hours of fasting, gastrocnemius weight was decreased by approximately 14% in WT mice, and by approximately 9% in *Myh6/Ghrl* mice, compared with fed animals (Figure 3A), which indicates that increased circulating UnAG results in 30% protection from fasting-induced loss in gastrocnemius mass. Accordingly, gastrocnemii CSA was reduced by 29% in WT mice and by 19% in *Myh6/Ghrl* mice compared with fed animals (Figure 3B), indicative of 34% protection. Similarly, extensor digitorum longus (EDL) muscle weight and mean fiber area of *Myh6/Ghrl* mice was reduced to a lesser extent than in WT animals (Figure 3, D and E). This protection was reflected by shift in CSA distributions of gastrocnemii and EDL — toward fibers with wider area — in *Myh6/Ghrl* compared with WT mice under fasting conditions (Figure 3, C and F).

After 48 hours of fasting, Atrogin-1 and MuRF1 expression in gastrocnemii of WT animals dramatically increased. In *Myh6/Ghrl* mice, the induction of Atrogin-1 was significantly reduced by one-third, while MuRF1 was only slightly, not significantly, decreased (Figure 3, G and H).

Plasma levels of glycerol and FFAs did not change in fasted *Myh6/Ghrl* and WT mice (Supplemental Figure 2, G and H), which indicates that fasting did not significantly affect either glycerol or FFA concentrations, consistent with previous reports in the FVB mouse background (48, 49). Moreover, hepatic phosphoenolpyruvate carboxykinase (PEPCK) expression was induced to the same extent in fasted *Myh6/Ghrl* and WT littermates (Supplemental Figure 2I). Together, these data suggest that muscle wasting–resistant properties of *Myh6/Ghrl* mice do not depend on effects of UnAG on energy balance.

Furthermore, *Myh6/Ghrl* mice were protected from denervation-induced muscle atrophy, an experimental procedure that does not affect animal daily food intake (Table 1). At 7 and 14 days after denervation, gastrocnemii weight of WT animals was reduced by 21% and 27%, respectively, while the loss of muscle weight in *Myh6/Ghrl* animals was significantly lower (Figure 4A). Consistently, gastrocnemii mean fiber CSA of WT animals was remarkably reduced at both 7 and 14 days after denervation, whereas CSA in *Myh6/Ghrl* animals was reduced to a lesser extent (Figure 4B). At 7 days after denervation, *Myh6/Ghrl* mice featured a mild shift of gastrocnemii CSA distribution that became impressive after 14 days (Figure 4, C and D). A strong inhibition of atrophy at 7 days after denervation was also evident in EDL (Figure 4, E and F) and tibialis anterior (TA) muscles (Figure 4, G and H).

Moreover, in gastrocnemii of *Myh6/Ghrl* mice, the induction of Atrogin-1 was reduced by 40% (Figure 4I). Conversely, MuRF1 was only slightly, not significantly, reduced (Figure 4J), consistent with the fasting-induced atrophy data. Together, these observations indicated that constitutive high levels of UnAG impair experimentally induced atrophy in vivo, likely through a mechanism independent of GHSR-1a and activation of the GH/IGF-1 axis.

UnAG pharmacological treatment induces antiatrophic signaling in muscle and inhibits fasting- and denervation-induced atrophy. Acute

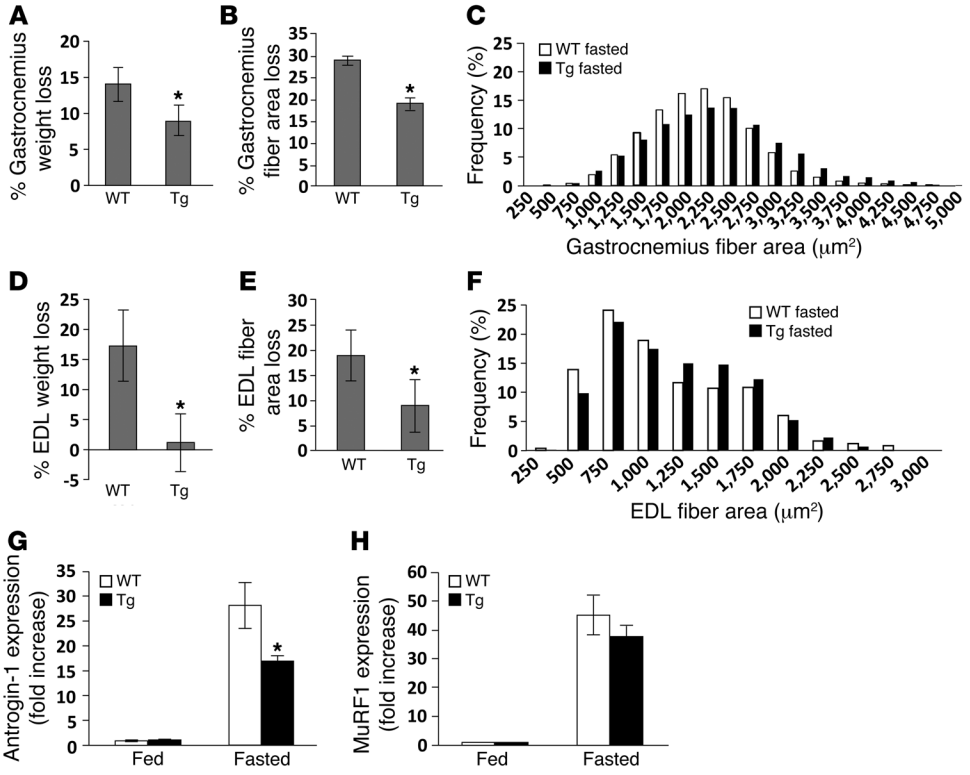

Figure 3

Myh6/Ghrl mice are protected from skeletal muscle atrophy induced by 48 hours of fasting. (**A**–**C**) Effect of fasting on gastrocnemii. Mean percentage of gastrocnemius weight loss (**A**) and CSA reduction (**B**) of fasted *Myh6/Ghrl* (Tg) mice and WT littermates compared with fed animals. (**C**) Frequency distribution of gastrocnemii CSA of fasted *Myh6/Ghrl* and WT mice. (**D**–**F**) Effect of fasting on EDL muscles. Mean percentage of EDL muscle weight loss (**D**), CSA reduction (**E**), and CSA frequency distribution (**F**) of fasted *Myh6/Ghrl* and WT littermates. (**G** and **H**) Atrogin-1 and MuRF1 expression in gastrocnemii of fed and fasted *Myh6/Ghrl* mice and their WT littermates, determined by real-time RT-PCR. **P* < 0.01 vs. WT. *n* = 7 (fed WT and *Myh6/Ghrl*); 5 (fasted WT); 6 (fasted *Myh6/Ghrl*); 3 (CSA loss and distribution, WT and *Myh6/Ghrl*).

administration of exogenous UnAG at 100 μg/kg, a dose previously used for in vivo studies (6), induced phosphorylation of Akt^{S473}, $FoxO3a^{T32}$, and $p38^{T180/Y182}$ in WT gastrocnemii (Figure 5, A–C), which indicates that, in vivo, UnAG activates the same antiatrophic signaling pathway as it does in C2C12 myotubes.

Repeated administration (every 12 hours) of UnAG protected mice from skeletal muscle atrophy induced by either fasting or denervation (Figure 5, D–I). UnAG treatment preserved gastrocnemii from weight and mean fiber CSA loss (Figure 5, D and E). Accordingly, frequency distribution of gastrocnemii CSA of fasted mice injected with UnAG showed a dramatic shift toward bigger fiber areas compared with saline-injected mice (Figure 5F).

Similarly, UnAG treatment of denervated mice resulted in a 25% protection from gastrocnemius weight loss and a significantly lower decrease of mean fiber CSA, although the CSA distribution of UnAG-injected mice showed only a very mild shift compared with saline-injected animals (Figure 5, G–I). Although the plasma concentration of UnAG after injection dropped to basal levels in about 2–4 hours (Supplemental Figure 3A), these data indicate that repeated acute stimulation is sufficient to protect from experimentally induced skeletal muscle atrophy without affecting muscular IGF-1 expression (Supplemental Figure 3B).

AG and UnAG induce antiatrophic signaling and impair muscle atrophy in Ghsr$^{-/-}$ *mice*. The findings reported above, along with previous data on common binding sites for AG/UnAG in C2C12 lacking *Ghsr* (16), strongly suggest that AG and UnAG stimulate antiatrophic signaling in skeletal muscle through activation of a receptor distinct from GHSR-1a. To verify this hypothesis, we assayed AG/UnAG antiatrophic signaling and activity in *Ghsr*$^{-/-}$ mice, in which AG fails to activate the GH/IGF-1a axis or stimulate appetite (50). Injection of either AG or UnAG induced Akt^{S473} phosphorylation in gastrocnemii of *Ghsr*$^{-/-}$ mice (Figure 6A). Consistently, treatment of *Ghsr*$^{-/-}$ mice with 100 μg/kg AG or UnAG twice daily reduced gastrocnemii weight loss induced by 48-hour fasting by 30% compared with saline-treated animals (Figure 6B). Moreover, the mean CSA loss of AG- and UnAG-injected mice strongly decreased compared with saline-injected animals, and CSA distribution shifted toward bigger areas (Figure 6, C and D).

In summary, these findings demonstrated that both AG and UnAG activate a direct antiatrophic signaling pathway in skeletal muscle and protect from experimentally induced muscle atrophy, independently of the AG receptor GHSR-1a.

Discussion

Several studies have shown that AG protects from cachexia and prevents muscle proteolysis in vivo, supposedly through stimulation of appetite and activation of the GH/IGF-1 axis mediated by AG binding to GHSR-1a (6, 7, 18–21). However, here we provided in vitro and in vivo evidence that AG and UnAG exert antiatrophic activity by acting directly on the skeletal muscle, even in *Ghsr*$^{-/-}$ mice.

Upregulation of circulating UnAG, which does not bind GHSR-1a and does not activate the GH/IGF-1 axis, counteracted muscle atrophy induced by either fasting or denervation. Consistently, UnAG has been reported to reduce burn-induced skeletal muscle proteolysis and local TNF-α upregulation (51).

We achieved upregulation of circulating UnAG either by myocardial *Ghrl* overexpression in *Myh6/Ghrl* mice or by repeated administration. The antiatrophic activity of UnAG cannot be mediated by its conversion to AG in the plasma, since acylation occurs only intracellularly on the ghrelin precursor by the ghrelin-specific acyltransferase GOAT (11, 12). The negligible myocardial expression of GOAT might explain the increase of only the unacylated form

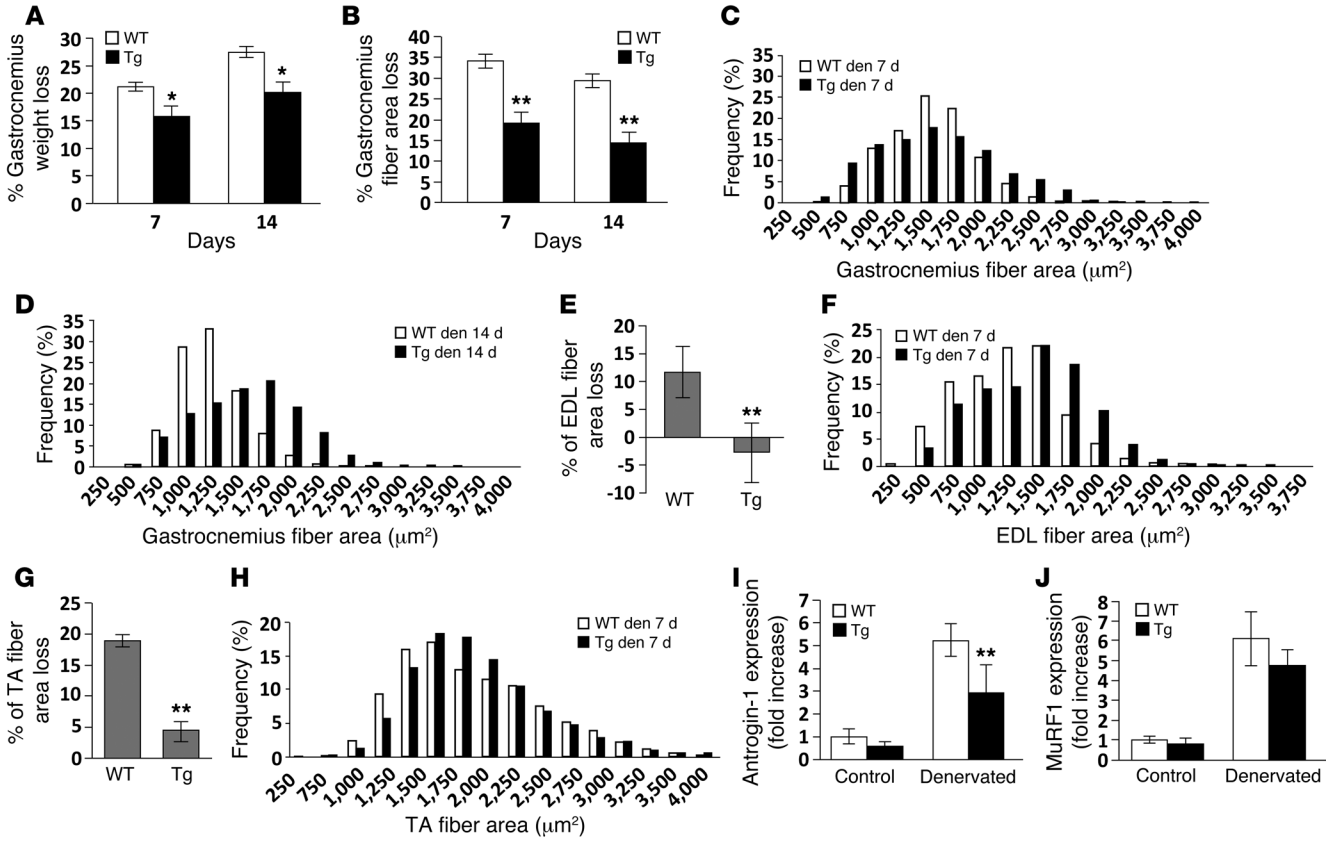

Figure 4

Myh6/Ghrl mice are protected from denervation-induced skeletal muscle atrophy induced by sciatic nerve resection. (**A** and **B**) Mean percentage of weight loss (**A**) and CSA reduction (**B**) of denervated gastrocnemius at 7 and 14 days after denervation, compared with the unperturbed side. (**C** and **D**) Frequency distribution of gastrocnemii CSA at 7 and 14 days after denervation in *Myh6/Ghrl* and WT mice. (**E**–**H**) CSA reduction and fiber area distribution of (**E** and **F**) EDL and (**G** and **H**) TA muscles at 7 days after denervation. (**I** and **J**) Atrogin-1 and MuRF1 expression, determined by real-time RT-PCR, in denervated gastrocnemii at 7 days after denervation, compared with the unperturbed side. $^{**}P < 0.01$, $^{*}P < 0.05$ vs. WT. $n = 6$ (WT); 5 (*Myh6/Ghrl*); 3 (CSA loss and distribution, WT and *Myh6/Ghrl*).

of circulating ghrelin in *Myh6/Ghrl* mice. This is in agreement with other tissue-specific *Ghrl* Tg mice featuring high UnAG circulating levels in the absence of significant changes of AG (43–45).

The observations that *Myh6/Ghrl* mice did not feature any change in circulating and muscular IGF-1 or in tibial or whole body length, along with the lack of skeletal muscle hypertrophy, further indicate that the GH/IGF-1 axis is not activated in these mice. Finally, the finding that both AG and UnAG impaired skeletal muscle atrophy in *Ghsr*$^{-/-}$ mice indicated that their antiatrophic activity is mediated by a receptor distinct from GHSR-1a. In these mice, AG exerted antiatrophic activity in the skeletal muscle independent of its role in modulating GH release and energy balance. Nevertheless, these data do not exclude the possibility that in WT animals, GHSR-1a may contribute to the antiatrophic activity of AG by also regulating the GH/IGF-1 axis and positive energy balance. For instance, AG has been suggested to prevent downregulation of muscular IGF-1 expression in an experimental model of cachexia through an indirect mechanism involving GHSR-1a activity on positive energy balance (20).

The hypothesis that AG/UnAG impairs muscle atrophy in vivo by acting directly on the skeletal muscle is further supported by our finding that UnAG administration rapidly stimulated antiatrophic signaling in the gastrocnemius. Moreover, AG/UnAG activated antiatrophic signaling in cultures of C2C12 myotubes, which do not express GHSR-1a, protecting them from dexamethasone-induced atrophy and atrogene upregulation. Although AG has previously been reported to fail in reducing dexamethasone-induced Atrogin-1 expression in C2C12 myotubes (20), the 10-fold lower dexamethasone concentration used in that study and the considerably weaker Atrogin-1 induction may explain the different results. Conversely, Sheriff et al. showed that UnAG reduces TNF-α/IFN-γ–induced cachexia in C2C12 myotubes in a PI3K/mTOR-dependent manner (51). The results of our present study not only confirmed the involvement of PI3K/mTOR pathways in AG/UnAG activity on skeletal muscle, but also showed the specific contribution of the mTORC2- over the mTORC1-mediated signaling pathway, which may explain, at least in part, the ability of AG/UnAG to protect from skeletal muscle atrophy without a concomitant induction of hypertrophy.

Indeed, the molecular mechanisms underlying AG/UnAG antiatrophic activity in the skeletal muscle involved the activation of mTORC2-mediated signaling pathways, leading to phosphorylation of Akt^{S473} and of its substrate FoxO3a^{T32}, which eventually impaired Atrogin-1 expression and muscle protein degradation. At

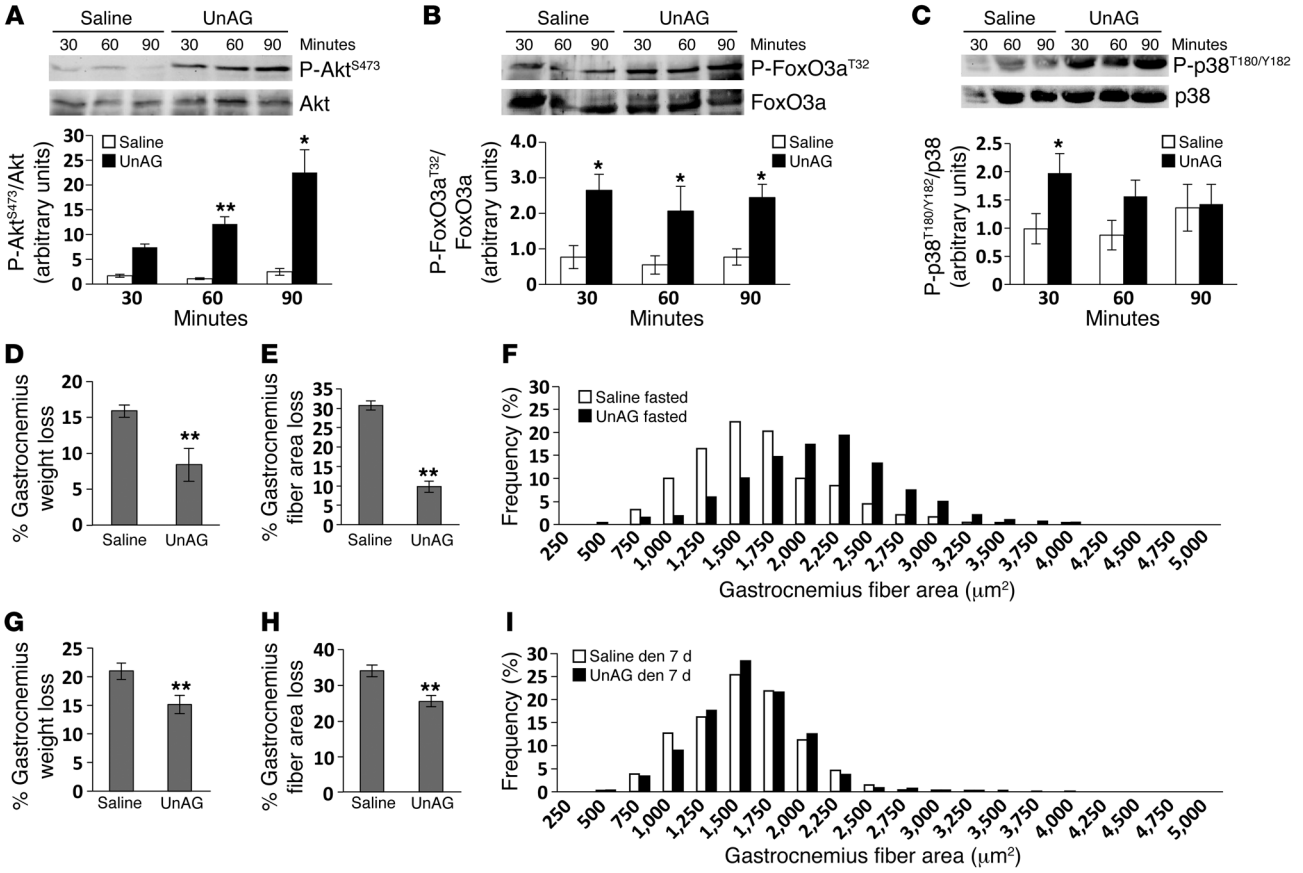

Figure 5

UnAG pharmacological treatment protects skeletal muscle from fasting- and denervation-induced atrophy in WT mice. (**A**–**C**) Phosphorylation of Akt^{S473}, FoxO3a^{T32}, and p38$^{T180/Y182}$ in gastrocnemii of WT mice treated with 100 μg/kg UnAG or saline. At the indicated time points, gastrocnemii were removed and processed for Western blot analysis. Shown are representative blots and densitometric analysis of 3 independent experiments, normalized to untreated animals (not shown). (**D**–**F**) Mean percent weight loss (**D**), CSA reduction (**E**), and CSA frequency distribution (**F**) of gastrocnemii from fed or 48-hour fasted mice treated twice daily with 100 μg/kg UnAG or saline (n = 5 per group). Frequency distribution was measured in 3 mice per group. In **D** and **E**, percent reduction shown is between fasted and fed mice. (**G**–**I**) Mean percent weight loss (**G**), CSA reduction (**H**), and CSA frequency distribution (**I**) of gastrocnemii from mice treated with 100 μg/kg UnAG or saline twice daily for 7 days after sciatic nerve resection (n = 5 per group). Frequency distribution was measured in 3 mice per group. In **G** and **H**, percent reduction shown is between denervated gastrocnemii and gastrocnemii from the unperturbed side. *P < 0.05, **P < 0.01 vs. saline treatment.

the same time, in C2C12 myotubes, AG/UnAG failed to stimulate mTORC1-mediated phosphorylation of S6K^{T389} and S6$^{S235/236}$, protein synthesis, and hypertrophy. Consistently, chronic upregulation of circulating UnAG in *Myh6/Ghrl* mice did not induce muscle hypertrophy. This finding highlights a remarkable difference between the antiatrophic activities of AG/UnAG and IGF-1 in the skeletal muscle, as IGF-1 stimulates both mTORC2-mediated impairment of protein degradation and mTORC1-dependent stimulation of protein synthesis and hypertrophy (23–26). Consistently, in TNF-α/IFN-γ–treated C2C12 myotubes, UnAG inhibited protein catabolism and impaired the induction of Atrogin-1 and MuRF1. Moreover, UnAG restored the basal phosphorylation state of proteins of mTORC1 and mTORC2 pathways, although the lack of UnAG-induced increase in Akt^{S473} phosphorylation observed herein may depend on receptor desensitization, given the higher concentration of UnAG used and the protracted treatment (51).

The finding that downregulation of the mTORC1-specific component raptor did not affect the antiatrophic activity of AG/UnAG, while impairing IGF-1 antiatrophic activity, further supports the conclusion that AG/UnAG antiatrophic activity does not involve mTORC1-mediated stimulation of protein synthesis. On the other hand, the finding that AG/UnAG antiatrophic activity was sensitive to downregulation of rictor, the specific component of mTORC2, demonstrated the key role of mTORC2 in mediating AG/UnAG antiatrophic activity. The finding that ghrelin-induced phosphorylation of Akt^{S473} was uncoupled from the activation of mTORC1-mediated pathways and hypertrophy may appear controversial, as IGF-1–induced phosphorylation of Akt^{S473} is associated with the activity of both mTOR complexes (29), and overexpression of constitutive active Akt in the skeletal muscle prevents denervation-induced atrophy and induces hypertrophy (22, 52). The lack of muscle hypertrophy observed in *Myh6/Ghrl* mice may depend on weaker stimulation of the PI3K/Akt pathway by UnAG. Indeed, although tissue-specific expression of constitutive active Akt in Tg mice induces strong phosphorylation of Akt and of its substrates (53), phosphorylation of Akt was not detectable in

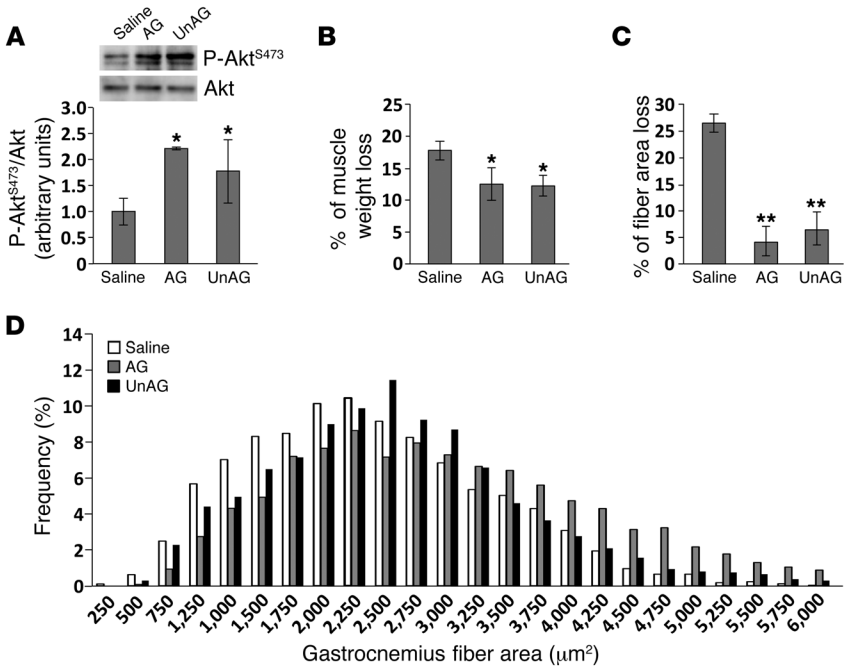

Figure 6
AG and UnAG pharmacological treatment of *Ghsr*$^{-/-}$ mice induces antiatrophic signaling and protects from fasting-induced skeletal muscle atrophy. (**A**) Phosphorylation of Akt^{S473} in gastrocnemii of *Ghsr*$^{-/-}$ mice injected with 100 μg/kg AG or UnAG or with saline. 60 minutes after treatment, gastrocnemii were removed and processed for Western blot analysis. Shown are representative blots and densitometric analysis of 3 independent experiments. (**B**–**D**) Mean percentage weight loss (**B**), CSA reduction (**C**), and CSA frequency distribution (**D**) of gastrocnemii from fed or 48-hour fasted *Ghsr*$^{-/-}$ mice injected s.c. twice daily with 100 μg/kg AG or UnAG or with saline (n = 5 per group). Frequency distribution was measured in 3 mice per group. In **B** and **C**, percent reduction is between fasted and fed mice. *P < 0.05, **P < 0.01 vs. saline treatment.

muscles of *Myh6/Ghrl* mice (data not shown). Indeed, we found that 2 distinct PI3K isoforms, namely PI3Kβ and PI3Kα, mediated the antiatrophic activity of AG/UnAG and IGF-1, respectively. This observation, along with the ability of a $G\alpha_s$-uncoupling drug to abolish the antiatrophic activity of AG/UnAG, but not IGF-1, is consistent with the hypothesis that the unknown receptor mediating the common activities of AG/UnAG is a GPCR (9). Moreover, these data further serve to rule out the hypothesis that AG/UnAG acts on myotubes by stimulating the autocrine release of IGF-1.

The inability of AG and UnAG to stimulate protein synthesis and hypertrophy in the skeletal muscle is consistent with their key role in the adaptive response to fasting and negative energy balance (13). The molecular mechanisms underlying the uncoupling of mTORC2 from mTORC1 remain to be investigated. AG and UnAG, which are released during fasting, might shift muscle metabolism toward amino acid oxidation, thereby decreasing the intracellular pool of free amino acids essential for mTORC1 activity (29). Alternatively, activation of PI3Kβ, whose enzymatic activity is lower than that of PI3Kα (54), may result in weaker activation of Akt. Finally, AMPK, which negatively regulates mTORC1 in skeletal muscle (55), may contribute to mTORC1 uncoupling, although AG was reported to be unable to stimulate AMPK in rat gastrocnemius (56).

The finding that p38 was required for AG/UnAG antiatrophic activity is consistent with previous findings that p38 cooperates with PI3K/Akt pathways to induce C2C12 differentiation (16, 57). However, the role of p38 in regulating muscle atrophy is complex, as its activation mediates muscle atrophy induced by oxidative stress and inflammatory cytokines (34, 36, 58). The role of p38 in signaling is determined by its association in distinct signaling complexes with different regulators and substrates and by its localization (35). Our findings are consistent with evidence indicating that, in myotubes, decreased p38 phosphorylation is associated with dexamethasone-induced atrophy, and that p38 mediates β-hydroxyl-β-methylbutyrate protection from dexamethasone-induced protein degradation (59, 60). Moreover, p38 activity can regulate cytoplasmic localization of FoxO3a independently of Akt, thereby impairing its transcriptional activity and Atrogin-1 induction (33, 61). Furthermore, activation of p38 stabilizes and activates the transcriptional coactivator PGC1α, which represses FoxO3a activity (62, 63). Although IGF-1 activated p38, this was dispensable for IGF-1 antiatrophic activity. In addition, IGF-1 and AG/UnAG antiatrophic activities differed in the inability of AG/UnAG to downregulate myostatin, a TGF-β–like inhibitor of muscle growth, which further supports the hypothesis that AG/UnAG and IGF-1 counteract muscle atrophy through distinct molecular mechanisms.

The data presented herein unveiled a novel component of the complex role of AG/UnAG, i.e., the direct activation of antiatrophic pathways in the skeletal muscle, eventually leading to reduced muscle wasting. This effect adds to the well-known capabilities of AG to stimulate appetite, regulate lipid metabolism, and release GH. Although the identity of the novel AG/UnAG receptor is yet unknown, these findings may have important biological and therapeutic implications, since they provide proof that UnAG has a strong and specific potential for the prevention or treatment of muscle atrophy, avoiding the diabetogenic side effects of AG (47) and the cancer risk associated with IGF-1 treatment (64).

Methods

Reagents. AG_{1-28} and $UnAG_{1-28}$ were purchased from PolyPeptide Laboratories. The PI3K p110α inhibitor PIK-75 hydrochloride was purchased from Axon Medchem, and the PI3K p110β inhibitor TGX-221 was a gift from U. Galli (Synthetic Medicinal Chemistry group, Università del Piemonte Orientale, Novara, Italy). Water-soluble dexamethasone and all other reagents, unless otherwise stated, were from Sigma-Aldrich. Anti–phospho-Akt^{S473}, anti-Akt, anti–phospho-FoxO3a^{T32}, anti-FoxO3a, anti–phospho-S6K^{T389}, anti-S6K, anti–phospho-S6$^{S235/236}$, anti-S6, anti-p38$^{T180/Y182}$, anti-p38, anti-raptor, and anti-rictor antibodies were from Cell Signaling Technology; anti-actin antibody was from Santa Cruz Biotechnology.

Cell cultures and myotube analysis. C2C12 myoblasts were differentiated in myotubes as previously described (16). For measurement of myotube diam-

eters, myotubes were fixed, and diameters were quantified by measuring a total of >100 myotube diameters from 5 random fields in 3 replicates at ×40 magnification using Image-Pro Plus software (MediaCybernetics) as described previously (24).

Raptor and rictor silencing. Raptor siRNA (*MISSION pre-designed siRNA* SASI_Mm01_00055293; Sigma-Aldrich), rictor siRNA (SASI_Mm01_00137731; Sigma-Aldrich), Block-iT, or siRNA negative control sequence (Invitrogen) were transfected with Lipofectamine2000 (Invitrogen) in C2C12 myotubes. Transfection efficiency was evaluated by the fluorescent siRNA negative control Block-iT, and silencing was verified by Western blot.

[^{3}H]-leucine incorporation assay. C2C12 myotubes were maintained for 24 hours with or without 10 nM AG or UnAG in differentiation medium supplemented with 2 μCi/ml [^{3}H]-leucine (Perkin Elmer) to evaluate the induction of protein synthesis. At the end of treatments, cells were washed with PBS, treated with 5% trichloroacetic acid, and lysed with 0.5 M NaOH and 0.5% SDS. The amount of incorporated [^{3}H]-leucine was evaluated by β counter (Tri-Carb 2800TR; Perkin Elmer) analysis. Data are the average of 4 replicates.

Western blot. C2C12 myotubes were serum starved overnight and then treated as indicated in the figure legends. Western blot was performed as previously described (16). Unless otherwise specified, after use of anti–phospho-specific antibodies, membranes were stripped with Re-Blot Plus (Chemicon, Millipore) and reblotted with the corresponding total protein antibodies.

Muscles of mice fasted for 6 hours were s.c. injected with 100 μg/kg UnAG or AG or with saline solution. At the indicated time points, gastrocnemii were removed, homogenized at 4°C in RIPA buffer (1% Triton X-100; 1% sodium deoxycholate; 0.1% SDS; 1 mM EDTA; 1 mM EGTA; 50 mM NaF; 160 mM NaCl; and 20 mM Tris-HCl, pH 7.4) containing 1 mM DTT, protease inhibitor cocktail, and 1 mM Na_3VO_4. Homogenates were then processed as above.

Tg animal generation and treatment. All experiments were conducted on young adult male FVB1 WT, FVB1 *Myh6/Ghrl*, and C57BL/6J *Ghsr*$^{-/-}$ mice (50), matched for age and weight.

Tg animals were obtained by cloning the murine ghrelin gene (*Ghrl*) under control of the cardiac promoter sequences of the β myosin heavy chain 3′ UTR and the first 3 exons of the α isoform *Myh6* (65). Transgene integration and expression were confirmed by PCR and real-time RT-PCR, respectively. Phenotypical characterization and experiments were carried out on hemizygote animals and littermate controls.

AG, UnAG, and IGF-1 plasmatic levels were measured by EIA kits (SPIbio Bertin Pharma for AG and UnAG; R&D Systems for IGF-1); insulin plasmatic levels were quantified with the Insulin (mouse) ELISA kit (ALPCO Diagnostics); and glycerol and free fatty acid plasmatic levels were evaluated by enzymatic assay kits (Cayman).

BMI was calculated as animal weight divided by the square of the nasoanal length.

Fasting-induced atrophy was achieved by 48 hours of food removal (63), while denervation-induced muscle atrophy was obtained by resection of the sciatic nerve under anesthesia with sevoflurane (Baxter) and evaluated 7 and 14 days later (66). Muscles were collected, weighed, and normalized for tibial length and processed either for RNA extraction or for histology.

Daily food intake was measured over a 12-day period, quantifying the food consumption of each mouse every day.

In all experiments with s.c. injection of AG and/or UnAG, controls were saline-injected animals.

Glucose and insulin tolerance tests. Glucose tolerance and insulin sensitivity tests were performed as previously described (43). For glucose tolerance evaluation, mice were injected i.p. with glucose at 1.5 mg/g body weight at 9:00 am, after 16 hours of fasting. Blood glucose was determined at the indicated time points on tail blood samples using the Accu-Chek Mobile blood glucose meter (Roche Diagnostics). For insulin sensitivity determination, Humulin R (0.75 U/kg body weight; Lilly) was administered i.p., and blood samples for glucose concentrations were collected as described above.

RNA extraction and analysis. Total RNA from cultured myotubes and from muscles was extracted by TRIreagent (Invitrogen). The RNA was retro-transcribed with High-Capacity cDNA Reverse Transcription Kit (Invitrogen), and real-time PCR was performed with the ABI7200 Sequence Detection System (Invitrogen) using the following assays: Mm00499518_m1 (*Fbxo32*, Atrogin-1), Mm01185221_m1 (*Trim63*, MuRF1), Mm00439560_m1 (*Igf1*), Mm00445450_m1 (*Ghrl*), Mm01254559_m1 (*Mstn*), Mm01247058_m1 (*Pck1*), Mm00446953_m1 (*Gusb*), and Mm00506384_m1 (*Ppif*).

Muscle sampling and staining for fiber size assessment. Muscles were embedded in Killik compound (Bio-optica) and frozen in liquid nitrogen–cooled isopentane. Serial transverse cryosections (7 μm thick) of the midbelly region of muscles were cut at –20°C and mounted on glass slides. The sections were air-dried, fixed for 10 minutes in 4% paraformaldehyde, and stained with H&E. The number of myofibers in TA, gastrocnemii, and EDL was measured from the histological preparations. Muscle fiber CSA was assessed as previously described (67). Data are expressed as fiber size distribution and as percent CSA reduction relative to controls.

Grip strength test. Skeletal muscle force was assessed using the BS-GRIP Grip Meter (2Biological Instruments) as previously described (68). Each animal was tested 3 times, and the average value of the maximum weight that the animal managed to hold was recorded and normalized to the mouse's weight.

Statistics. Data are presented as mean ± SEM. Variation among groups was evaluated using nonparametric Wilcoxon and Mann-Whitney *U* tests. Statistical significance was assumed for *P* values less than 0.05. All statistical analyses were performed with SPSS for Windows version 17.0.

Study approval. All animal experimental procedures were approved by the Institutional Animal Care and Use Committee at Università del Piemonte Orientale "Amedeo Avogadro."

Acknowledgments

We are grateful to Riccarda Granata and Cristina Grande for insulin measurements and to Thien-Thi Nguyen, Christian Zurlo, Laura Badà, and Giulia Bettas Ardisson for technical assistance. This work was supported by Telethon (grant no. GGP030386 to A. Graziani), Regione Piemonte CIPE (to A. Graziani, S. Geuna, and I. Perroteau), Regione Piemonte Ricerca Sanitaria (to A. Graziani), Italian Ministry for University and Research (PRIN grant to A. Graziani, S. Geuna, and I. Perroteau), and Opera Pia Eletto Lualdi.

Received for publication December 23, 2011, and accepted in revised form November 1, 2012.

Address correspondence to: Nicoletta Filigheddu, Department of Translational Medicine, Università del Piemonte Orientale "Amedeo Avogadro," Via Solaroli 17, 28100 Novara, Italy. Phone: 39.0321660529; Fax: 39.0321620421; E-mail: nicoletta.filigheddu@med.unipmn.it.

Paolo E. Porporato's present address is: Unit of Pharmacology and Therapeutics, Université Catholique de Louvain, Brussels, Belgium.

Viola F. Gnocchi's present address is: Research Center for Genetic Medicine, Children's National Medical Center, Washington, DC, USA.

Federica Chianale's present address is: Oncological Sciences Department, Systems Biology Unit, IRCC, Candiolo (TO), Italy.

1. Dodson S, et al. Muscle wasting in cancer cachexia: clinical implications, diagnosis, and emerging treatment strategies. *Annu Rev Med*. 2011;62:265–279.
2. Kojima M, Hosoda H, Date Y, Nakazato M. Ghrelin is a growth-hormone-releasing acylated peptide from stomach. *Nature*. 1999;402(6762):656–660.
3. Tschöp M, Smiley DL, Heiman ML. Ghrelin induces adiposity in rodents. *Nature*. 2000; 407(6806):908–913.
4. Nakazato M, Murakami N, Date Y, Kojima M. A role for ghrelin in the central regulation of feeding. *Nature*. 2001;409(6817):194–198.
5. Howard AD, Feighner SD, Cully DF, Arena JP. A receptor in pituitary and hypothalamus that functions in growth hormone release. *Science*. 1996; 273(5277):974–977.
6. Nagaya N, et al. Chronic administration of ghrelin improves left ventricular dysfunction and attenuates development of cardiac cachexia in rats with heart failure. *Circulation*. 2001;104(12):1430–1435.
7. Nagaya N, et al. Effects of ghrelin administration on left ventricular function, exercise capacity, and muscle wasting in patients with chronic heart failure. *Circulation*. 2004;110(24):3674–3679.
8. Baldanzi G, et al. Ghrelin and des-acyl ghrelin inhibit cell death in cardiomyocytes and endothelial cells through ERK1/2 and PI 3-kinase/AKT. *J Cell Biol*. 2002;159(6):1029–1037.
9. Granata R, et al. Acylated and unacylated ghrelin promote proliferation and inhibit apoptosis of pancreatic beta-cells and human islets: involvement of 3′,5′-cyclic adenosine monophosphate/protein kinase A, extracellular signal-regulated kinase 1/2, and phosphatidyl inositol 3-Kinase/Akt signaling. *Endocrinology*. 2007;148(2):512–529.
10. Chung H, Seo S, Moon M, Park S. Phosphatidylinositol-3-kinase/Akt/glycogen synthase kinase-3 beta and ERK1/2 pathways mediate protective effects of acylated and unacylated ghrelin against oxygen-glucose deprivation-induced apoptosis in primary rat cortical neuronal cells. *J Endocrinol*. 2008;198(3):511–521.
11. Yang J, Brown MS, Liang G, Grishin NV, Goldstein JL. Identification of the acyltransferase that octanoylates ghrelin, an appetite-stimulating peptide hormone. *Cell*. 2008;132(3):387–396.
12. Gutierrez JA, et al. Ghrelin octanoylation mediated by an orphan lipid transferase. *Proc Natl Acad Sci U S A*. 2008;105(17):6320–6325.
13. Chen C-Y, Asakawa A, Fujimiya M, Lee S-D, Inui A. Ghrelin gene products and the regulation of food intake and gut motility. *Pharmacol Rev*. 2009; 61(4):430–481.
14. Delhanty PJD, et al. Ghrelin and unacylated ghrelin stimulate human osteoblast growth via mitogen-activated protein kinase (MAPK)/phosphoinositide 3-kinase (PI3K) pathways in the absence of GHS-R1a. *J Endocrinol*. 2006;188(1):37–47.
15. Sato M, et al. Effects of ghrelin and des-acyl ghrelin on neurogenesis of the rat fetal spinal cord. *Biochem Biophys Res Commun*. 2006;350(3):598–603.
16. Filigheddu N, et al. Ghrelin and des-acyl ghrelin promote differentiation and fusion of C2C12 skeletal muscle cells. *Mol Biol Cell*. 2007;18(3):986–994.
17. Delhanty PJD, et al. Unacylated ghrelin rapidly modulates lipogenic and insulin signaling pathway gene expression in metabolically active tissues of GHSR deleted mice. *PLoS One*. 2010;5(7):e11749.
18. Nagaya N, et al. Treatment of cachexia with ghrelin in patients with COPD. *Chest*. 2005;128(3):1187–1193.
19. Balasubramaniam A, et al. Ghrelin inhibits skeletal muscle protein breakdown in rats with thermal injury through normalizing elevated expression of E3 ubiquitin ligases MuRF1 and MAFbx. *Am J Physiol Regul Integr Comp Physiol*. 2009;296(4):R893–R901.
20. Sugiyama M, et al. Ghrelin improves body weight loss and skeletal muscle catabolism associated with angiotensin II-induced cachexia in mice. *Regul Pept*. 2012;178(1–3):21–28.
21. DeBoer MD. Emergence of ghrelin as a treatment for cachexia syndromes. *Nutrition*. 2008;24(9):806–814.
22. Bodine SC, et al. Akt/mTOR pathway is a crucial regulator of skeletal muscle hypertrophy and can prevent muscle atrophy in vivo. *Nat Cell Biol*. 2001; t3(11):1014–1019.
23. Rommel C, et al. Mediation of IGF-1-induced skeletal myotube hypertrophy by PI(3)K/Akt/mTOR and PI(3)K/Akt/GSK3 pathways. *Nat Cell Biol*. 2001;3(11):1009–1013.
24. Sandri M, et al. Foxo transcription factors induce the atrophy-related ubiquitin ligase atrogin-1 and cause skeletal muscle atrophy. *Cell*. 2004;117(3):399–412.
25. Stitt TN, et al. The IGF-1/PI3K/Akt pathway prevents expression of muscle atrophy-induced ubiquitin ligases by inhibiting FOXO transcription factors. *Mol Cell*. 2004;14(3):395–403.
26. Latres E, et al. Insulin-like growth factor-1 (IGF-1) inversely regulates atrophy-induced genes via the phosphatidylinositol 3-kinase/Akt/mammalian target of rapamycin (PI3K/Akt/mTOR) pathway. *J Biol Chem*. 2005;280(4):2737–2744.
27. Bodine SC, et al. Identification of ubiquitin ligases required for skeletal muscle atrophy. *Science*. 2001;294(5547):1704–1708.
28. Foster KG, Fingar DC. Mammalian target of rapamycin (mTOR): conducting the cellular signaling symphony. *J Biol Chem*. 2010;285(19):14071–14077.
29. Laplante M, Sabatini DM. mTOR signaling in growth control and disease. *Cell*. 2012;149(2):274–293.
30. Copp J, Manning G, Hunter T. TORC-specific phosphorylation of mammalian target of rapamycin (mTOR): phospho-Ser2481 is a marker for intact mTOR signaling complex 2. *Cancer Res*. 2009; 69(5):1821–1827.
31. Sarbassov DD, et al. Prolonged rapamycin treatment inhibits mTORC2 assembly and Akt/PKB. *Mol Cell*. 2006;22(2):159–168.
32. Lamming DW, et al. Rapamycin-induced insulin resistance is mediated by mTORC2 loss and uncoupled from longevity. *Science*. 2012;335(6076):1638–1643.
33. Clavel S, Siffroi-Fernandez S, Coldefy AS, Boulukos K, Pisani DF, Dérijard B. Regulation of the intracellular localization of Foxo3a by stress-activated protein kinase signaling pathways in skeletal muscle cells. *Mol Cell Biol*. 2010;30(2):470–480.
34. Li YP, et al. TNF-alpha acts via p38 MAPK to stimulate expression of the ubiquitin ligase atrogin1/MAFbx in skeletal muscle. *FASEB J*. 2005; 19(3):362–370.
35. Cuadrado A, Nebreda AR. Mechanisms and functions of p38 MAPK signalling. *Biochem J*. 2010; 429(3):403–417.
36. McClung JM, Judge AR, Powers SK, Yan Z. p38 MAPK links oxidative stress to autophagy-related gene expression in cachectic muscle wasting. *Am J Physiol Cell Physiol*. 2010;298(3):C542–C549.
37. Kim J, et al. p38 MAPK participates in muscle-specific RING Finger 1-mediated atrophy in cast-immobilized rat gastrocnemius muscle. *Korean J Physiol Pharmacol*. 2009;13(6):491–496.
38. Hohenegger M, et al. 1998. Gsalpha-selective G protein antagonists. *Proc Natl Acad Sci U S A*. 1998; 95(1):346–351.
39. Jia S, et al. Essential roles of PI(3)K-p110beta in cell growth, metabolism and tumorigenesis. *Nature*. 2008;454(7205):776–779.
40. Ciraolo E, et al. Phosphoinositide 3-kinase p110beta activity: key role in metabolism and mammary gland cancer but not development. *Sci Signal*. 2008;1(36):ra3.
41. Morissette MR, Cook SA, Buranasombati C, Rosenberg MA, Rosenzweig A. Myostatin inhibits IGF-I-induced myotube hypertrophy through Akt. *Am J Physiol Cell Physiol*. 2009;297(5):1124–1132.
42. Trendelenburg AU, Meyer A, Rohner D, Boyle J, Hatakeyama S, Glass DJ. Myostatin reduces Akt/TORC1/p70S6K signaling, inhibiting myoblast differentiation and myotube size. *Am J Physiol Cell Physiol*. 2009;296(6):C1258–C1270.
43. Zhang W, Chai B, Li J-Y, Wang H, Mulholland MW. Effect of des-acyl ghrelin on adiposity and glucose metabolism. *Endocrinology*. 2008;149(9):4710–4716.
44. Iwakura H, et al. Analysis of rat insulin II promoter-ghrelin transgenic mice and rat glucagon promoter-ghrelin transgenic mice. *J Biol Chem*. 2005; 280(15):15247–15256.
45. Ariyasu H, et al. Transgenic mice overexpressing des-acyl ghrelin show small phenotype. *Endocrinology*. 2005;146(1):355–364.
46. Musarò A, et al. Localized Igf-1 transgene expression sustains hypertrophy and regeneration in senescent skeletal muscle. *Nat Genet*. 2001;27(2):195–200.
47. Delhanty PJ, van der Lely AJ. Ghrelin and glucose homeostasis. *Peptides*. 2011;32(11):2309–2318.
48. Mandard S, et al. The fasting-induced adipose factor/angiopoietin-like protein 4 is physically associated with lipoproteins and governs plasma lipid levels and adiposity. *J Biol Chem*. 2006;281(2):934–944.
49. Sharara-Chami RI, Zhou Y, Ebert S, Pacak K, Ozcan U, Majzoub JA. Epinephrine deficiency results in intact glucose counter-regulation, severe hepatic steatosis and possible defective autophagy in fasting mice. *Int J Biochem Cell Biol*. 2012;44(6):905–913.
50. Sun Y, Wang P, Zheng H, Smith RG. Ghrelin stimulation of growth hormone release and appetite is mediated through the growth hormone secretagogue receptor. *Proc Natl Acad Sci U S A*. 2004; 101(13):4679–4684.
51. Sheriff S, Kadeer N, Joshi R, Friend LA, James JH, Balasubramaniam A. Des-acyl ghrelin exhibits pro-anabolic and anti-catabolic effects on C2C12 myotubes exposed to cytokines and reduces burn-induced muscle proteolysis in rats. *Mol Cell Endocrinol*. 2012;351(2):286–295.
52. Pallafacchina G, Calabria E, Serrano AL, Kalhovde JM, Schiaffino S. A protein kinase B-dependent and rapamycin-sensitive pathway controls skeletal muscle growth but not fiber type specification. *Proc Natl Acad Sci U S A*. 2002;99(14):9213–9218.
53. Skurk C, et al. The FOXO3a transcription factor regulates cardiac myocyte size downstream of AKT signaling. *J Biol Chem*. 2005;280(21):20814–20823.
54. Zhao JJ, et al. The p110alpha isoform of PI3K is essential for proper growth factor signaling and oncogenic transformation. *Proc Natl Acad Sci U S A*. 2006;103(44):16296–16300.
55. Gwinn DM, et al. AMPK phosphorylation of raptor mediates a metabolic checkpoint. *Mol Cell*. 2008; 30(2):214–226.
56. Barazzoni R, et al. Ghrelin regulates mitochondrial-lipid metabolism gene expression and tissue fat distribution in liver and skeletal muscle. *Am J Physiol Endocrinol Metab*. 2005;288(1):E228–E235.
57. Serra C, et al. Functional interdependence at the chromatin level between the MKK6/p38 and IGF1/PI3K/AKT pathways during muscle differentiation. *Mol Cell*. 2007;28(2):200–213.
58. Puigserver P, et al. Cytokine stimulation of energy expenditure through p38 MAP kinase activation of PPARgamma coactivator-1. *Mol Cell*. 2001; 8(5):971–982.
59. Kewalramani G, et al. Acute dexamethasone-induced increase in cardiac lipoprotein lipase requires activation of both Akt and stress kinases. *Am J Physiol Endocrinol Metab*. 2008;295(1):E137–E147.
60. Aversa Z, Alamdari N, Castillero E, Muscaritoli M, Rossi Fanelli F, Hasselgren PO. beta-Hydroxy-beta-methylbutyrate (HMB) prevents dexamethasone-induced myotube atrophy. *Biochem Biophys Res Commun*. 2012;423(4):739–743.
61. Qin W, Pan J, Wu Y, Bauman WA, Cardozo C. Protection against dexamethasone-induced muscle atrophy is related to modulation by testosterone of FOXO1 and PGC-1α. *Biochem Biophys Res Commun*.

2010;403(3–4):473–478.
62. Hong T, et al. Fine-tuned regulation of the PGC-1α gene transcription by different intracellular signaling pathways. *Am J Physiol Endocrinol Metab*. 2011;300(3):E500–E507.
63. Sandri M, et al. PGC-1alpha protects skeletal muscle from atrophy by suppressing FoxO3 action and atrophy-specific gene transcription. *Proc Natl Acad Sci U S A*. 2006;103(44):16260–16265.
64. Fürstenberger G, Senn HJ. Insulin-like growth factors and cancer. *Lancet Oncol*. 2002;3(5):298–302.
65. De Acetis M, et al. Cardiac overexpression of melusin protects from dilated cardiomyopathy due to long-standing pressure overload. *Circ Res*. 2005; 96(10):1087–1094.
66. Hishiya A, Iemura S, Natsume T, Takayama S, Ikeda K, Watanabe K. A novel ubiquitin-binding protein ZNF216 functioning in muscle atrophy. *EMBO J*. 2006;25(3):554–564.
67. Geuna S, Tos P, Guglielmone R, Battiston B, Giacobini-Robecchi MG. Methodological issues in size estimation of myelinated nerve fibers in peripheral nerves. *Anat Embryol (Berl)*. 2001;204(1):1–10.
68. Tos P, et al. Employment of the mouse median nerve model for the experimental assessment of peripheral nerve regeneration. *J Neurosci Methods*. 2008;169(1):119–127.

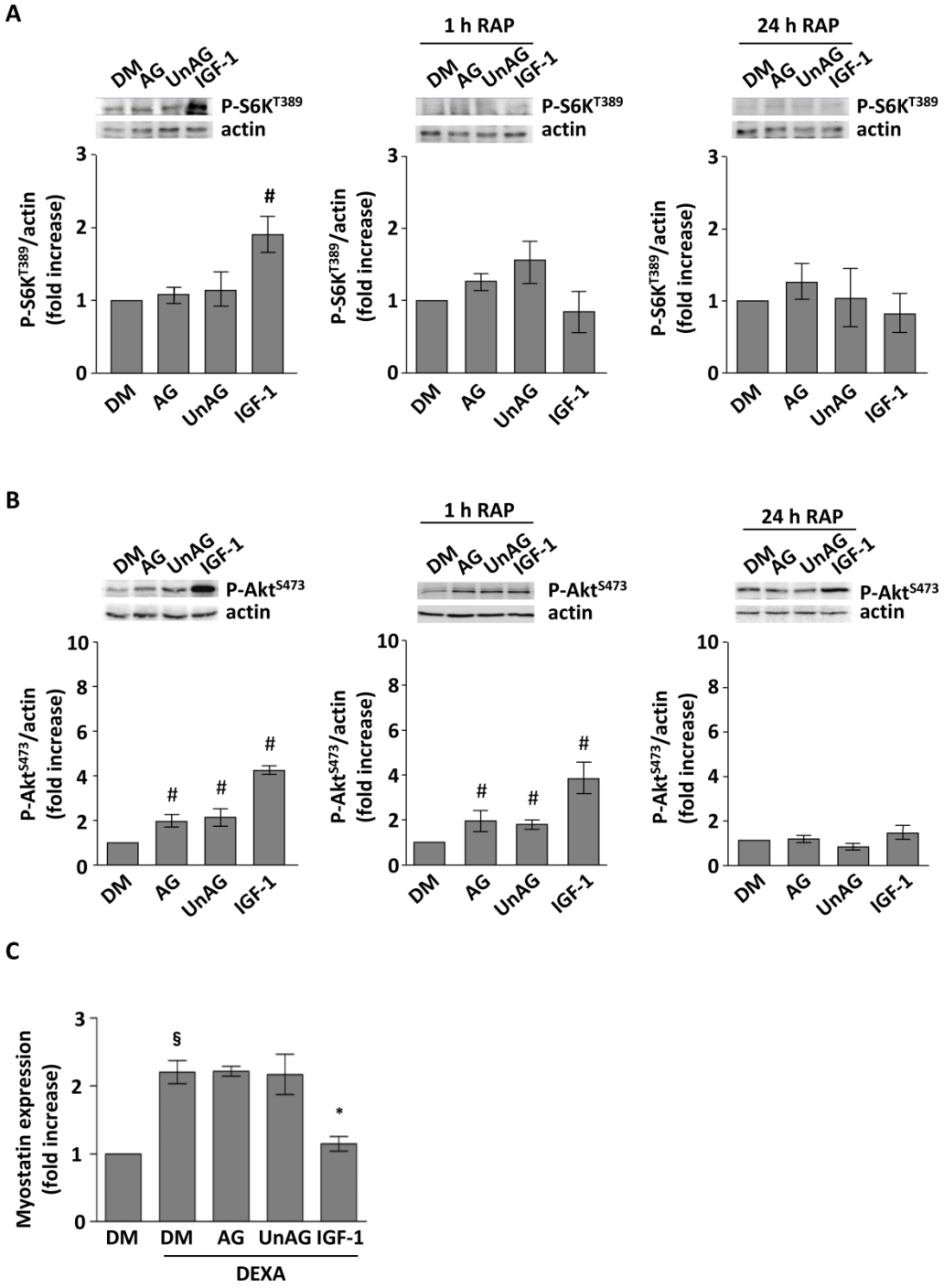

Figure S1.

Long rapamycin treatment impairs both mTORC1 and mTORC2 activities in C2C12 myotubes. (**A**-**B**) Phosphorylation of S6K^{T389} and Akt^{S473} detected by western blotting upon treatment for 20 min with 1 μM AG or UnAG. Upper panels: representative blots; lower panels: quantifications of 3 independent experiments. Rapamycin (RAP) 20 ng/ml was used for 1 h or 24 h. After short rapamycin treatment (1 h), mTORC1-mediated phosphorylation of S6K^{T389} is completely abolished (**A**), while the activity of mTORC2-mediated phosphorylation of Akt^{S473} is spared (**B**). On the other hand, upon 24 h of rapamycin treatment, Akt^{S473} phosphorylation is also abrogated, indicating that long rapamycin treatments affect mTORC2 activity as well as mTORC1 in C2C12 myotubes. #$P < 0.05$ versus control cells in DM.

(**C**) AG and UnAG do not affect dexamethasone (DEXA)-induced myostatin expression, measured by real-time RT-PCR. C2C12 myotubes were treated in DM for 24 h with 1 μM DEXA in the presence or absence of 10 nM AG or UnAG, or 10 ng/ml IGF-1 and processed for myostatin expression analysis. §$P < 0.01$ versus control cells in DM; *$P < 0.01$ versus DEXA-treated cells.

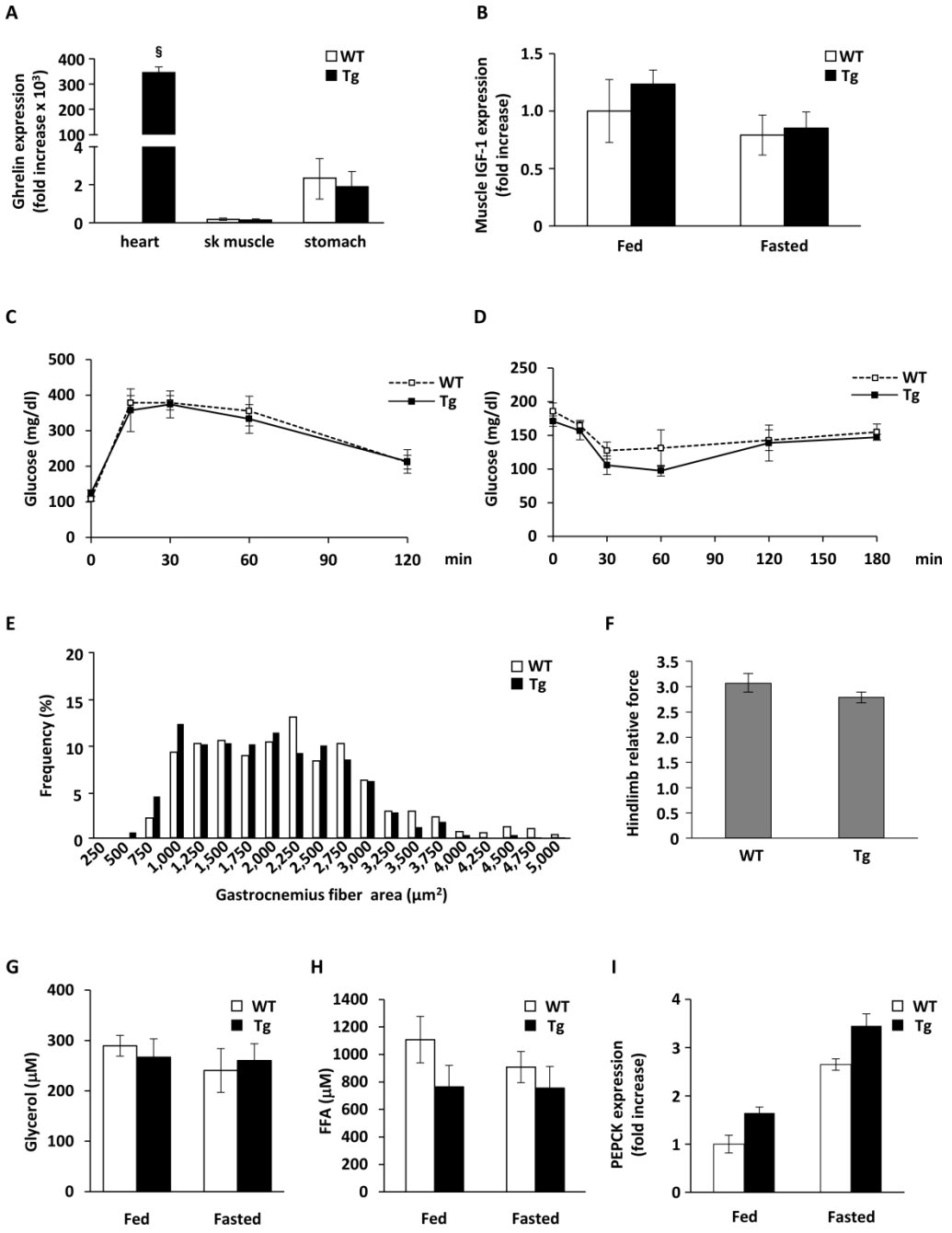

Figure S2.

(**A**) Ghrelin expression is specifically induced in the hearts of *Myh6/Ghrl* mice without any leaky expression in skeletal muscle. The expression in the stomach, the main source of AG and UnAG, is not altered in *Myh6/Ghrl* animals. §$P < 0.01$ versus WT mice. (**B**) IGF-1 expression in skeletal muscle is not altered in *Myh6/Ghrl* mice, either fed or starved animals (fed WT and Tg, n = 5; starved WT, n = 5; staved Tg, n = 6). (**C** and **D**) *Myh6/Ghrl* mice do not feature significant differences in glucose uptake (**C**) and insulin resistance (**D**) compared to WT littermates. For the glucose tolerance test, mice were injected after 16 h of fasting (WT and Tg, n = 5). (**E** and **F**) *Myh6/Ghrl* mice do not feature significant differences in muscle-fiber distribution and force compared to WT littermates. (**E**) Gastrocnemii were removed from fed animals and mean fiber CSA and distribution were analyzed (WT and Tg, n = 3). Mean gastrocnemius CSA of fed animals ± SEM (μm²) WT: 2,165.65 ± 290.85; Tg: 1,871.15 ± 100.86. (**F**) The weight that WT and Tg animals managed to hold up before losing grip was measured through a Grip Meter device and normalized to the weight of animals (WT and Tg, n = 5). (**G-I**) *Myh6/Ghrl* mice do not feature significant differences in plasmatic glycerol (**G**) and FFA (**H**), nor in liver PEPCK expression (**I**) compared to WT animals, in either fed or starved animals (n = 5 for each group).

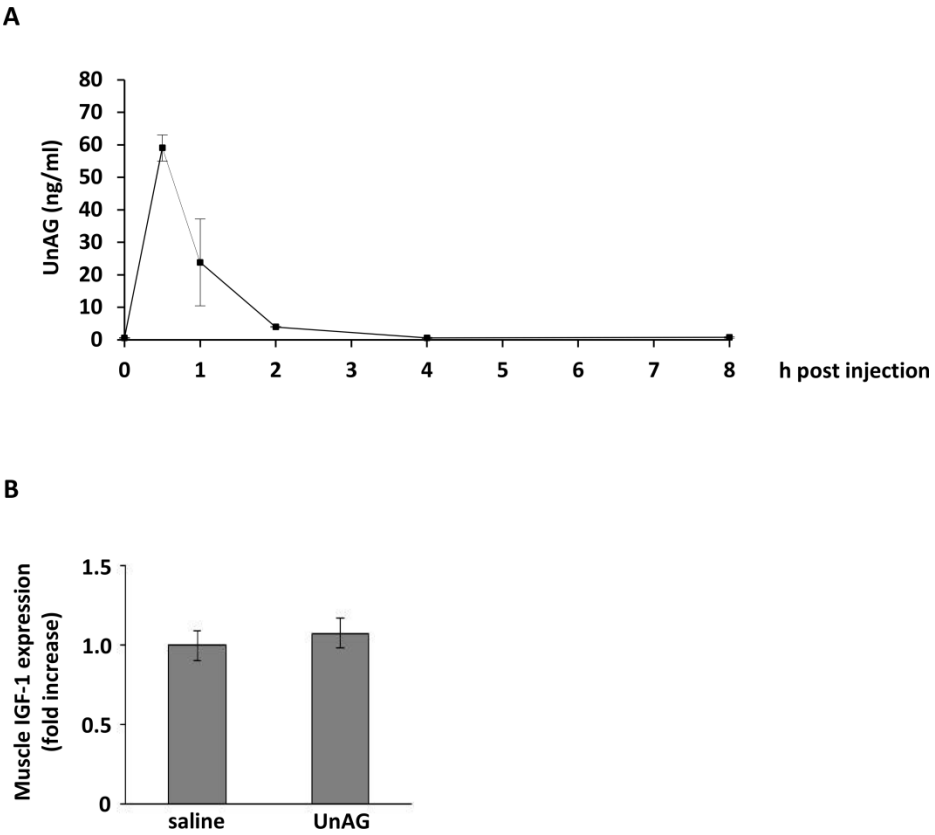

Figure S3.
(**A**) UnAG plasma concentration upon UnAG treatment. WT mice (n = 2) were injected s.c. with 100 µg/kg UnAG and, at the indicated time points, blood samples were collected by retro-orbital puncture and processed for EIA determination of plasmatic UnAG concentration. Each sample was loaded in triplicates and mean values ± SD are represented. (**B**) IGF-1 expression in skeletal muscle is not altered after UnAG injection compared to saline treatment (n = 5 for each group).